The Finite Element Method Simulation of Active Optimal Vibration Attenuation in Structures

A Thesis

Submitted to the College of Graduate Studies and Research

in Partial Fulfillment of the Requirements

for the Degree of

Master of Science

in the

Department of Mechanical Engineering

University of Saskatchewan

Saskatoon, Saskatchewan

Canada

By

Manish Baweja

PERMISSION TO USE

In presenting this thesis in partial fulfillment of the requirements for a Master's degree from the University of Saskatchewan, the author has agreed that the Libraries of this University may make it freely available for inspection. The author further agrees that permission for copying of this thesis in any manner, in whole or in part, for scholarly purposes may be granted by the professor or professors who supervised my thesis work or, in their absence, by the Head of the Department or the Dean of the College in which my thesis work was done. It is understood that any copying or publication or use of this thesis or parts thereof for financial gain shall not be allowed without the author's written permission. It is also understood that due recognition shall be given to the author and to the University of Saskatchewan in any scholarly use which may be made of any material in my thesis.

Requests for permission to copy or to make other use of material in this thesis in whole or part should be addressed to:

Head of the Department of Mechanical Engineering
University of Saskatchewan
Saskatoon, Saskatchewan, Canada S7N 5A9

ABSTRACT

The Finite Element Method (FEM) based computational mechanics is applied to simulate the optimal attenuation of vibrations in actively controlled structures. The simulation results provide the forces to be generated by actuators, as well as the structures response.

Vibrations can be attenuated by applying either open loop or closed loop control strategies. In open loop control, the control forces for a given initial (or disturbed) configuration of the structure are determined in terms of time, and can be preprogrammed in advance. On the other hand, the control forces in closed loop control depend only on the current state of the system, which should be continuously monitored.

Optimal attenuation is obtained by solving the optimality equations for the problem derived from the Pontryagin's principle. These equations together with the initial and final boundary conditions constitute the two-point-boundary-value (TPBV) problem.

Here the optimal solutions are obtained by applying an analogy (referred to as the beam analogy) between the optimality equation and the equation for a certain problem of static beams in bending. The problem of analogous beams is solved by the standard FEM in the spatial domain, and then the results are converted into the solution of the optimal vibration control problem in the time domain. The concept of the independent-modal-space-control (IMSC) is adopted, in which the number of independent actuators control the same number of vibrations modes.

The steps of the analogy are programmed into an algorithm referred to as the Beam Analogy Algorithm (BAA). As an illustration of the approach, the BAA is used to simulate the open loop vibration control of a structure with several sets of actuators. Some details, such as an efficient meshing of the analogous beams and effective solving of the target condition are discussed.

Next, the BAA is modified to handle closed loop vibration control problems. The algorithm determines the optimal feedback gain matrix, which is then used to calculate the actuator forces required at any current state of the system. The method's accuracy is also analyzed.

ACKNOWLEDGEMENTS

The author would like to express his gratitude and appreciation to his supervisor Dr. Walerian Szyszkowski for his guidance and assistance throughout the Master's program. The advice and encouragement provided by him is thankfully acknowledged.

Thanks are due to the members of the advisory committee, Dr. L. G. Watson and Dr. R. T. Burton of the Mechanical Engineering Department.

The author is thankful to Mr. I. J. MacPhedran, Mr. T. Zintel and Mr. Randy Hickson from Engineering Computing Services for their assistance in computer software and system operation.

Special thanks are extended to the author's parents, Mr. Harish Baweja and Mrs. Shakuntala Baweja and all other family members for their constant encouragement and support in making this work a reality. But for their assistance, this work would not have been possible.

Financial support provided by the Natural Sciences and Engineering Research Council (NSERC) of Canada in the form of the operating grant of Dr. W. Szyszkowski is gratefully acknowledged.

Finally, I also thank all my friends in Saskatoon for their useful advice and support throughout this research work.

DEDICATION

This thesis is dedicated to:

My Parents

Mr. Harish Baweja and Mrs. Shakuntala Baweja

&

My Family Members

For their continuous love and unwavering support

TABLE OF CONTENTS

LIST OF FIGURES

Figure **Page**

LIST OF TABLES

NOMENCLATURE

Listed below are the symbols and abbreviations used most frequently in the text. Occasionally, the same symbol may have a different meaning defined in the text.

$A,\ \hat{A},$ $B,\hat{B},\widetilde{C},\hat{C}$	Matrices
C	Damping coefficient
D	Matrix
d_e	Element deflection vector
DOF	Degrees of freedom
EI	Bending stiffness of the analogous beam
$E\hat{I}$	Bending stiffness
F	Force
F_a	Actuator forces vector
F_c	Control force vector
FEM	Finite element method
F^e	Element force vector
F_s	Vector of static forces
G	Constant feedback gain matrix
g	function
g_{id}	Modal gain for displacement
g_{iv}	Modal gain for velocity
H	Hamiltonian
I	Identity matrix
IMSC	Independent modal space control
J	Performance index
K	Stiffness matrix
K^e	Element stiffness matrix
k_f	Elastic foundation stiffness
k	Spring stiffness
L	Length of analogous beams
L_{eff}	Effective length
LHS	Left hand side
M_b	Bending moment
M	Mass matrix
n	Number of DOFs
ODE	Ordinary Differential Equation
P	Compressive force on analogous beams
P_{cr}	Critical compressive force
p_d	Costates related to position

P	Costates
p_v	Costates related to velocity
Q	Weighting matrix
$\hat{Q}$, $\hat{Q}_v$	Weighting matrix related to kinetic energy
q_v $\hat{q}_v$	Weighting functions related to kinetic energy
$\hat{Q}$	Weighting matrix in modal space
Q_d $\hat{Q}_d$	Weighting matrix related to strain energy
$q_{d,}\hat{q}_d$	Weighting functions related to strain energy
R, $\hat{R}$	Weighting matrices for control effort
$r,\hat{r}$	Weighting functions for control effort
RHS	Right hand side
s	number of modes
T	Shear Force
t	Time
t_{eff}	Effective time
t_f	Final time
U	Modal control force vector
uy	DOFs in Y direction
v,θ	Deflection and slope vectors of the analogous beam
$\dot{x}$	Velocity vector
x_f	Final position vector
x	Position vector
x_0	Initial position vector
x_s	Static displacements
y_d	Output vector
z	States
z_f	Final states
z_0	Initial states
$\alpha_1...\alpha_3$	Constants
$\beta_1...\beta_3$	
$\gamma_1...\gamma_3$	
α_c,β_c	Rayleigh damping
$\dot{\eta}$	First derivative of modal vector
ω	Angular velocity
Δ	Modal damping matrix
Φ_i	Eigenmodes
Ω	Modal stiffness matrix
ε	Convergence tolerance
η	Modal vector

ξ	Damping coefficient	Γ	Weighting constants for maneuver time
δ, τ	Beam parameter		
Φ	Mass normalized transformation matrix	λ, ς	Optimal control parameter

Chapter 1. Introduction

1.1 Computational Mechanics and Actively Controlled Structures

Computational mechanics nowadays plays an important role in the analysis and design of structures and mechanisms. Thanks to the availability of sophisticated finite element software and powerful computers the behaviour of even very complex mechanical systems can be analyzed and simulated with high accuracy. The simulations help in understanding and examining the system performance prior to performing any physical experiments. The big advantage of computer simulations is that once the computer model is prepared, it can be changed and rerun many times with minimal cost. Usually the cost of preparing and running such virtual experiments is incomparably smaller to performing the real experiments. Also, the computational effort is somewhat independent of the physical scale of the problem; it may be similar when considering either large objects in outer space or extremely small components of micro/nano mechanisms. Therefore, various new products and ideas can be quickly and thoroughly analyzed, verified, corrected, modified, optimized, etc. to make them better before even entering any physical testing.

While finite element method (FEM) based computational mechanics is widely popular with 'regular structures' it is essentially not used at all for actively controlled structures. Such structures, also referred to as smart structures, have sets of actuators built in, the role of which is to force the structure to perform a predefined task. How exactly the actuators act is typically determined by applying some control methodologies. The problem is that, the actuators' forces defined from control considerations are typically either not known explicitly or are in a form which is incompatible with computational mechanics standards (this is explained in more details later). Consequently, the structure and the control are considered separately and typically different software for mechanical and control aspects are typically used when analyzing and simulating such structures.

A large diameter reflector for astrophysical observatories (Figure 1.1a) is an example of an actively controlled structure. The reflector has to maintain its shape with tolerance in the range of micrometers despite of temperature variations and changing gravity forces. This is achieved by using actuators that act on the supporting truss structure (Figure 1.1 b) to adjust it according to the current conditions [Tzou, H.S. and Anderson, G.L., 1992].

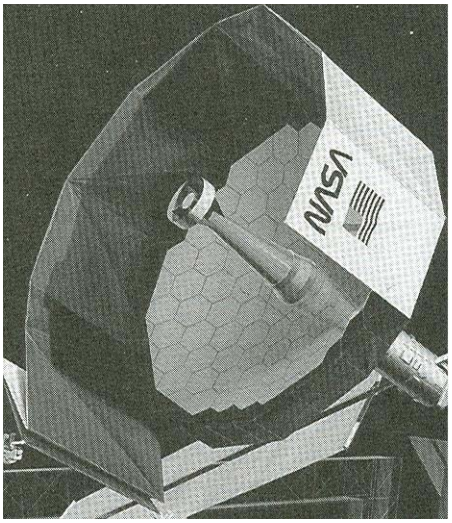

Figure 1.1a Large Diameter Reflector

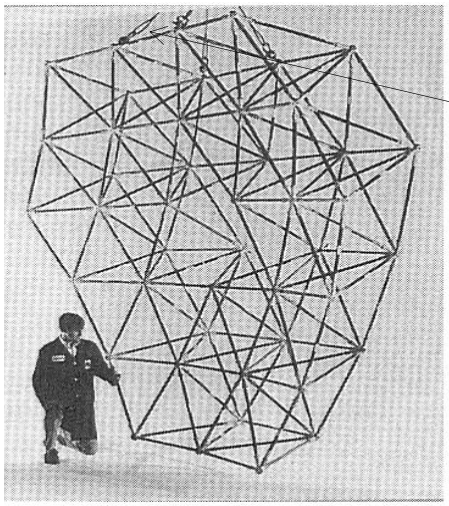

Figure 1.1 b Reflector Support Structure

Active control is used to reduce swaying in tall buildings. Figure 1.2 shows the frame of a 21-story building that is to be controlled by sixty-two actuators [Saleh, A. and Adeli, H., 1999]. The actuators are located in the upper level of the structure (Section 2) and are to eliminate the horizontal displacements due to the dynamic loads such as earthquakes and wind.

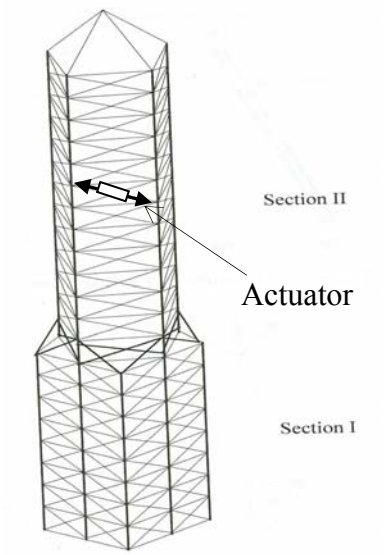

Figure 1.2 21-Story Frame Structure

The concept of active vibration control is illustrated in a simple two-story structure (Figure 1.3) controlled by two actuators. These actuators, by generating appropriate forces acting at points *A* and *B*, should be capable of eliminating any disturbances imposed on the structure. This structure was analyzed in [Grewal, I. S. and Szyszkowski, W., II, 2002].

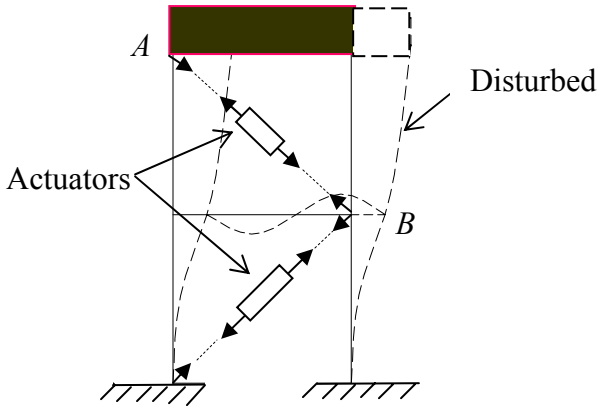

Figure 1.3 Two Story Structure

The main challenge in design of actively controlled structures is to select appropriate actuators. The forces to be generated by the actuators depend generally on their location and the dynamic characteristics of the structure. It would be beneficial to be able to determine these forces for any particular structure and the actuators' configurations from the computer simulations. By performing such a simulation the designers can determine in advance the magnitude of the forces required to control the structure, and from that they can decide which type and how many actuators are needed.

The focus of this thesis is on the computer simulation of actively controlled structures. Once the required actuators' actions are determined, the selection of real physical actuators will be easy, this being beyond the scope of this thesis. Clearly the actuation forces and physical actuators may be relatively small for the reflector in Figure 1.1 and quite large for the structure shown in Figure 1.2.

The simulation method presented in this thesis is based on FEM. It is assumed that the above mentioned structures can be modelled with sufficient accuracy by using standard FEM. In this study ANSYS (the ANSYS 6.1 version), a commercial FEM program was used for this purpose. Any types of elements, that are appropriate for the analysis of a particular structure, can be used in the FEM model. It is also assumed that the number of elements is generally very large in comparison with the number of actuators. In the next section a brief overview of the finite element method is presented.

1.2 Comments on the Finite Element Method

A large variety of structures can be modeled and simulated using the FEM methods of computational mechanics [Bathe, K. J., 1996]. The FEM is based on the idea of building a complicated object with simple blocks, or, dividing a complicated object into small pieces using small elements. Then the behaviour of each piece is analyzed by using a set of relatively simple approximate functions to solve the equations defining the problem considered. Mathematically speaking the FEM converts the set of governing differential equations for a problem into a set of equations in the form:

$$M\ddot{x} + C\dot{x} + Kx = F(t) \tag{1.1}$$

Vector x represents nodal displacements, and the dot indicates the first time derivative. M, C and K are mass, damping and stiffness matrices, respectively. For the vibration problems analyzed here these matrices can be considered constant. $F(t)$ is the vector of active nodal forces. The components of x are also referred to as the degree of freedom of the system (DOF). The set of 2^{nd} order differential equations (1.1) can be integrated in time starting from the known initial conditions:

$$x(0) = x_0 \text{ and } \dot{x}(0) = \dot{x}_0 \tag{1.2}$$

If $F(t)$ is known, such a problem will be referred to as a transient dynamic problem. If the motion is negligible (and the inertial terms $M\ddot{x}$ and $C\dot{x}$ can be omitted) then equation (1.1) becomes the equation of static equilibrium:

$$Kx_s = F_s \tag{1.3}$$

where F_s is the vector of static nodal forces and x_s is the corresponding vector of static displacements.

Such static problems are handled relatively easily by solving the set associated of algebraic equations.

Another problem that can be solved without much effort is the problem of free vibrations with small damping. Assuming $F(t) = 0$ and a harmonic motion for x (for example $x = \Phi \sin \omega t$) the following eigenvalue problem is formulated.

$$(K - \omega_i{}^2 M)\Phi_i = 0 \tag{1.4}$$

The solution of this problem gives the set of frequencies ω_i and the modes of vibrations Φ_i. Theoretically for the problem with n DOFs one can obtain n number of modes (typically listed in the ascending order of frequency).

The main goal of this thesis is to handle actively controlled structures and in particular to find suitable control forces using computational mechanics. The shape and size of the structure does not matter since it will be converted into a standard FEM model. Here the fin structure shown in Figure 1.4 is considered. This structure is complex enough to necessitate the use of FEM. On the other hand the FEM related calculation will not be excessive so the focus can be made on the control aspect of the problem.

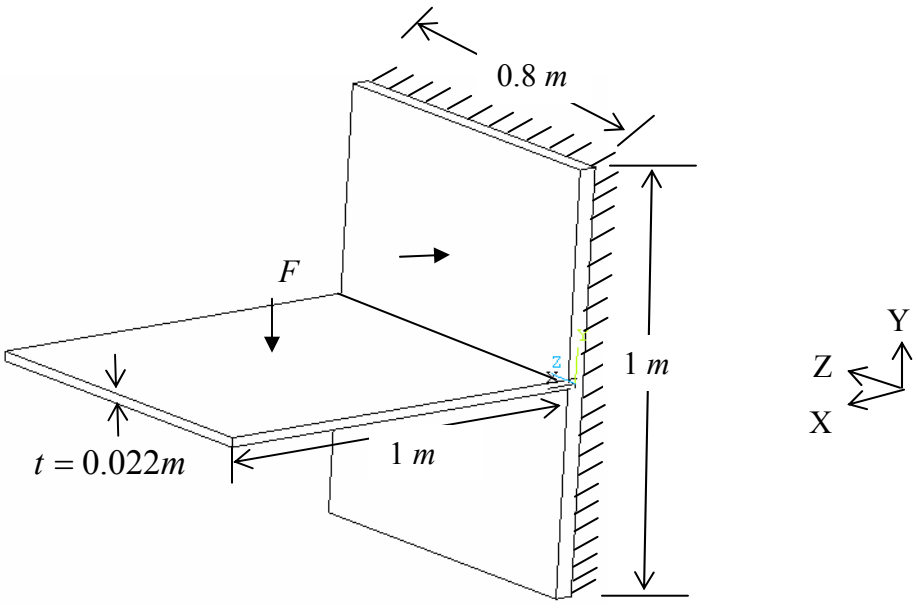

Figure 1.4 Model of Fin Structure

The structure is modeled using the ANSYS software. The FEM model (Figure 1.5) that will be considered in this thesis is built of 300 SHELL63 elements from the ANSYS element library, and has approximately 2000 DOFs (which provide sufficient accuracy for the FEM calculations). The SHELL63 elements have both bending and membrane capabilities. Also in-plane and normal loads are permitted. The element has six degrees of freedom at each node. It should be emphasised that the FEM model with any number of DOFs will be treated in the same way.

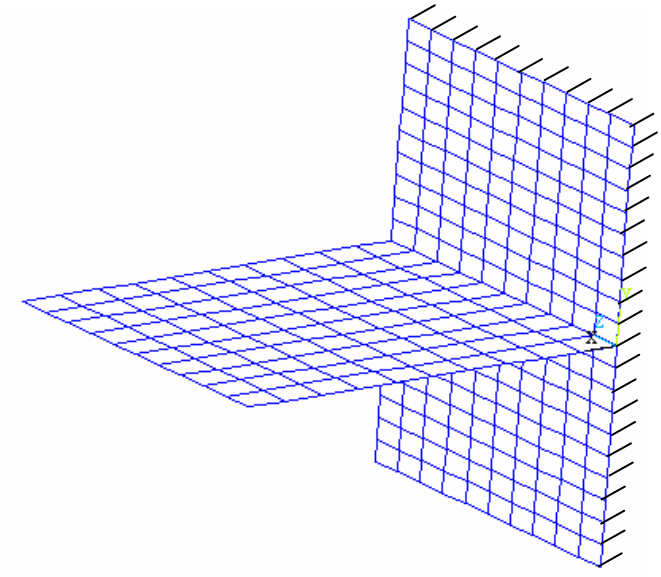

Figure 1.5 Meshed FEM Model

It should be emphasized again that the FEM analysis mentioned can be used only if the force vector $F(t)$ is known. In actively controlled structures, however, typically only the initial and final configurations are known. The forces needed to maneuver the structure from the initial to final configurations have to be determined. The problem of finding proper control forces can be classified as an active structural control problem. In the next chapter active control is explained in detail.

Chapter 2. Comments on Active Control

2.1 Introduction

As stated in the previous chapter, any type of complex mechanical structure can be modelled and different types of FEM analysis can be performed as long as the forces exerted on the structure are known. Since the initial conditions (1.2) are known, such an analysis will constitute a standard transient dynamics initial value problem. However, in active control the initial and final configurations (final boundary conditions) of a problem may be known, and the control forces generated by the actuators are to be determined. In control, such problems are also referred to as the two-point-boundary-value (TPBV) problems (the conditions are given for the two points of the time domain).

In control theory, the state of the system (which represents the mathematical model of the dynamic system) is usually written in the form of the first order differential equations using state variables [Takahashi, Y., and Robins, M. J., and Auslander, D.M., 1972]. Introducing the state variables $z_i = x_i$ and $z_{n+i} = \dot{x}_i$, $i=1....n$ (which represent positions and velocities respectively) the governing equations Eq. (1.1) for the structure under the vector of nodal control forces $F_c(t)$ can be written in the form

$$\dot{z} = Az + BF_c(t) \tag{2.1}$$

where

$$A = \begin{bmatrix} 0 & I \\ -M^{-1}K & -M^{-1}C \end{bmatrix}_{2n\times 2n} \tag{2.2}$$

$$B = \begin{bmatrix} 0 \\ M^{-1} \end{bmatrix}_{2n\times n} \tag{2.3}$$

and z is the vector of state variables and n is the number of DOFs of the FEM model.

As can be seen a dynamic system of second order with n DOFs can be converted into a set of first order equations with $2n$ state variables.

In the active control besides the initial conditions (1.2), the final boundary conditions are also specified as:

$$x(t_f) = x_f \text{ and } \dot{x}(t_f) = \dot{x}_f \tag{2.4}$$

In terms of state variables the boundary conditions Eqs. (1.2) and (2.4) can be written in the form:

$$z(0) = z_0 \text{ and } z(t_f) = z_f \tag{2.5}$$

where z_0 and z_f represent the system's states (the positions and velocities) at the beginning and at the end of the maneuver.

In active structural control it is desired to use actuators generating the control force vector $F_c(t)$ to move the structure from one configuration to another. It is assumed that the initial and final configurations are known. Specifically for vibration attenuation the disturbed configuration will be denoted by z_0, and the vibration-free state as z_f. The location of actuators is not known a priori; but suitable places to position the actuators can be found (this will be discussed in chapter 5 section 5.5). Two approaches for how to execute the maneuver from the state z_0 to the state z_f are presented next: open loop control and closed loop control.

2.2 Open Loop Control

A schematic block diagram of the open loop control system is shown in Figure 2.1. As explained before, in control practitioners generally use the system's states. In open loop control the control forces, $F_c(z_0, t)$, are calculated in terms of time, and the initial configuration of the structure. Such in advance predetermined forces are then applied on the structure to execute the maneuver. Since the control forces for a particular initial disturbance are calculated in advance and then applied to get the desired configuration, the corresponding algorithm is referred to as an *off-line algorithm.*

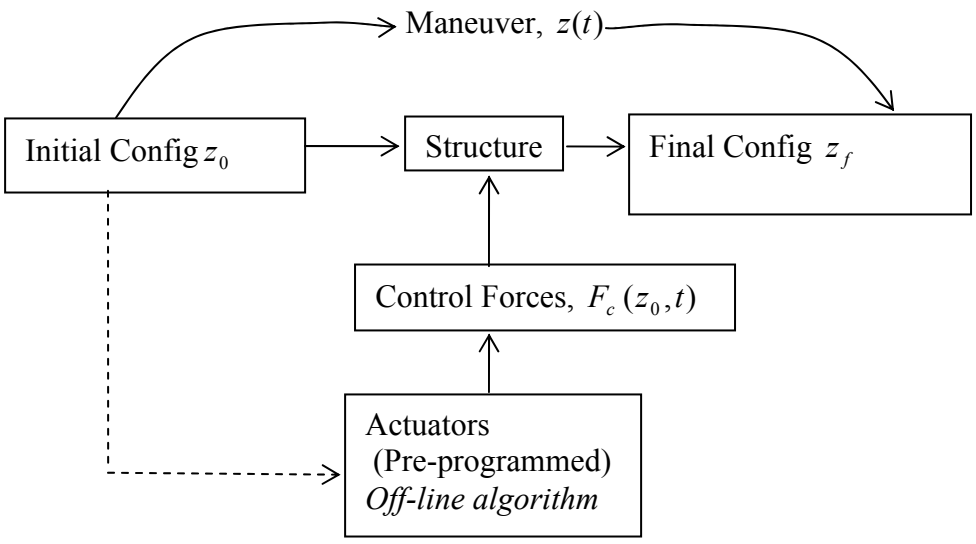

Figure 2.1 Open Loop Control

2.3 Closed Loop Control

In the closed loop control system the control forces depend on the current state of the system. This dependence is typically written in the form: $F_c(t) = -Gz(t)$ where G is the real constant matrix called the feedback gain matrix. This means that for the known gain matrix one can determine the control forces for any state of the system independently of the initial configuration. A schematic diagram of the closed loop control system is shown in Figure 2.2. Error (in the form of states at particular time t) is calculated from sensors placed on the structure, and fed to the gain matrix (controller) to determine the control forces. These forces are, in turn, applied to the structure to get the desired configuration. Again in Figure 2.2 the term *on-line algorithm* is used as control forces are calculated directly from the current states of the system.

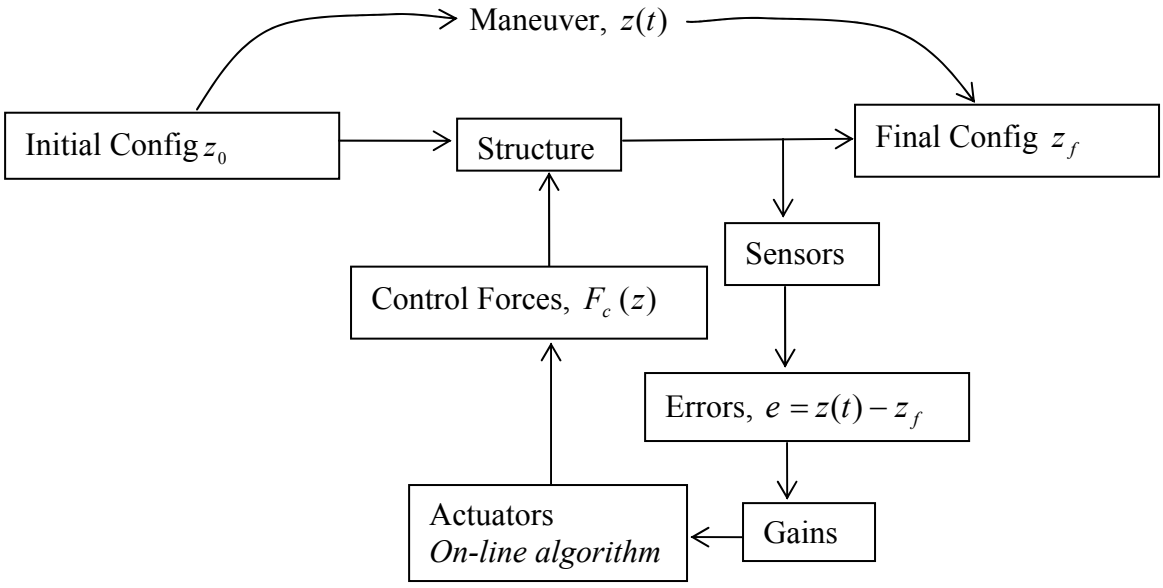

Figure 2.2 Closed Loop Control

As outlined above, the main goal of active vibration control is to determine the control forces for the whole maneuver that would satisfy the initial and final boundary conditions. Clearly, the maneuver can be executed in different ways, and for each maneuver there will be a different pattern of the control forces. The question of which option of executing maneuver is better and how to select the best control forces can be answered by the optimal control methodology. Such methodology is discussed in detail in next chapter.

Chapter 3. Optimal Control and Its Solution Techniques

3.1. Introduction to Optimal Control

As explained earlier there are several ways in active structural control to find the forces and to execute the predefined maneuver. The main interest is in finding the 'best' way to perform such maneuvers. Optimal control methodology will be used for this purpose. The word 'optimal' in its general sense means, the 'best' or most desirable. An optimal control problem requires the mathematical model of a process to be controlled, the statement of physical constraint, and a performance measure [Takahashi, Y., Robins, M. J. and Auslander, D.M., 1972].

As explained in chapter 2 section 2.1, in control one generally deals with the system's state, so the governing equation of dynamics will be in the form of Eq. (2.1) with corresponding boundary conditions (2.5). The performance measure may be given by:

$$J = \int_{t_0}^{t_f} g(z, F_c)dt \rightarrow \min \tag{3.1}$$

where g represents a function of the states and controls.

Eq. (3.1) imposes an extra constraint on the variables $F_c(t)$ and $z(t)$ related already through the governing equation of dynamics (2.1).

Formally, minimizing the performance index (3.1) compels the search for the best $F_c(t)$, to be combined with trajectory $z(t)$ into one optimizing process. It is expected that, at least one combination of $F_c(t)$ and $z(t)$ exists that satisfy the condition. Such a solution is recognized as an optimal solution.

3.2 Formulation of Optimal Control Problem

To obtain the desired trajectory and optimal actuator forces, the performance index (measure) is minimized. In optimal control performance can be either minimized or maximized, to reach a desired state.

The execution of such an optimal control depends on the particular form of $g(z, F_c)$. Some physical meaning may be assigned to this function. If $g = g_1(z) = z^T Kz$, where

$z^T = [x^T, 0]$ and K is the matrix representing the system's stiffness, then g represents the strain energy during maneuver. If $g = g_2(F_c) = F_c^T R F_c$, where R is a weighting matrix, the corresponding performance can be used to minimize the magnitude of the control forces. If $g = c$, where c is a constant, then $J = ct_f$ and the performance index minimizes the maneuver time.

The performance index for most mechanical systems is specified as quadratic in terms of DOFs and controls, and is given by:

$$J = 1/2 \int_0^{t_f} [x^T Q_d x + \dot{x}^T Q_v \dot{x} + F_c^T R F_c + \Gamma] dt \rightarrow \min \tag{3.2}$$

where positive definite weighing matrices Q_d, Q_v, and R are to control the displacements, the velocities, and the level of control forces of the system respectively.

Γ is a positive constant weighting the maneuver time. Note that if following substitutions are made: $Q_d \rightarrow K$, $Q_v \rightarrow M$ and $R \rightarrow K^{-1}$ then one can deal directly with the strain energy, kinetic energy, and control energy of the system.

3.3 Solution to Optimal Control Problems

To control a mechanical system driven by forces F_c from the initial to the final states, z_0 to z_f, one can require that:

$$J(F_c) = \int_0^{t_f} g(z, F_c) dt \rightarrow \min \tag{3.3}$$

Note that formally the left hand side of Eq. (3.3) should be written as $J(z, F_c)$; however, since forces F_c and z are related via the state equation (2.1), i.e. $z = z(F_c)$, ultimately the performance is dependant only on the control.

Optimal control problems have been attacked by researchers and engineers by applying direct optimization methods. The main idea of such methods is to determine two sets of F_c^k and F_c^{k+1} in two consecutive iterations k and $k+1$ in such a way that $J(F_c^{k+1}) < J(F_c^k)$. Thus the performance is directly minimized, while trying to meet all constraints. This approach is also referred to as parametric optimization. An alternate way

of solving optimal control problems is to derive the optimality conditions using Pontryagin's principle. The optimal control forces and optimal paths must meet these constraints. This approach is more analytical and is called the indirect method.

3.4 Direct Search Technique

Various direct search general optimization techniques based mostly on the gradient are used to minimize $J(F_c)$. Such a parametric optimization technique is discussed in some detail next.

3.4.1 Parametric Optimization Technique

An algorithm for the direct search technique is explained here on the example of the fin structure introduced in chapter 1 section 1.2. Assume the fin structure is disturbed (Figure 3.1) and is to reach the final undisturbed configuration at a given time t_f with the help of force $F_c(t)$ generated by an attached actuator.

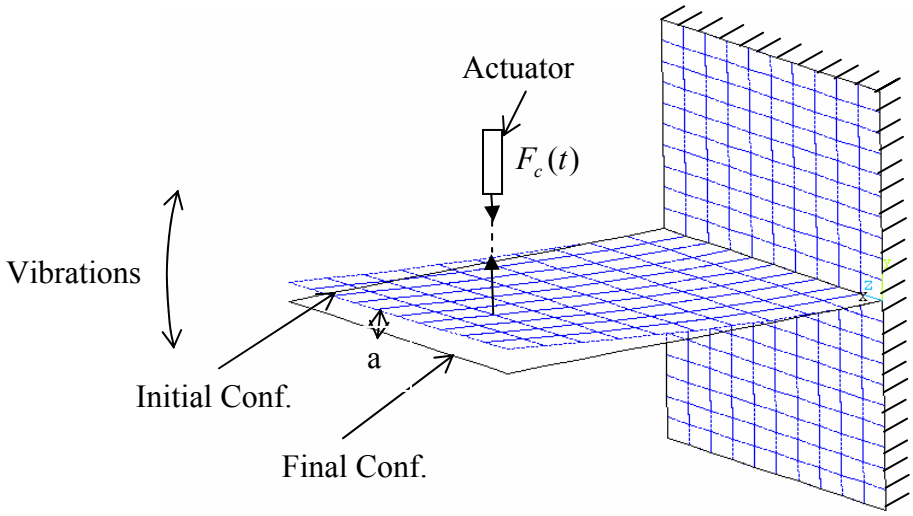

Figure 3.1 Disturbed Structure

In order to apply the parametric optimization technique the optimal control problem must be converted into an algebraic form with a finite number of optimization variables (here the objective function is written in terms of DOFs will be considered):

(a): $J = \int_0^{t_f} g(x, \dot{x}, F_c)dt \rightarrow \min$

subject to (b): $M\ddot{x} + C\dot{x} + Kx = F_c(t)$

and the boundary conditions (c): $x(0) = x_0$, $\dot{x}(0) = \dot{x}_0$, $x(t_f) = x_f$, $\dot{x}(t_f) = \dot{x}_f$

An algorithm for parametric optimization can be developed as follows:

1) *Parameterizations of optimization variables* (*OV*): Divide t_f into k intervals and assume some force values $F_1^0, ..F_{k+1}^0$ at each time t_j as *OV*. The force may be varying linearly within the interval, (between points j and $j+1$) as indicated in Figure 3.2.

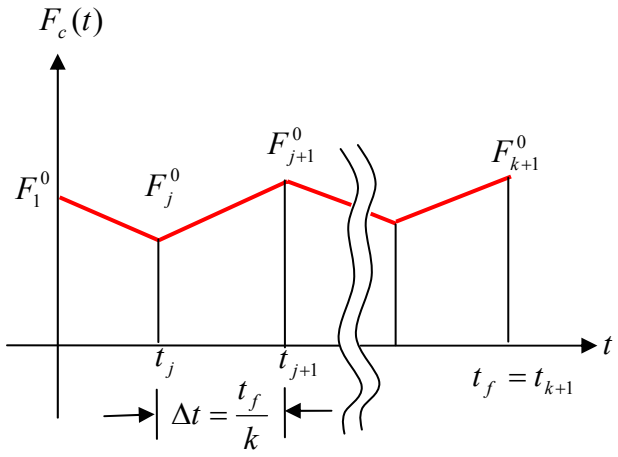

Figure 3.2 Parameterization of Control Forces

2) *Satisfying the equation of dynamics*: Use the ANSYS transient dynamic analysis with $F_c^0(t) = F_j^0\left(\frac{t_{j+1} - t}{\Delta t}\right) + F_{j+1}^0\left(\frac{t - t_j}{\Delta t}\right)$

to calculate $x(t)$ and $\dot{x}(t)$ for $t_j \le t \le t_{j+1}$ by integrating Eq. (b) starting with x_0 and $\dot{x}_0$

3) *Meeting the final boundary conditions*: Determine and calculate a certain norm of the error at t_f i.e. $e_f = \left\|x(t_f) - x_f\right\| + \left\|\dot{x}(t_f) - \dot{x}_f\right\|$

4) *Calculating the performance*: Substitute $x(t)$, $\dot{x}(t)$ and $F(t)$ into the performance. Integrate it numerically to obtain: $J = \int_0^{t_f} g(x, \dot{x}, F_c)dt = J(F_1^0, ..F_{k+1}^0)$

5) *Updating the OV:* Minimize $J(F_1..F_{k+1})$ with the constraint $e_f = 0$ to obtain a new set of $F_1^1, ..F_{k+1}^1$. This constraint optimization problem can be converted into the unconstrained problem by using either the penalty or Lagrange multipliers.

6) Repeat the process until the constraint is met and $J(F_c)$ is minimized

This approach becomes computationally expensive and tiresome if the number of intervals increases. The convergence is usually very poor [Abdullah, M.M., 1998; Saleh, A. and Adeli, H., 1999]

The alternative approach referred to as indirect methods to solve optimal control problems are discussed in next section.

3.5 Indirect methods to Solve Optimal Control Problems

Indirect methods are more analytical than the direct methods. The conditions to be met on the optimal path are derived first. These conditions are derived from Pontryagin's Principle and are the necessary conditions for an optimal solution. The next step is to determine the control and the trajectory that meet these conditions.

3.5.1 Optimality Conditions using Pontryagin's Principle

Optimality conditions using Pontryagin's principle [Pinch, E.R., 1993] are formulated for the problem given by Eq. (2.1) and the performance index given Eq. (3.1). Solving the optimality conditions should allow the practitioner to get the optimal maneuver time (t_f) (if unknown) and the optimal control force vector in time F_c(t).

The performance index, to be optimized for the maneuver from z_0 to z_f of the system defined by the Eq. (2.1), is defined by:

$$J = 1/2 \int_0^{t_f} (z^T Q z + F_c{}^T R F_c + \Gamma) dt \rightarrow \min \qquad (3.4)$$

where Q and R are positive definite matrices of order $2n$ and n respectively

and Γ is a positive constant. Q and R are generally expressed as:

$$Q = \begin{bmatrix} Q_d & \\ & Q_v \end{bmatrix}_{2n\times 2n} \text{ and } \quad R = [R]_{n\times n} \tag{3.5}$$

In order to apply Pontryagin's principle for the state given by Eq. (2.1) the Hamiltonian is defined as:

$$H = -1/2(z^T Q z + F_c{}^T R F_c + \Gamma) + p^T (Az + BF_c) \rightarrow \min \tag{3.6}$$

where p is the vector of costates with $2n$ components.

For optimal motion the costates must satisfy the equation:

$$\dot{p} = -\frac{\partial H}{\partial z} = Qz - A^T p \tag{3.7}$$

Also, the Hamiltonian has to be minimum with respect to control, that is:

$$\frac{\partial H}{\partial F_c} = -RF_c + B^T p = 0 \tag{3.8}$$

Eq. (3.8) gives the modal optimal control as:

$$F_c = R^{-1} B^T p \tag{3.9}$$

where R^{-1} exists as R must be positive definite.

After substituting Eq. (3.9) into Eq. (2.1) one obtains:

$$\dot{z} = Az + BR^{-1} B^T p \tag{3.10}$$

which means there are now two sets of differential equations i.e. (3.7) and (3.10) to solve. One should note, however, that the boundary conditions are given for states only i.e.

$z(0) = z_0$ and $z(t_f) = z_f$

Also, at t_f the following target condition must be met

$$H(t_f)\delta t_f = 0 \tag{3.11}$$

If t_f is given then $\delta t_f = 0$, and the target condition is met automatically. On the other hand if t_f is not given then $\delta t_f \neq 0$ and one has to satisfy the target condition in the form $H(t_f) = 0$.

Typically these optimality conditions are problem dependent and become very complicated mathematically. The above equations are very difficult to solve mainly because Eq. (3.7) cannot be effectively integrated without knowing the initial values of

costates, $p(0)$. In the next section a different approach to handle optimal control problems is presented in which the costates are eliminated.

3.5.2 The Riccati Equation

The main problem in solving optimality conditions using Pontryagin's principle is that the initial conditions for the costates are not known. If costates can be changed into some form of states then perhaps the problem can be solved. For that assume [Junkins, J.L. and Kim, Y., 1993]:

$$p = C(t)z \tag{3.12}$$

where C is a symmetric matrix of dimension n.

Substituting back into Eq. (3.7) one has:

$$\dot{C}z + C\dot{z} = Qz - A^T Cz \tag{3.13}$$

From Eq. (3.8) and Eq. (3.12):

$$F_c = R^{-1}B^T Cz \tag{3.14}$$

Now substituting Eqs. (2.1) and (3.14) back into Eq. (3.13):

$$\dot{C} + CA + CBR^{-1}B^T C - Q + A^T C = 0 \tag{3.15}$$

This equation is referred to as the Riccati equation. Note that the third term contains multiplication of matrices C. If C can be found by solving the Riccati equation then it can be substituted into the Eqs.(3.14), (3.12) and (2.1) to get the controls, costates and trajectories of the optimal maneuver. However, the equation is non linear, has a matrix form, and it is generally difficult to solve if the size of C increases [Saleh, A., and Adeli, H., 1994].

Also the boundary condition for Eq. (3.15) is related to the target conditions and has the form $C(t_f) = C_f$ which requires integration backward in time. Eq. (3.15) simplifies somewhat if the duration time is assumed infinite: i.e.: if $t_f \to \infty$ for such a case $\dot{C} = 0$ and the Riccati equation can be obtained in the form of

$$CA + CBR^{-1}B^T C - Q + A^T C = 0 \tag{3.16}$$

Eq. (3.16) is known as algebraic Riccati's equation (ARE).

Also, the matrix $R^{-1}B^TC$ in Eq. (3.14) becomes constant and the control-state relation can be written in the form:

$$F_c = -Gz(t) \tag{3.17}$$

where constant $G = -R^{-1}B^TC$ is called feedback gain matrix.

The solution to Eq. (3.16) is still very difficult. Due to nonlinearities some iterative methods must be used, which do not always converge to the correct solutions [Junkins, J.L. and Kim, Y., 1993].

The question arises, is there any way that one can handle optimal control problems relatively easier?

The answer to this question is positive, as it is demonstrated in the next section. In the section that follows the optimality equation is derived in a different form. This form is also independent of costate, but does not have nonlinear terms as in Eq. (3.15).

3.6 Removing Costates from Optimality Equation

It can be concluded from the previous section that solution to the optimal control problem is a tedious and uncertain task, irrespective of whether it is a direct or indirect method.

Indirect methods are generally more precise and reliable than the direct methods, but the presence of the costates makes it a difficult task to solve practical problems. This suggests that one should find some way to eliminate the costates from the problem. It is possible by formally combining Eqs. (2.1), (3.7) and (3.9), to eliminate the costates and to obtain the equations of optimal states as:

$$\ddot{z} + [DA^TD^{-1} - A]\dot{z} - [DA^TD^{-1}A + DQ]z = 0 \tag{3.18}$$

where

$$D = BR^{-1}B^T \tag{3.19}$$

However, for the mechanical systems defined by Eq. (1.1), matrix D is singular because the top row of matrix B defined by Eq. (2.3) is *zero* and consequently Eq. (3.18) cannot be used.

3.6.1 New Form of Optimality Equation

As mentioned above the optimality conditions can be derived in terms of the states only, however, Eq. (3.18) is useless for mechanical systems due to the singularity of term D. However, singularity can be removed provided the costates related to the displacement, p_d, are considered separately from the costates related to the velocity, p_v [Szyszkowski, W., and Hoetzel, M., 1999; Szyszkowski, W. and Grewal, I. S., 2000, 2002].

The costate vector can be decomposed into:

$$p = \begin{bmatrix} p_d \\ p_v \end{bmatrix} \tag{3.20}$$

Now, using the degrees of freedom $x(t)$, instead of the costates $z(t)$, the costate equation, Eq. (3.7), can be rewritten in the form:

$$\dot{p} = \begin{bmatrix} \dot{p}_d \\ \dot{p}_v \end{bmatrix} = -\frac{\partial H}{\partial x} = Qx - A^T p \tag{3.21}$$

$$= \begin{bmatrix} Q_d x + [M^{-1}K]^T p_v \\ Q_v \dot{x} - p_d + [M^{-1}C]^T p_v \end{bmatrix} \tag{3.22}$$

The optimal control force from Eq. (3.9) becomes:

$$F_c = R^{-1} M^{-1} p_v \tag{3.23}$$

Note that the set of $3n$ equations comprising of Eqs. (1.1) and (3.22) contain three sets of variables x, p_d, p_v with n components each. After long but straightforward transformations the costates p_d and p_v can be written in terms of x as:

$$p_d = Q_v \dot{x} - MR[M\dddot{x} + C\ddot{x} + K\dot{x}] + [M^{-1}C]^T MR[M\ddot{x} + C\dot{x} + Kx] \tag{3.24}$$

$$p_v = MR[M\ddot{x} + C\dot{x} + Kx] \tag{3.25}$$

Finally, eliminating the costates and using the symmetry of *K, C* and *M* one obtains the optimality equation in a new form.

$$MRM\ddddot{X} + [2KRM - Q_v - CRC]\dddot{X} + [KRK + Q_d]\ddot{X} = 0 \tag{3.26}$$

The boundary conditions for the equations are the same as given by Eq. (3.27)

$$x(0) = x_0, \frac{dx}{dt}(0) = \dot{x}_0 \text{ and } x(t_f) = x_f, \frac{dx}{dt}(t_f) = \dot{x}_f \tag{3.27}$$

This approach formulates problems of optimal control in the form of a set of *n* fourth order equations (3.26). Together with the boundary conditions (3.27) it constitutes a well defined TPBV problem.

If the maneuver time is also optimized, then the target condition (3.11) must be satisfied. The Hamiltonian (3.6), using (3.21) and (3.22) can be now derived in terms of DOF's and its derivatives as:

$$
\begin{aligned}
H(t_f) &= -\frac{1}{2} x_f^T Q_d x_f - \frac{1}{2} \dot{x}_f^T Q_v \dot{x}_f - \frac{1}{2}\Gamma \\
&- \frac{1}{2}(2\dddot{x}_f^T MRM \dot{x}_f - \ddot{x}_f^T (MRM \ddot{x}_f + MRC \dot{x}_f \\
&- 2CRM \dot{x}_f - MRKx_f) + \dot{x}_f^T (CK^{-1} M \ddot{x}_f \\
&- 2MK^{-1} C \ddot{x}_f + 2M\dot{x}_f - CK^{-1} C\dot{x}_f + Cx_f) \\
&- x_f^T (M\ddot{x}_f + C\dot{x}_f + Kx_f))
\end{aligned}
\tag{3.28}
$$

For the final boundary conditions in the form $x_f = \dot{x}_f = 0$, the target condition is reduced to:

$$
2H(t_f) = \ddot{x}_f{}^T MRM \ddot{x}_f - \Gamma = 0 \tag{3.29}
$$

3.6.2 Similarity between the New Form of Optimality Equation and Problems in the Finite Element Method

As mentioned before (chapter 1 section 1.2) FEM essentially solves a problem of ordinary or partial differential equations in the spatial domain with the given boundary conditions or the so-called boundary value problem.

The TPBV optimal control problem deals in the same way with the boundary value problem in the time domain. This clearly means one can form some kind of analogy between optimal control problems and problems in the FEM.

The ODE (3.26) with conditions (3.27) forms the boundary value problem of the fourth order and can formally be handled by the FEM with C^1 class elements in the time domain. Such time elements would provide the inter-elemental continuity of the velocity field in the dynamic considerations. It should also be noted that due to the presence of only even derivatives in Eq. (3.26), the corresponding stiffness matrices (which can be derived by applying the Galerkin formula) in the *FE* formulation will be symmetric. Once

the optimal vector $x(t)$ is determined from (3.26), the control forces $F_c(t)$ can be calculated directly from the equation of motion, Eq. (1.1).

Before further discussion of the analogy between the FEM problems and optimal control problems, and the new methodology based on this analogy, a brief review of the literature pertaining to the optimal control of structures is presented.

3.7 Literature Review

A large number of research papers and books covering various aspects of optimal control have been published in recent years. The topics considered here are categorized into two groups. The review section 3.7.1, briefly describes the research that has been published in the area for open loop optimal control problems and then in section 3.7.2, the research that has been published in the field of closed loop optimal control problems.

3.7.1 Review for Open Loop Control Problems

The problem of optimal control of structural vibrations, containing a linear set of the state equations and a quadratic performance index, is usually formulated as the so-called linear-quadratic regulator problem [Takahashi, Y. and Robins, M. J., and Auslander, D.M., 1972]. The optimality equations for such a problem can be derived in the form of Eq. (3.7) and (3.10). The solutions to the optimality equations may theoretically be obtained in the form of matrix exponentials [Athans, M. and Falb, P.L., 1966]. Also, the set of ODE representing the optimality conditions can be transformed into various forms of the matrix Riccati equations [Junkins, J.L. and Kim, Y., 1993]. However, either the matrix exponentials or the Riccati equations are generally difficult to handle numerically, especially for the problems with a finite duration of the optimal control process for which the Riccati equations are differential ones.

Optimal control of structures has been analyzed numerically mostly by the parametric optimization approach combining the software for mathematical optimization, control, and structural analysis. For example, a package integrating the NEWSUMT-A (gradient based optimization technique) with ORACLS (optimal control of linear systems) software was applied to analyze optimal control of a large space structure in [Fonseca, I.

and Bainum; Fonseca, Ijar M., Bainum, Peter, M. and Paulo Lourenção, T. M., 2002]. The parametric optimization approach and the well-known Davidon-Fletcher-Powell variable metric algorithm were used in [Abdullah, M.M., 1998], with the performance index directly minimized in terms of the assumed gains and the placement of actuators and sensors. Due to the necessity of repetitive evaluations of the objective and its derivatives in terms of a large number of parameters, the use of parametric optimization and general-purpose optimization software is usually computationally intensive; a super computer and a parallel algorithm were used in [Saleh, A. and Adeli, H., 1999].

The optimal control problems become more tractable if the Independent Modal Space Control (IMSC) approach is applied [Meirovitch, L. and Baruh, H., 1982; Lin, Y.H., 1989]. In such an approach a particular vibration mode can be handled independently from the other modes. Also, the concept of independent modal controls to be 'coupled' with the corresponding mode of vibrations is introduced. As a consequence the corresponding Riccati equations decouple. For steady state time-invariant cases these equations can be derived as a set of independent second order algebraic equations whose solutions are available in closed forms. However, if the control's duration cannot be assumed infinite (as is the case for the time-invariant problems), the methods based on Riccati's equations are much less convenient to use. If the number of modes is the same as of the number of actuators, the modal controls results can be easily converted into the forces in the actuators.

Following the modal controls concept the corresponding physical modal actuators made of thin laminate piezoelectric materials have been constructed [Kim, S.J., Hwang, J.S., and Mok, J., 2000; Kim, J., Hwang J.S. and Kim, S.J., 2001]. Standard parametric optimization and a genetic algorithm were used to obtain the optimal shape of the laminate, lamination angles, and the electrode patterns.

The motion of an actively controlled structure is governed by the set of 1^{st} order ODE representing the optimality equations, which with the given initial and final conditions creates a boundary value problem in the time domain. Theoretically, such a problem should be tractable by the FEM approach with the domain divided into proper one-dimensional *time elements*.

Unfortunately, in several attempts reported in the literature, the FEM methodology and discretization of the time domain were applied to rather inconvenient formulations of the TPBV problems. For example, in [Hodges, D. H. and Bless, R. R., 1991; Warner, M. S. and Hodges D. H., 2000] the FEM was used directly to the variational forms, which were equivalent to solving the optimality equations in the standard form of the first order ODE Eq. (3.7) and (3.10). Such a formulation the optimality equations contain the states and costates, while the initial and final boundary conditions are imposed on the states only. While the approach used was quite general and applicable to nonlinear problems, the required manipulations on 'time elements', and the method of imposing the boundary conditions posed a challenge. The 'time elements' with linear approximation functions were used in [Hodges, D. H. and Bless, R. R., 1991], while higher order polynomials were proposed in [Warner, M. S. and Hodges D. H., 2000]. The approach was not used for controlling structures.

An iterative procedure to tackle the linear-quadratic regulator by the FEM was reported in [Zhong, W., Lin, J. and Qiu, C., 1992]. In that paper an iterative solution of the optimality equations represented by the Riccati equations was attempted, however, no particular optimal control problem was solved. A serious disadvantage of such an approach is that the matrix Riccati equation is non linear (despite the state and costate equations being linear for the linear-quadratic regulator problems) and generally difficult to handle numerically.

3.7.2 Closed Loop Control Problems

Optimal gains for active vibration attenuation can be determined by solving the corresponding Riccati equations for the problem in the form of coupled non-linear matrix equations [Junkins, J.L. and Kim, Y., 1993; Saleh, A. and Adeli, H., 1999]. Although several iterative algorithms have been proposed to get optimal gains from these equations, ‘the solutions of the Riccati equation are the most time-consuming part of any optimal control problem’ ([Saleh, A. and Adeli, H., 1999], p. 109). Besides being very intensive numerically these algorithms ‘do not universally guarantee stable and accurate computation’ ([Junkins, J.L. and Kim, Y., 1993], p. 248).

Potter's method was used in [Wang, S. Y., Quek, S. T. and Ang, K. K., 2001] to obtain the optimal gains for control of piezoelectric plates. In such a method the gains are determined by first solving the complex eigenvalue problem of an asymmetric matrix (referred to as Hamiltonian's matrix) formed of the matrices defining the states and the performance index (weighting matrices).

A different approach, in which the gains are iteratively improved, was proposed in [Levine, W. S. and Athans M., 1970]. However, the corresponding algorithm is essentially intuitive without a proof of convergence. The approach was somewhat refined in [Mendel, J. M., 1974].

Optimal gains can also be calculated by using the parametric optimization techniques. In such an approach first the controls and then the states are expressed in terms of gains and substituted into the performance index. Next, treating the gains as the optimization variables, the performance is gradually improved until the minimum is reached [Preumont, A., 2002]. A genetic algorithm was used for that purpose in [He, Y. P., McPhee, J., 2002], while gradient-based algorithms were applied in [Kelkar, A. G., Mao Y., Joshi and S. M., 2001; Choi, S. S. and Sirisena, H. R., 1977; Moerder, D. D. and Calise, A. J., 1985]. The above approach is numerically very intensive. In order to facilitate its convergence, various auxiliary optimality conditions were derived and used as extra constraints while minimizing the performance. The constrained optimization process was converted into an unconstrained one by using either the Lagrange multipliers [Kelkar, A. G., Mao Y., Joshi and S. M., 2001; Moerder, D. D. and Calise, A. J., 1985], or a penalty method [Choi, S. S. and Sirisena, H. R., 1977].

The concept of independent modal-space control (IMSC) methodology was used in [Meirovitch, L. and Baruh, H., 1982] in which the gains for each independent mode are calculated explicitly. The weighting matrices, however, had a special form (the control weighting matrix was diagonal and one term was infinite), for which Riccati's equations were solved analytically.

From the above discussion it can be concluded that there are several approaches to solve optimal control problems but none of them used the FEM (at least not efficiently) to get optimal actuator forces, maneuver and constant feedback gains. This shows the

motivation, which compelled this research to find a new methodology to be referred to as the *beam analogy*.

How to change the form of the optimality equation (3.26) with the BCs (3.27) to make it suitable to be solved by the FEM is presented next.

Chapter 4. A Beam Analogy Approach

It should be noted that applying the FE method directly to n coupled components of vector $x(t)$ in Eq. (3.26) would be challenging. For example, if the time domain is discretized into m time elements, then one has to deal with $n \times m$ DOF in the space-time domain. Also, the bandwidth of matrices in Eq. (3.26) becomes approximately m times larger than the bandwidth of matrices in Eq. (1.1), which makes its direct solution very difficult.

In the next section it is shown how to decouple these equations and solve them by the FEM.

4.1 The Modal Space

Certain problems of the transient dynamics are solved very effectively by the FEM if the modal space is used. In such a space the set of Eq. (1.1) with coupled DOF is converted into a set of equations with separated modes. By doing so one can deal with each mode independently in the FEM software. The modal frequencies, ω_i and the corresponding modal shapes, Φ_i of the system given by Eq. (1.1), are obtained by solving the eigenvalue problem:

$$(K - \omega_i^2 M)\Phi_i = 0\,,\ i = 1,...,n \tag{4.1}$$

The eigenmodes, Φ_i, are orthogonal and normalized in such a way that

$$\Phi_i^T M \Phi_j = \delta_{ij} \text{ and } \Phi_i^T K \Phi_j = \omega^2{}_i \delta_{ij} \tag{4.2}$$

where $\delta_{ij} = \begin{matrix} 1 & if\ i = j \\ 0 & if\ i \neq j \end{matrix}$

The normalized eigenmodes are assembled into the transformation matrix as:

$$\Phi = \left[\Phi_1, \Phi_2, ..., \Phi_n\right]_{n \times n} \tag{4.3}$$

Matrix Φ is used to relate the DOF vector x to the modal co-ordinates vector η:

$$x = \Phi \eta \tag{4.4}$$

Since $\eta = \Phi M x$, the initial conditions that are given by $x(0) = x_0$ and $\dot{x}(0) = \dot{x}_0$ can be transformed into the initial values for modal variables $\eta(0) = \eta_o$ and $\dot{\eta}(0) = \dot{\eta}_o$.

Substituting Eq. (4.4) into Eq. (1.1) and pre-multiplying by Φ^T one obtains:

$$\Phi^T M \Phi \ddot{\eta} + \Phi^T C \Phi \dot{\eta} + \Phi^T K \Phi \eta = \Phi^T F \tag{4.5}$$

If the Rayleigh damping is assumed i.e. $C = \alpha_c M + \beta_c K$ then:

$$\Phi_i^T C \Phi_i = \Phi_i^T [\alpha_c M + \beta_c K] \Phi_i = \Delta_{ii} = \alpha_c + \beta_c \omega^2{}_i = 2\omega_i \xi_i \tag{4.6}$$

Thus, using Eqs. (4.2) and (4.6), Eq. (4.5) is transferred into:

$$I\ddot{\eta} + \Delta\dot{\eta} + \Omega\eta = U \tag{4.7}$$

where I is an identity matrix of dimension $n \times n$ and matrices Δ and Ω are diagonal with terms:

$$\Delta_{ii} = \alpha_c + \beta_c \omega^2{}_i = 2\omega_i \xi_i,\ \Omega_{ii} = \omega^2{}_i, i = 1,...,n \tag{4.8}$$

where ξ_i represents the modal damping ratio.

The modal forces are defined as:

$$U = \Phi^T F \tag{4.9}$$

Since all matrices in Eq.(4.7) are diagonal each mode must satisfy the equation

$$\ddot{\eta}_i + 2\omega_i \xi \dot{\eta}_i + \omega_i^2 \eta_i = U_i \qquad i = 1....s.....n \tag{4.10}$$

Typically only $s << n$ modes are needed to simulate the structure's dynamics accurately. This is used in the mode superposition method to efficiently run the transient dynamic FEM analysis of the model with even very large numbers of DOF.

The modal variables that decoupled Eq. (1.1) can be used in a similar manner to decouple the optimality equation given by Eq. (3.26). In the modal space Eq. (4.7) represents the equation of motion equivalent to Eq. (1.1). Consequently, Eqs. (2.1) can be rewritten in this space as:

$$\dot{z} = \hat{A} z + \hat{B} U \tag{4.11}$$

where $z_i = \eta_i$ and $z_{n+i} = \dot{\eta}_i$, $i = 1,...,n$ and $U = \Phi^T F_c = \Phi^T B_a F_a$

Here vector $F_c(t)$ is assumed to be uniquely determined in terms of n_a independent actuator forces vector (F_a), and the placement matrix B_a (dimension $m \times n_a$) as:

$$F_c = B_a F_a \tag{4.12}$$

Matrices $\hat{A}$ and $\hat{B}$ assume the form:

$$\hat{A} = \begin{bmatrix} 0 & I \\ -\Omega & -\Delta \end{bmatrix}_{2n\times 2n} \tag{4.13}$$

$$\hat{B} = \begin{bmatrix} 0 \\ I \end{bmatrix}_{2n\times n} \tag{4.14}$$

Similarly, substituting Eq. (4.4) in to Eq. (3.4), the performance index in the modal space is transformed into:

$$J = 1/2\int_0^{t_f} [\eta^T \Phi^T Q \Phi \eta + U^T [(\Phi^T)^{-1}]^T R (\Phi^T)^{-1} U + \Gamma] dt \tag{4.15}$$

$$= 1/2\int_0^{t_f} [\eta^T \Phi^T Q_d \Phi \eta + \dot{\eta}^T \Phi^T Q_v \Phi \dot{\eta} U^T [(\Phi^T)^{-1}]^T U^T [\Phi^T R^{-1} \Phi]^{-1} U + \Gamma] dt \to \min \tag{4.16}$$

The following transformed weighting matrices are introduced:

$$\hat{Q} = \begin{bmatrix} \hat{Q}_d & \\ & \hat{Q}_v \end{bmatrix}_{2n\times 2n} = \begin{bmatrix} \Phi^T Q_d \Phi & \\ & \Phi^T Q_v \Phi \end{bmatrix}_{2n\times 2n} \tag{4.17}$$

$$\hat{R} = [\Phi^T R^{-1} \Phi]_{n\times n}^{-1} \tag{4.18}$$

The performance index can be re-written in the form:

$$J = 1/2\int_0^{t_f} [\eta^T \hat{Q}_d \eta + \dot{\eta}^T \hat{Q}_v \dot{\eta} + U^T \hat{R} U + \Gamma] dt \to \min \tag{4.19}$$

The Hamiltonian in Eq. (3.6) transforms into:

$$H = -1/2(\eta^T \hat{Q} \eta + U^T \hat{R}_c U + \Gamma) + p^T (\hat{A}\eta + \hat{B}U) \to \min \tag{4.20}$$

The set of Eqs. (3.7)-(3.9) now become:

$$\dot{p} = -\frac{\partial H}{\partial \eta} = \hat{Q}\eta - \hat{A}^T p \tag{4.21}$$

$$\frac{\partial H}{\partial U} = -\hat{R}U + \hat{B}^T p = 0 \tag{4.22}$$

$$U = \hat{R}^{-1}\hat{B}^T p \tag{4.23}$$

Additionally, the target condition Eq. (3.11) becomes:

$$H(t_f) = -\frac{1}{2}[\eta^T \hat{Q}\eta + U^T \hat{R}U + \Gamma] + p^T[\hat{A}\eta + \hat{B}U] = 0 \tag{4.24}$$

Similarly as before, separating the costates according to Eq. (3.20) one obtains:

$$\dot{p} = \begin{bmatrix} \dot{p}_v \\ \dot{p}_d \end{bmatrix} = -\frac{\partial \hat{H}}{\partial \eta} = \hat{Q}\eta - \hat{A}^T p = \begin{bmatrix} \hat{Q}_d \eta + \Omega p_v \\ \hat{Q}_v \dot{\eta} - p_d + \Delta p_v \end{bmatrix} \tag{4.25}$$

Equations (3.23)-(3.25) now become:

$$U = \hat{R}^{-1} p_v \tag{4.26}$$

$$p_d = \hat{Q}_v \dot{\eta} - \hat{R}[I\ddot{\eta} + \Delta\dot{\eta} + \Omega\eta] + \Delta\hat{R}[I\dot{\eta} + \Delta\eta + \Omega\eta] \tag{4.27}$$

$$p_v = \hat{R}[I\dot{\eta} + \Delta\eta + \Omega\eta] \tag{4.28}$$

Eliminating costates one gets the new form of the differential equation, Eq.(3.26), representing the optimal control problem in the modal space as:

$$\hat{R}\dddot{\eta} + [2\Omega\hat{R} - \hat{Q}_v - \Delta\hat{R}\Delta]\ddot{\eta} + [\Omega\hat{R}\Omega + \hat{Q}_d]\eta = 0 \qquad i = 1...n \tag{4.29}$$

The boundary conditions for the maneuver now transform to:

$$\eta(0) = \eta_0, \frac{d\eta}{dt}(0) = \dot{\eta}_0 \quad \text{and} \quad \eta(t_f) = \eta_f, \frac{d\eta}{dt}(t_f) = \dot{\eta}_f \tag{4.30}$$

The target condition in the modal space is:

$$\begin{aligned} H(t_f) = & -\frac{1}{2}\eta_f^T \hat{Q}_d \eta_f - \frac{1}{2}\dot{\eta}_f^T \hat{Q}_v \eta_f - \frac{1}{2}\Gamma \\ & - \frac{1}{2}(2\ddot{\eta}_f^T \hat{R}\dot{\eta}_f - \ddot{\eta}_f^T(\hat{R}\ddot{\eta}_f + \hat{R}\Delta\dot{\eta}_f \\ & - 2\Delta\hat{R}\dot{\eta}_f - \hat{R}\Omega\eta_f) + \dot{\eta}_f^T(\Delta\Omega^{-1}\ddot{\eta}_f \\ & - 2\Omega^{-1}\Delta\ddot{\eta}_f + 2\dot{\eta}_f - \Delta\Omega^{-1}\Delta\dot{\eta}_f + \Delta\eta_f) \\ & - \eta_f^T(I\ddot{\eta}_f + \Delta\dot{\eta}_f + \Omega\eta_f)) \end{aligned} \tag{4.31}$$

For zero final boundary conditions i.e. $\eta_f = \dot{\eta}_f = 0$ in modal space the target condition will again reduce to:

$$2H(t_f) = \ddot{\eta}_f^T \hat{R}\ddot{\eta}_f - \Gamma = 0 \tag{4.32}$$

Having determined vector $\eta(t)$ from (4.32), the modal controls $U(t)$ can be found from (4.10).

Thus switching of the real space coordinates x into the modal space coordinates η, results in the following transformations:

$$M \to I, C \to \Delta, K \to \Omega, F_c \to U, Q \to \hat{Q}, R \to \hat{R} \tag{4.33}$$

whether the new matrices $\hat{Q}_d$, $\hat{Q}_v$ and $\hat{R}$ are diagonal or not, depends only on the form of matrices Q, R, M, K, C and Φ. However M, K, C and Φ are related through Eq. (4.2) and (4.6). In general, matrices $\hat{Q}_d$, $\hat{Q}_v$ and $\hat{R}$ become diagonal if the weighting matrices Q and R in performance index, Eq.(3.2) are assumed in the form:

$$Q = \begin{bmatrix} Q_d & \\ & Q_v \end{bmatrix}_{2n\times 2n} = \begin{bmatrix} \alpha_1 M + \alpha_2 K + \alpha_3 C & \\ & \beta_1 M + \beta_2 K + \beta_3 C \end{bmatrix}_{2n\times 2n} \tag{4.34}$$

$$R = [\gamma_1 M + \gamma_2 K + \gamma_3 C]^{-1}_{n\times n} \tag{4.35}$$

where $\alpha_1, \alpha_2, \alpha_3, \beta_1, \beta_2, \beta_3, \gamma_1, \gamma_2$ and γ_3 are constants.

Substituting Eq. (4.34) into Eq. (4.17) and using Eqs. (4.2) and (4.6) it is easy to obtain the diagonal terms of the positive definite matrices in the form:

$$\hat{Q}_{iid} = \alpha_1 + \alpha_2\omega_i^2 + 2\alpha_3\omega_i\xi_i \,,\; \hat{Q}_{iiv} = \beta_1 + \beta_2\omega_i^2 + 2\beta_3\omega_i\xi_i \tag{4.36}$$

Similarly, substituting Eq. (4.35) into Eq. (4.18) and using Eqs. (4.2) and (4.6) diagonal terms for positive matrix $\hat{R}_{ii}$ take the following form:

$$\hat{R}_{ii} = (\gamma_1 + \gamma_2\omega_i^2 + 2\gamma_3\omega_i\xi_i)^{-1} \tag{4.37}$$

Substituting Eqs. (4.36) and (4.37) into Eq. (4.29) one obtains the decoupled optimality equation for each mode respectively [Szyszkowski, W. and Grewal, I. S., 2000, 2002]:

$$\hat{R}_{ii}\ddot{\eta}_i + [2\Omega_{ii}\hat{R}_{ii} - \hat{Q}_{viii} - \Delta_{ii}\hat{R}_{ii}\Delta_{ii}]\dot{\eta}_i + [\Omega_{ii}\hat{R}_{ii}\Omega_{ii} + \hat{Q}_{dii}]\eta_i = 0 \qquad i = 1...n \tag{4.38}$$

4.2 Analogy with the Beam Equation

Here it is shown how Eq. (4.38) is solved in the time domain by using the static beam equation. This equation is normally used to calculate the deflections, slopes, bending moments and shear forces of beams in the spatial domain. The static beam will be referred to as the analogous beam and will be used in optimal vibration control to determine the positions and velocities imposed by optimal control forces on the structure in the time domain.

Consider small static deflections of a beam of length L_i and bending stiffness EI_i Supported on elastic foundations of stiffness K_{fi}. The beam can be loaded only at both ends by bending moments M_{oi} and M_{fi}, shear forces T_{oi} and T_{fi} at both the ends, and axial forces P_i (compressive force is assumed positive).

The deflection in the beam is governed by the well-known fourth order differential equation:

$$EI_i \frac{d^4 v_i}{dy^4} + P_i \frac{d^2 v_i}{dy^2} + k_{fi} v_i = 0 \tag{4.39}$$

The geometrical boundary conditions are in the form:

$$v_i(0) = v_{i0}, \frac{dv_i}{dy}(0) = \theta_{i0} \quad \text{and} \quad v_i(L_i) = v_{if}, \frac{dv_i}{dy}(L_i) = \theta_{if} \tag{4.40}$$

Using the sign convention indicated in Figure 4.1, the bending moment and shear force in the beam are:

$$M_{bi} = EI_i \frac{d^2 v_i}{dy^2} \text{ and } T_i = EI_i \frac{d^3 v_i}{dy^3} \tag{4.41}$$

The problem defined by Eqs. (4.39) and (4.40) can routinely be solved by applying any structural FEM software, which provide a beam element that includes the elastic foundation stiffness. In the ANSYS software this beam problem is solved by using beam element called BEAM54 (the solution technique is explored in section 4.3).

The FEM solution provides all the information about the deflection, slope, bending moments and the shear forces at the nodal points. Thus the above beam bending problem can be solved completely with little effort if only the length L_i, the bending stiffness EI_i, the axial force P_i, the elastic foundation stiffness k_{fi}, and, the boundary conditions (4.40) are known.

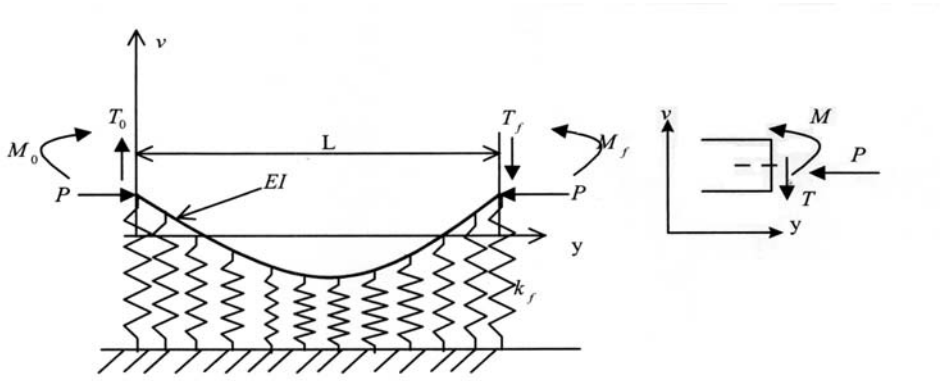

Figure 4.1 Beam on Elastic Foundation

Comparing Eq. (4.38) and Eq. (4.39) one to one correspondence is obtained between the independent modes (representing the optimal control problem) and the set of independent beams (representing the static beam problem) [Szyszkowski, W. and Grewal, I. S., 2000, 2002]. These are:

$$v_i \equiv \eta_i ,$$

$$EI_i \equiv \frac{1}{\gamma_1 + \gamma_2 \omega^2{}_i + \gamma_3 2\omega_i \zeta_i} ,$$

$$P_i \equiv \left[2\omega^2{}_i \frac{1}{\gamma_1 + \gamma_2 \omega^2{}_i + \gamma_3 2\omega_i \zeta_i} - \left(\beta_1 + \beta_2 \omega^2{}_i + \beta_3 2\omega_i \zeta_i \right) + \left(4\zeta^2{}_i \omega^2{}_i \frac{1}{\gamma_1 + \gamma_2 \omega^2{}_i + \gamma_3 2\omega_i \zeta_i} \right) \right],$$

$$k_{f_i} \equiv \left[\omega^4{}_i \frac{1}{\gamma_1 + \gamma_2 \omega^2{}_i + \gamma_3 2\omega_i \zeta_i} + \left(\alpha_1 + \alpha_2 \omega^2{}_i + \alpha_3 2\omega_i \zeta_i \right) \right] \qquad \text{(4.42-a,b,c,d)}$$

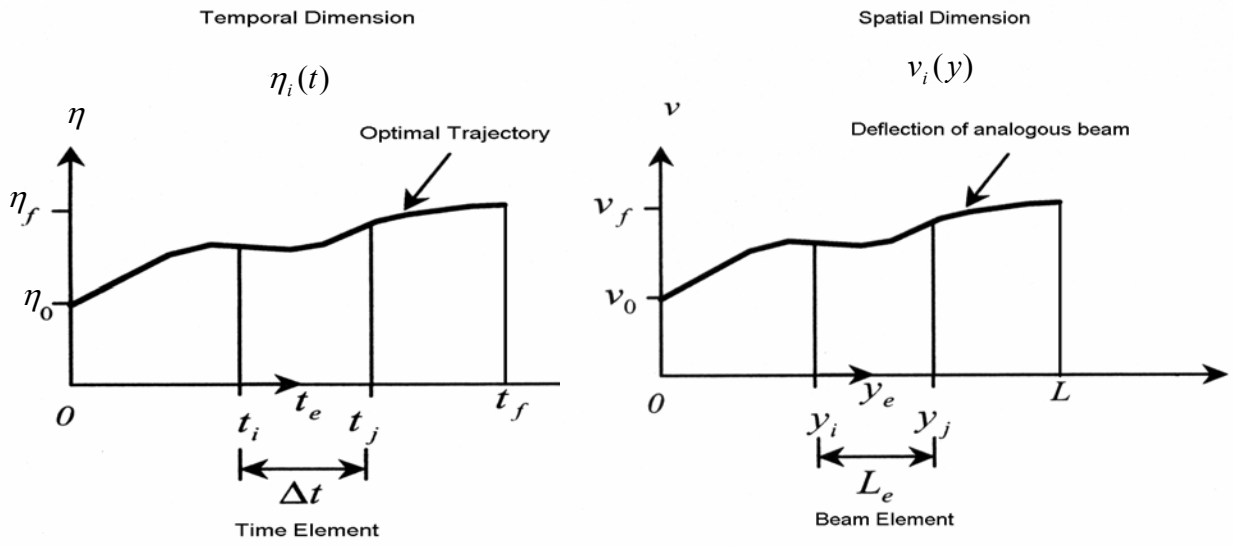

Figure 4.2 Presentation of Temporal and Spatial Domain

The analogy and the corresponding domains are shown in Figure 4.2. In particular, if numerically $L = t_f$ then the deflection of analogous beam $v_i(y),\ 0 \le y \le L$ is numerically equal to $\eta_i(t), \text{for } 0 \le t \le t_f$. Then the motion of the controlled structure can be obtained from:

$$x(x,t) = \sum \Phi_i(x)\eta_i(t) \tag{4.43}$$

All modal functions and their derivatives have simple interpretations in terms of analogous beams parameter namely:

$$\eta_i \equiv v_i, \quad \dot{\eta}_i \equiv \theta_i, \ddot{\eta}_i \equiv \frac{M_{bi}}{EI_i} \text{ and } \dddot{\eta}_i \equiv \frac{T_i}{EI_i} \tag{4.44}$$

The modal control parameter can be derived in terms of the beam parameter as:

$$U_i(M_{bi},\theta_i,v_i) \equiv \frac{M_{bii}}{EI_i} + 2\omega_i\xi_i\theta_i + \omega^2{}_i v_i \tag{4.45}$$

Having determined the modal vector U, the control force in Eq. (4.9) can be calculated from:

$$F_c = \tilde{\Phi}^{-1}U \tag{4.46}$$

where $\widetilde{\Phi} = \Phi^T B_a$

Here the IMSC approach is used in which n_a actuators control $s = n_a$ modes so that the dimension of the $\Phi^T B_a$ is $s \times s$ and where B_a is the placement matrix explained in section 4.1 Eq. (4.12).

As an illustration, suppose there are $n_a = 2$ actuators and they are acting in one direction (vertical) on two different nodes on the structure in chapter 5 Figure 5.2. Then matrix B_a will have a *unit* value for each node (in the vertical direction) and *zero* for the rest. This matrix B_a will be of dimension $n \times n_a$ and will reduce the dimension of $\widetilde{\Phi}$ to $n_a \times n_a$ i.e. 2×2.

The characteristics of matrix $\widetilde{\Phi}$ reflect controllability of the system, which measures the particular actuator input configuration's ability to obtain the information needed to estimate all system states. A simple way to think about controllability is as a measure of the performance of the actuators to control the structure at a particular placement. In our case, a system is said to be completely controllable if the inverse of $\widetilde{\Phi}$ exists.

Finally the target condition $H(t_f)$ in terms of the beam's parameter for zero final boundary conditions ($v_f = 0$ and $\theta_f = 0$) is calculated as:

$$2H(t_f) = \sum_{i=1}^{n} \frac{1}{c_1 + c_2 \omega^2{}_1 + c_3 2\omega_i \zeta_i} \left[\frac{M_{bi}}{EI_i} \right]^2 - \Gamma = 0 \qquad (4.47)$$

Thus, the length of the analogous beams representing the optimal maneuver must be such that the moments at the ends satisfy the above equation. Note that if $\Gamma = 0$, the sum of the moments M_{bi} (at the end *y = L)* of each beam must vanish.

4.3 Solving the Analogous Beams by the FEM

Bending of beams is conveniently solved in the FEM by using Hermitian polynomials as interpolation functions. The beam equation, Eq. (4.39) is converted into:

$$K^e d^e = [K_e^e - K_g^e + K_f^e][d^e] = [F^e] \qquad (4.48)$$

where:

$$K_e^e = \frac{EI}{L_e^3}\begin{bmatrix} 12 & 6L_e & -12 & 6L_e \\ & 4L_e^2 & -6L_e & 2L_e^2 \\ & & 12 & -6L_e \\ & & & 4L_e^2 \end{bmatrix} \tag{4.49}$$

$$K_g^e = \frac{EI}{L_e^3}\begin{bmatrix} \frac{36}{L_e} & 3 & -\frac{36}{L_e} & 3 \\ & 4L_e & -3 & -L_e \\ & & -\frac{36}{L_e} & -3 \\ & & & 4L_e \end{bmatrix} \tag{4.50}$$

$$K_f^e = k_f L_e\begin{bmatrix} \frac{13}{35} & \frac{11L_e}{210} & \frac{9}{70} & -\frac{13L_e}{420} \\ & \frac{L_e^2}{105} & \frac{13L_e}{420} & -\frac{L_e^2}{420} \\ & & \frac{13}{35} & -\frac{11L_e}{210} \\ & & & \frac{L_e^2}{105} \end{bmatrix} \tag{4.51}$$

The element deflection vector is defined as:

$$(d^e)^T = [v_i \quad \theta_i \quad v_j \quad \theta_j] \tag{4.52}$$

and the element forces vector is:

$$(F^e)^T = \left[T_i + P\frac{dv_i}{dx} \quad -M_{bi} \quad -T_j - P\frac{dv_i}{dx} \quad M_{bj}\right] \tag{4.53}$$

The length of the beam element is denoted by L_e and would correspond to the time increment Δt if Eq. (4.26) were explicitly integrated in time.

After assembling Eq. (4.52), the global deflection vector representing the deflection and slope at all nodes can be written in the form:

$$(d)^T = [d_0 \quad d_1 \quad d_L] \tag{4.54}$$

where $(d_0)^T = [v_0 \quad \theta_0]$ and $(d_L)^T = [v_L \quad \theta_L]$ are given by the initial and final conditions. Vector d_1 represents the slope and deflection at the inside nodes of the beam. According to the analogy outlined in the previous sections, the inside nodes are not loaded. Therefore, all components of *F* corresponding to d_1 are zero. The global stiffness

matrix can be decomposed into the matrices corresponding to d_0, d_1 and d_L respectively and the governing equations for the whole beam system can be written in the form:

$$\begin{bmatrix} K_0 & K_{01} & K_{02} \\ K_{01}^T & K_1 & K_{10} \\ K_{02}^T & K_{10}^T & K_{Ll} \end{bmatrix} \begin{bmatrix} d_0 \\ d_1 \\ d_L \end{bmatrix} = \begin{bmatrix} F_0^e \\ 0 \\ F_L^e \end{bmatrix} \tag{4.55}$$

The unknown values for the nodes between the beam ends are found in terms of the given boundary values from:

$$d_1 = -K_1^{-1}(K_{01}^T d_0 + K_{10} d_L) \tag{4.56}$$

When vector d_1 is calculated, forces F_0^e and F_L^e at both ends of the beam can be found by substituting Eq. (4.55) back into Eq. (4.56). In particular the values of shear forces, T_L, and moments, M_L at each end of beam need to be calculated to evaluate the Hamiltonian at the target condition (see Eq. (4.47)).

4.4 Why use the Beam Analogy?

The beam analogy can be considered as an alternative to the method based on the Riccati equation. The advantage of beam analogy is that most problems can be solved using easily available FEM software. In the next chapter the use of analogous static beams to solve the problems of active optimal vibration control of elastic structures for the open loop controls is discussed. A Beam Analogy Algorithm (BAA) is developed, which can be used to control any number of modes of arbitrary linear elastic structures.

Chapter 5. Open Loop Control

5.1 Introduction

An algorithm that solves open loop optimal vibration attenuation problems for an arbitrary linear structure is presented. The algorithm is referred to as the BAA (Beam Analogy Algorithm), it is based on the beam analogy methodology. The BAA is used to obtain the optimal action of actuators and the corresponding structure's response. Effects of the number of actuators, their placements and the values of optimization parameters are also investigated.

5.2 The Beam Analogy Algorithm

The BAA is a step by step procedure of beam analogy written in an orderly manner to obtain optimal control forces, maneuver time etc. The procedure needs a structural FEM software (the ANSYS program was used) to run the modal analysis of the structure, and to solve the analogous beams problem. The BAA consists of five steps as shown in Figure 5.1. The steps are consecutive, with no looping. Iterations are required only if the maneuver time t_f is also to be determined, in that case then the non linear target condition, i.e. $|H| \le \varepsilon$, is satisfied iteratively in step 3.

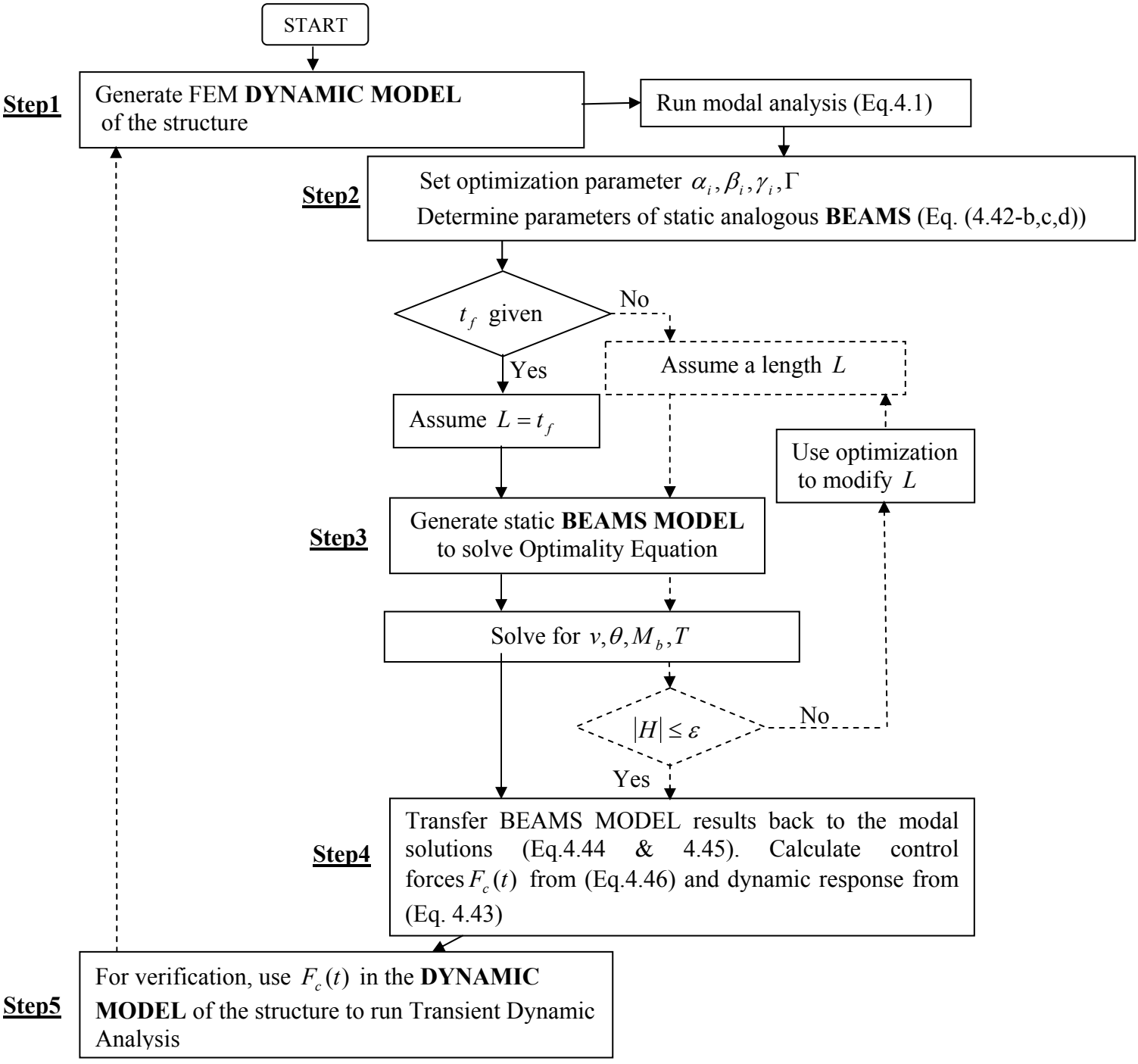

Figure 5.1 Flowchart of the BAA

5.3 Details of the Beam Analogy Algorithm

Step 1

With the help of the finite element software (ANSYS) and using suitable elements, a dynamic model of the continuous structure (to be controlled) is generated. The modal frequencies of this structure are of interest, since the frequency of each mode is used in calculating the beam parameters (beam analogy) and the boundary conditions at both ends.

Step2

Select optimization parameters according to the particular requirement (discussed in the section 5.6). The analogous beam parameters can be obtained from Eq. (4.42-b,c,d). If the time, i.e. length of the beam, is not known in advance then assume some length (very small to avoid missing the first optimal point in the design optimization module of the finite element software; this problem is explained in the chapter 6 section 6.11).

Step3

Create a file (ANSYS codes) to model analogous beams (the number of beams depends on the number of modes to be controlled) using a suitable element (BEAM54) and all boundary conditions in terms of analogous beam parameters (calculated from Eq. (4.42-b,c,d)). The beam length is either known or should be found from the target condition. Run the design optimization module in ANSYS, with L as the only optimization variable, to satisfy the target condition i.e. $|H| \leq \varepsilon$.

Once the analogous beam length i.e. the maneuver time t_f, is known the required variables v, θ, M_b and T can be determined.

Step4

After getting v, θ, M_b and T get the modal solutions, the control forces and the dynamic responses by using Eq. (4.44-4.46) and (4.43).

Step5

Finally, for verification purposes, apply control forces (obtained in Step 4) to the structure (modeled in the step1) and run the dynamic analysis. Step 5 is explained in detail in the section 5.4.2.1 of this chapter.

5.4 Optimal Vibration Control of a 3-D Structure

For demonstration of the BAA consider the elastic aluminium fin as shown in Figure 1.5 section 1.2. In open loop control, control forces depend on the initial configuration of the structure. Hence, a disturbed configuration of the structure is needed. In order to create a disturbed configuration a set of somewhat arbitrary forces are statically applied at several points. These forces are suddenly released at $t = 0$ causing vibrations (Figure 5.2). The actuators are used to bring the structure to a complete rest.

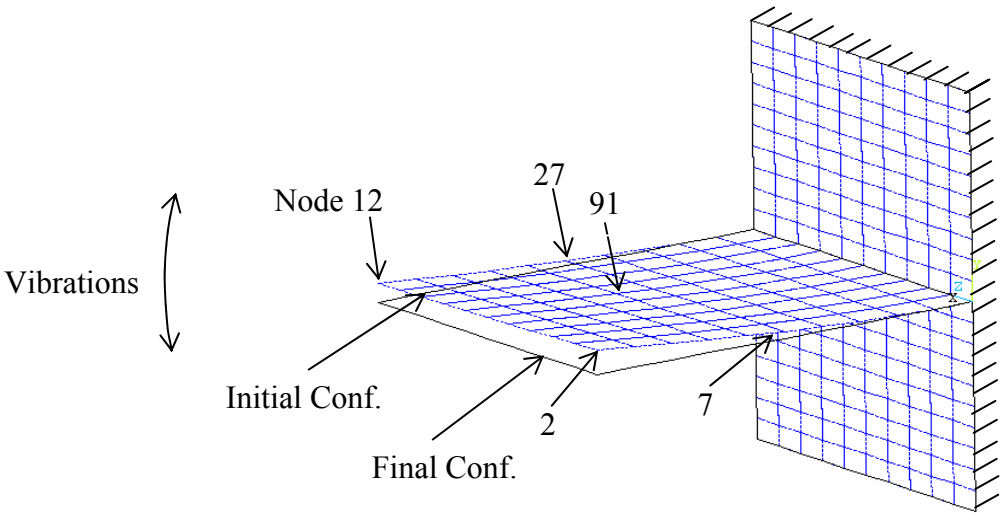

Figure 5.2 Disturbed Structure with Node Locations

Note that vector x has nearly 2000 DOF components and the same number of eigenmodes Φ_i. In reality, higher modes are typically naturally damped due to the presence of some structural damping (related to stresses or environment) therefore these modes have less practical importance and can be neglected. Up to the first four modes of vibration of the structure will be controlled in the simulation presented.

The disturbed configuration is identical for all the control cases considered. Some values of the DOF's for selected nodes are (in meters): $uy_2 = 0.01939$, $uy_7 = 0.005344$, $uy_{12} = 0.01476$, $uy_{27} = 0.003984$, $uy_{91} = 0.006641$. The symbol uy_k denotes the vertical displacements at the k-th node. The nodes location is shown in Figure 5.2.

The modal analysis of the structure is performed in **Step 1** using the DYNAMIC MODEL. The first four vibration modes ($\Phi_1,....,\Phi_4$) are shown in Figure 5.3.

The disturbed configuration can now be defined in terms of the modal variables. Using Eq. (4.4) the initial values of the first four modal variables are:

$\eta_1(0) = 0.05819,\ \eta_2(0) = 0.004670,\ \eta_3(0) = 0.002789,\ \eta_4(0) = 0.0009948.$

Also, $\dot{\eta}_i(0) = 0$, and $\eta_i(t_f) = \dot{\eta}_i(t_f) = 0$ for the final configuration.

This completes **step 1** of the algorithm.

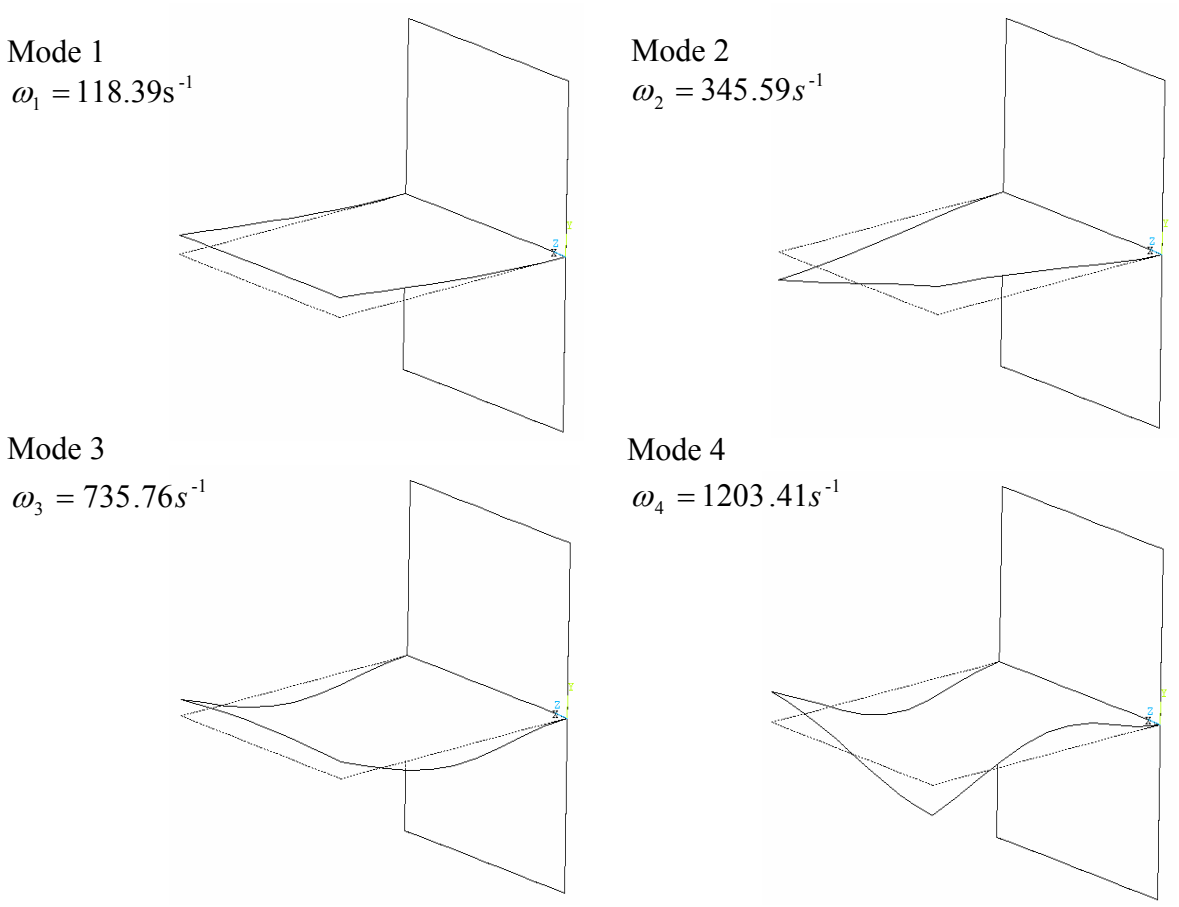

Figure 5.3 Modal Shapes

To initiate **step 2** one has to assume the values of optimization parameters.

The following values were used here: $\alpha_2 = 1,\ \beta_1 = 1,\ \gamma_2 = 0.01$ and $\Gamma = 0.5 Nm$ (the remaining optimization parameters were assumed zero values) resulting in

$$J = 1/2 \int_0^{t_f} [x^T K x + \dot{x}^T M \dot{x} + 100 F_c^T K^{-1} F_c + 0.5] dt \rightarrow \min. \qquad (5.1)$$

In Eq. 5.1 the parameters are selected in such a way that the strain energy, kinetic energy and work of control forces can be dealt with directly. Particular interest is in optimizing the control forces, that is why more weight is given to the control force terms. The convergence parameter for the target condition was $\varepsilon = 10^{-9}$.

Several control cases with different numbers and placements of actuators will be considered. For each case it is assumed that the actuators generate forces that are perpendicular to the horizontal plate. For case 1 the maneuver time t_f is considered unknown.

5.4.1 Case1: Two Actuators (t_f is unknown)

Before moving further an important step is to decide where to place the actuators in order to make the system controllable and also to get maximum control over the disturbed structure. Fortunately following the BAA a different number of locations can be tried and compared. In this example, the actuators are positioned at the two extreme nodes (2 and 12) of the free end of the fin structure to generate two forces F_1 and F_2 (Figure 5.4).

Two fictitious analogous beams are required to analyze the problem. Only two modes of the vibration will be controlled. The parameters of these beams are calculated from Eq. (4.42-b,c,d) and are shown in Figure 5.4.

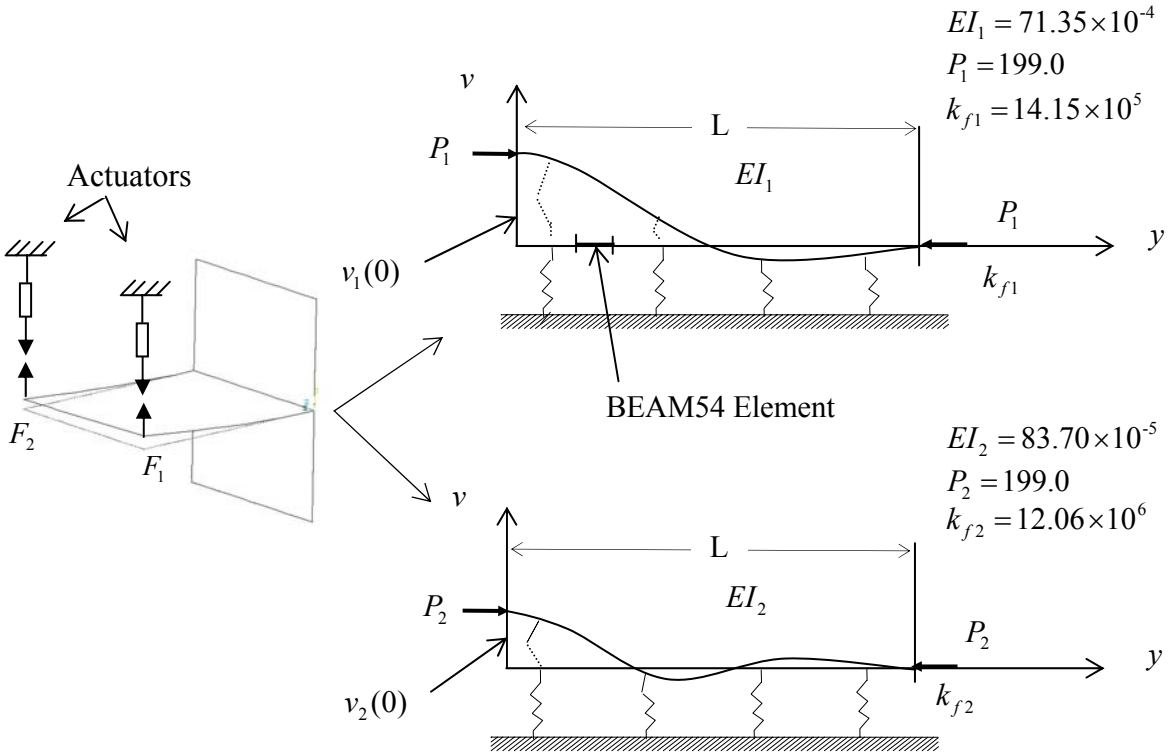

Figure 5.4 Analogous Beams for 2 Actuators

The analogous beams are meshed with 48 BEAM54 elements (comment on the meshing pattern is drawn in the chapter 6 section 6.10) for each beam. Initially the length $L = 0.0025\,m$ was assumed somewhat arbitrarily (it is recommended to start with a small value for L in order to find the smallest root of Eq. (4.47) (see the explanation in chapter 6 section 6.11). The deflections and rotations on the left end of the beams are the same as the initial values of the model variables i.e.: $v_1(0) = 0.05819,\ \theta_1(0) = 0,\ v_2(0) = .004670$ and $\theta_2(0) = 0.$ The beams are then solved by the ANSYS software to obtain deflections, rotations and bending moments in terms of the coordinate *y*. In particular, the value of $M_i(L)$ are obtained and substituted into the target condition, Eq. (4.47). The length L (or the maneuver time t_f) that meets this condition was easily found using the ANSYS optimization routine. After four optimization loops the length was found to be $L = 0.05301\,m,$ which corresponds to $t_f = 0.05301s$. This concludes **step 3** of the algorithm.

Now the results obtained from the fictitious static BEAMS MODEL can be converted into the optimal time variation of modal variables and controls (**step 4**).

The modal variables of the structure are numerically identical to the displacement of analogous beams (see Eq. (4.44)) and are shown in Figure 5.5.

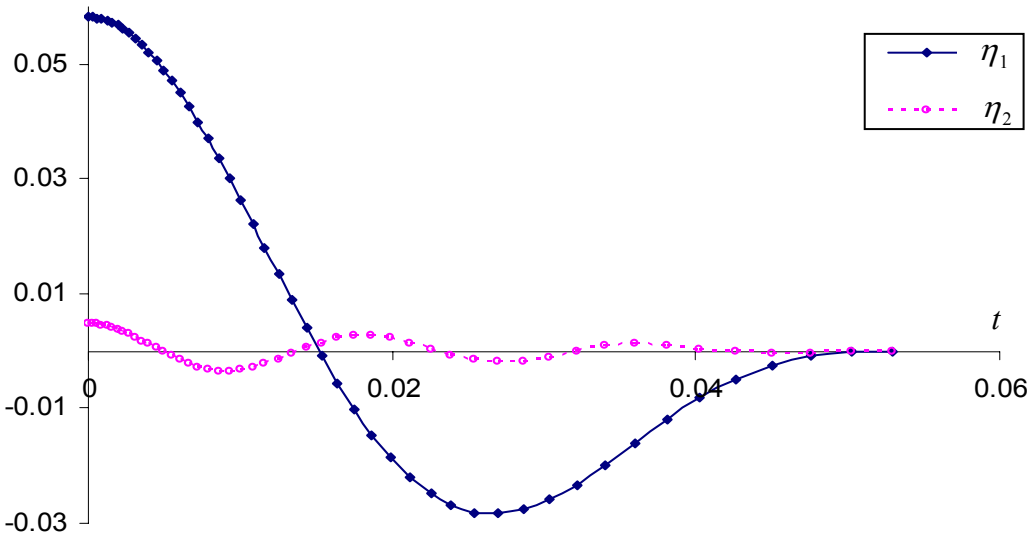

Figure 5.5 Modal Variables

The modal controls are obtained from Eq. (4.45) and are plotted in Figure 5.6. Note that while the modal variables are zero at the final time, the values of modal controls are not.

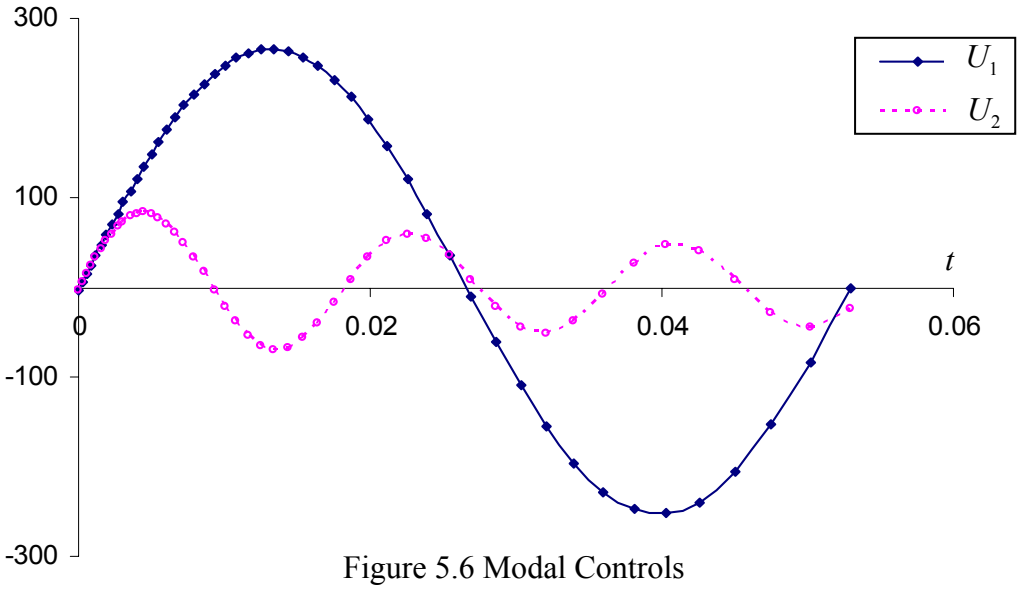

Figure 5.6 Modal Controls

Magnitudes of the control forces can be obtained from Eq. (4.46), which takes the form: $\begin{bmatrix} F_1 \\ F_2 \end{bmatrix} = \widetilde{\Phi}^{-1} U = \begin{bmatrix} \Phi_1^{(2)} & \Phi_1^{(12)} \\ \Phi_2^{(2)} & \Phi_2^{(12)} \end{bmatrix}^{-1} \begin{bmatrix} U_1 \\ U_2 \end{bmatrix}$ for the two modes considered.

where $\Phi_i^{(j)}$ denotes the DOF's representing the vertical displacement at node j for mode i (forces F_1 and F_2 are applied at nodes 2 and 12 respectively). If the structure is controllable the inverse $\widetilde{\Phi}$ matrix exists.

Substituting *U's* from Figure 5.6 one obtains the forces shown in Figure 5.7. The maximum values of F_1 and F_2 are 423*N* and 557*N* respectively.

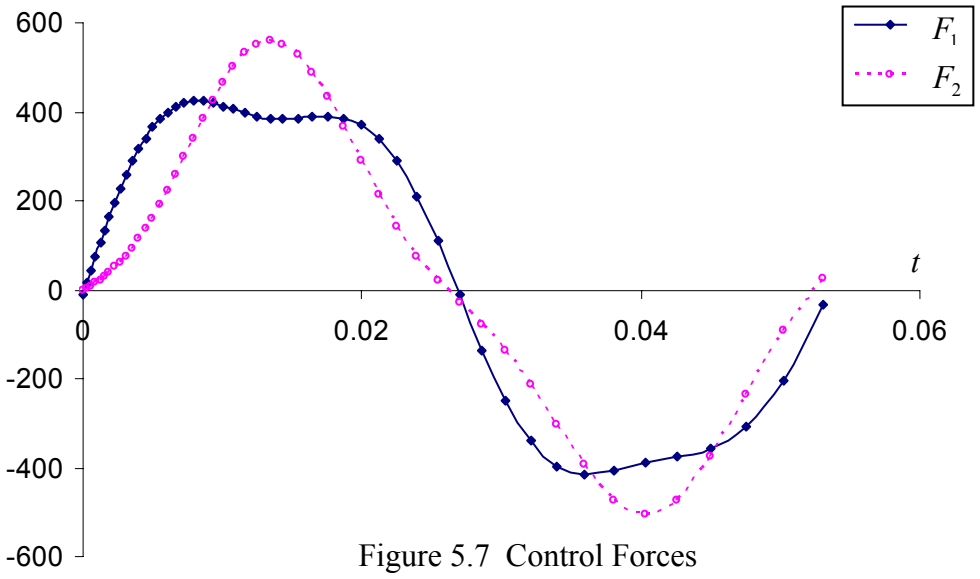

Figure 5.7 Control Forces

The histograms of DOF's over the entire process can be obtained from Eq. (4.43) in the form $x_{(2)} = \Phi_1 \eta_1 + \Phi_2 \eta_2$. The symbol $x_{(j)}$ denotes the values calculated using $j = 2$ modes only. The vertical displacements at the selected nodes are as shown in Figure 5.8.

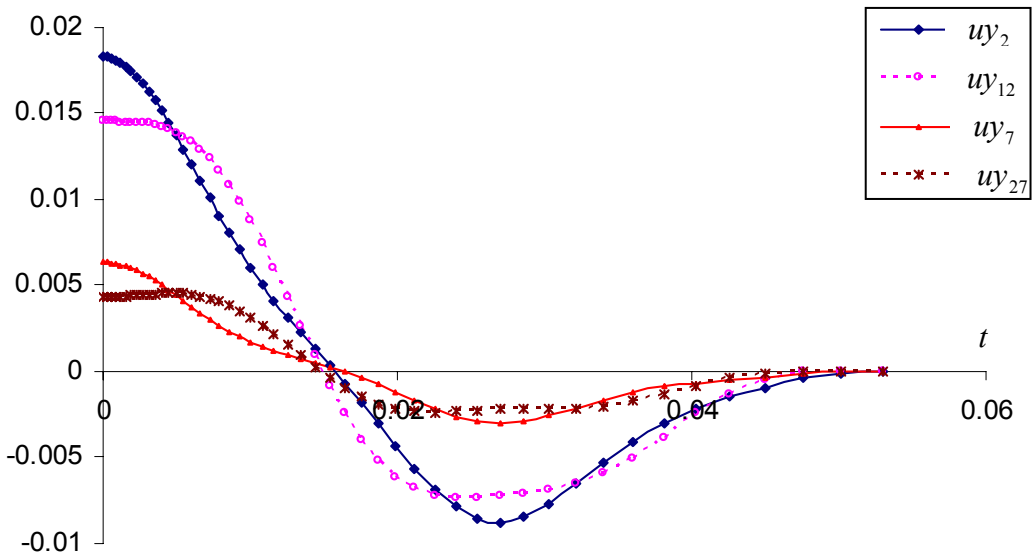

Figure 5.8 Displacements

This completes **Step 4** of the BAA.

5.4.2 Verification

An important step is to verify whether or not the BAA method is providing correct results. There are several means available to confirm the accuracy of the presented method (Beam Analogy). Some, like building the prototype and performing the real experiment, may be very costly. One method, which is neither time consuming nor expensive, is performing a computer simulation in which the expected dynamic response of the structure to the given forces is recreated very precisely.

Here such computer simulations, which use the dynamic FEM procedures available in ANSYS, are presented.

The results from the beam analogy are verified by writing the control forces vs. time history (shown in Figure 5.7) into the ANSYS load file and then by running the transient dynamic analysis (TDA) of the DYNAMIC MODEL (see **step 5** of the BAA).

5.4.2.1 Transient Dynamic Analysis (TDA)

The transient dynamic analysis (sometimes called the time-history analysis) is a technique used to determine the dynamic response of a structure under the action of any

general time-dependent loads. This type of analysis is used to determine the time-varying displacements, strains, stresses, and forces in a structure as it responds to any combination of static, transient, and harmonic loads.

The basic equation of motion solved by a transient dynamic analysis is given by Eq. (1.1). The ANSYS program uses the Newmark time integration method to solve these equations at discrete timepoints. The load is defined at two time instances and interpolated linearly between them. This is defined as a load step. The time increment used for integrating within each load step is called the *integration time step*. The time steps may be adjusted automatically to secure proper accuracy.

One can either integrate all the DOFs in Eq. (1.1) using so called full dynamics, or the Mode Superposition Method (MSUP), which integrates only some relatively small number of modes then sums them up. The advantages of MSUP are that it can provide similar accuracy but it is faster and less expensive than the full method for many problems. The main disadvantage of the MSUP is that only linear problems can be handled. Since the problem simulated here is linear, for verification purposes MSUP is adopted in this thesis. It has been found that for the structure in Figure 5.2, using *ten* modes is equivalent to using the full transient method.

5.4.2.2 Mode Superposition (MSUP) Transient Dynamic Analysis on Fin Structure for Verification

As explained earlier in this chapter first two modes of the continuous structure by using modal space are controlled. The BAA was used to calculate the forces to control these modes. For verification these control forces are applied back to the structure (Figure 5.7), to obtain the complete (i.e. including all uncontrolled modes) dynamic response (the response restricted to two modes only was shown in Figure 5.8). For this purpose the MSUP method with *ten* modes included is used. After applying the forces the structure's response, represented by the displacement patterns for nodes 2, 7, 12 and 27, is shown in Figure 5.9.

Clearly, the displacements patterns in Figure 5.8 and 5.9 are similar but not identical. The difference is due to $x - x_{(2)} \cong x_{(10)} - x_{(2)} = \Phi_3 \eta_3 + ...\Phi_{10}\eta_{10} \neq 0$ and reflects the spillover effect, resulting from the omission of the higher modes in determining the control forces. In particular, note some 'residual' vibrations of higher frequencies after the attenuation processes is terminated (for $t > t_f$).

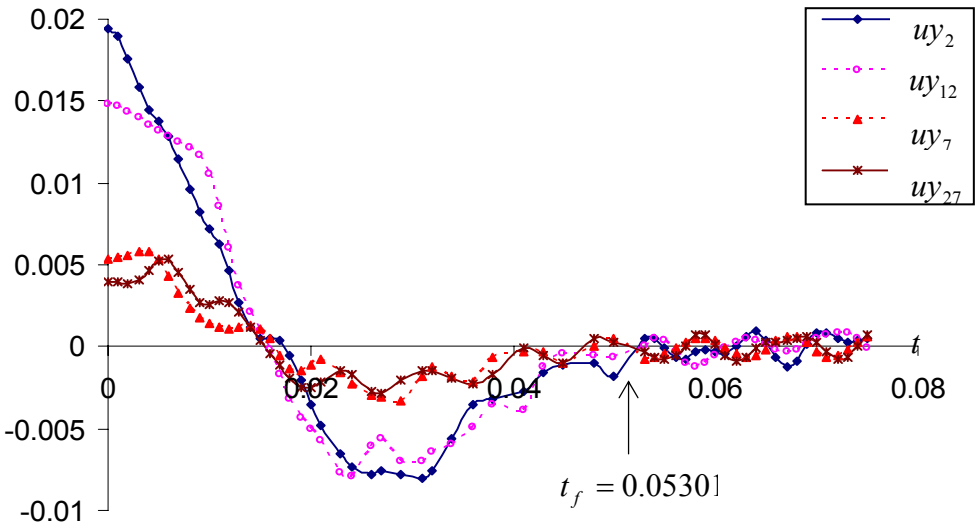

Figure 5.9 Displacements from Transient Dynamic Analysis

5.4.3 Case2a: Three Actuators (t_f is unknown)

In the previous section the fin structure was controlled by two actuators. Consequently some spillover effect occurred due to higher uncontrolled modes. This effect can be decreased by adding one more actuator and control one more mode, which can be easily done using the BAA. The third actuator is positioned at node 91 of the fin structure. All the actuators are therefore placed at nodes 2, 12 and 91 to generate forces F_1, F_2 and F_3 respectively (Figure 5.10). Step 1 and 2 of the BAA will be the same as before except that in order to determine the three forces one has to consider three vibration modes. Consequently, the BEAMS MODEL now consists of three fictitious static analogous

beams instead of two. The parameters of these beams are calculated from Eq. (4.42-b,c,d) (for the first two beams they are the same as those in Figure 5.4).

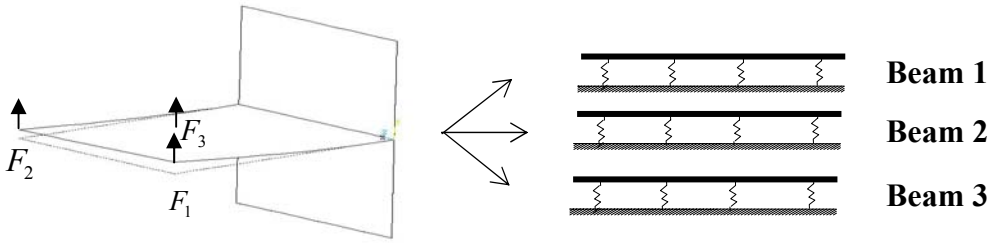

Figure 5.10 Analogous Beams for 3 Actuators

Following **Step 3** and **Step 4** of the BAA, the modal variables shown in Figure 5.11 are obtained. Note that now the maneuver time $t_f = 0.079311$ is longer then for the case of two actuators (for which $t_f = 0.05301$).

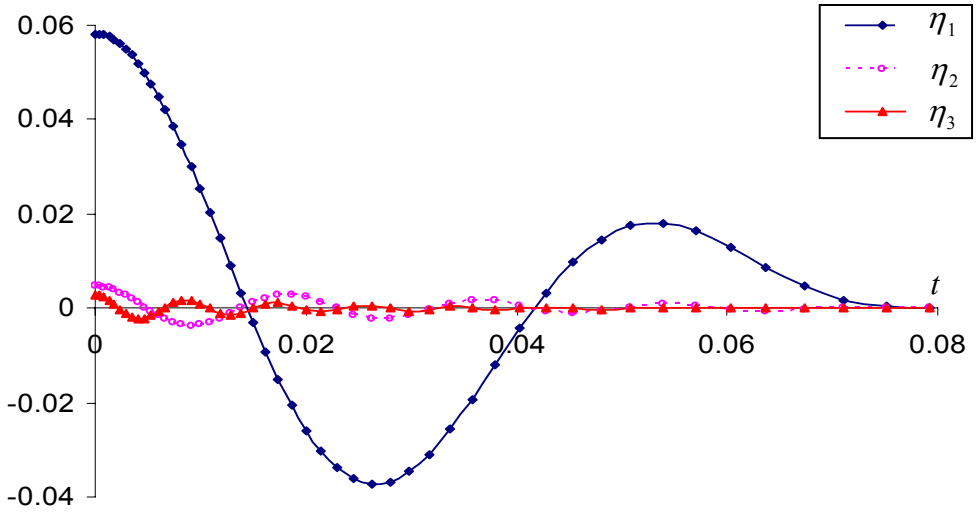

Figure 5.11 Modal Variables

The corresponding modal controls are plotted in Figure 5.12.

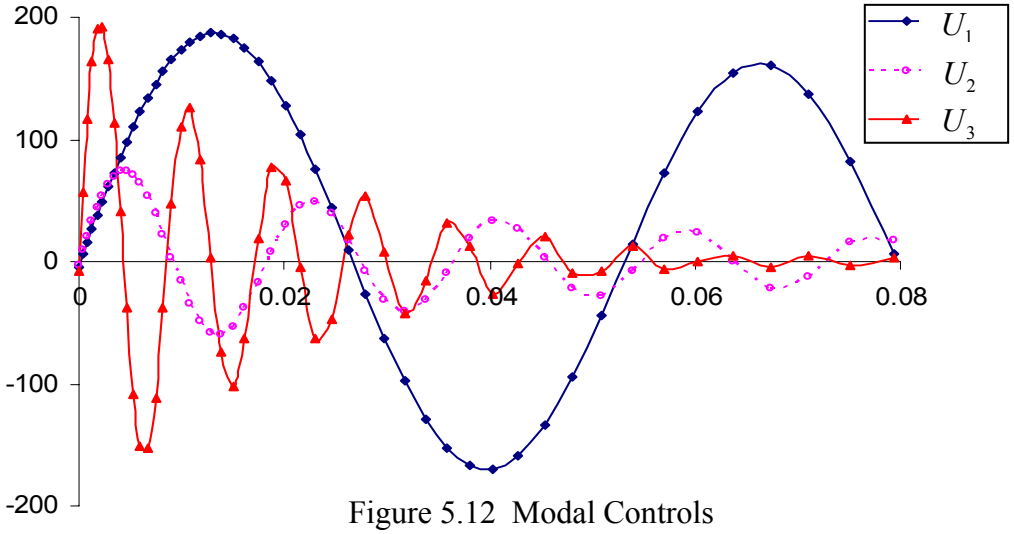

Figure 5.12 Modal Controls

As three actuators are placed at nodes 2, 12 and 91 in the vertical direction to control the structure, only at three places will there be *unity* terms and at all other places there will be *zeros* in the placement matrix B_a (3×3). Therefore the control forces matrix will also be of dimension 3×3. Once again controllability of the structure can be checked by inverting $\widetilde{\Phi}$.

$$\begin{bmatrix} F_1 \\ F_2 \\ F_3 \end{bmatrix} = \begin{bmatrix} \Phi_1^{(2)} & \Phi_1^{(12)} & \Phi_1^{(91)} \\ \Phi_2^{(2)} & \Phi_2^{(12)} & \Phi_2^{(91)} \\ \Phi_3^{(2)} & \Phi_3^{(12)} & \Phi_3^{(91)} \end{bmatrix}^{-1} \begin{bmatrix} U_1 \\ U_2 \\ U_3 \end{bmatrix}$$

where now the contribution of the three modes is included. These forces are shown in Figure 5.13. As can be seen the force F_3 is dominant, its maximum value is about $1030N$. In comparison to the two actuator case presented in Figure 5.7, the maximum magnitudes of forces F_1 and F_2 are reduced to $262N$ and $329N$ respectively. Note rapid cycling of F_3 with the frequency roughly the same as ω_3 in the early phase of the process. This cycling is related to variations of U_3 and disappear in the final phase of the maneuver.

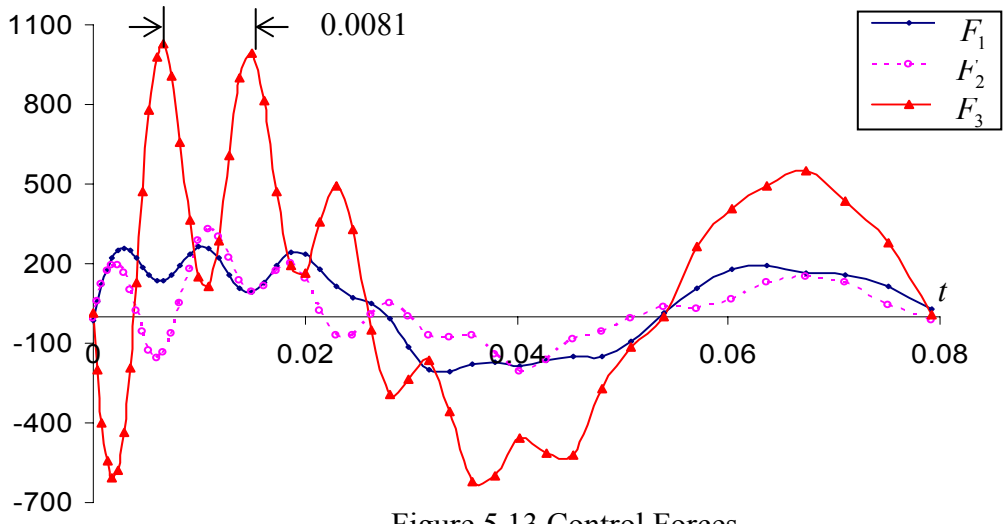

Figure 5.13 Control Forces

The corresponding displacements $x_{(3)} = \Phi_1\eta_1 + \Phi_2\eta_2 + \Phi_3\eta_3$ are shown in Figure 5.14.

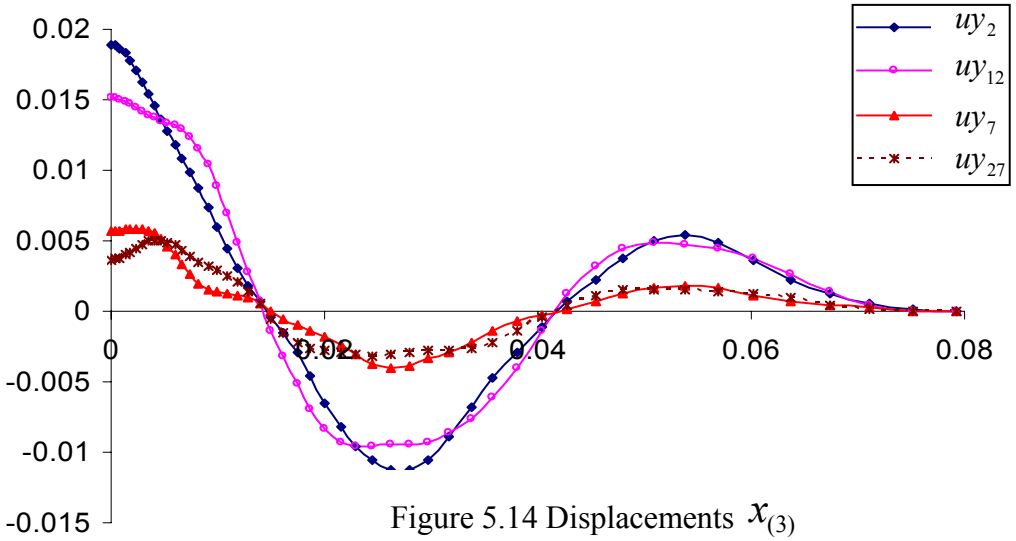

Figure 5.14 Displacements $x_{(3)}$

5.4.4 Case2b: Three Actuators, and t_f given

Next, in order to demonstrate the option with the known t_f (see the flow chart in Figure 5.1 step 2) the three actuator case for $t_f = 0.05301,$ is recalculated i.e. the same as the maneuver time for the case with two actuators. Since the t_f is known, there is no need to run the design optimization loop in ANSYS, because the target condition is automatically

met. After following the rest of the steps in the BAA, the modal variables and controls are shown in Figure 5.15 and 5.16 respectively.

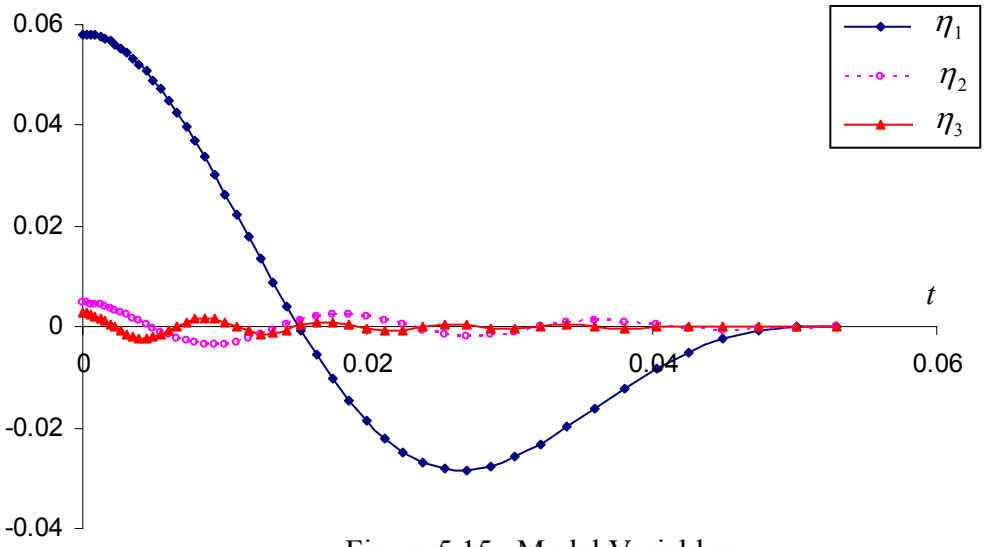

Figure 5.15 Modal Variables

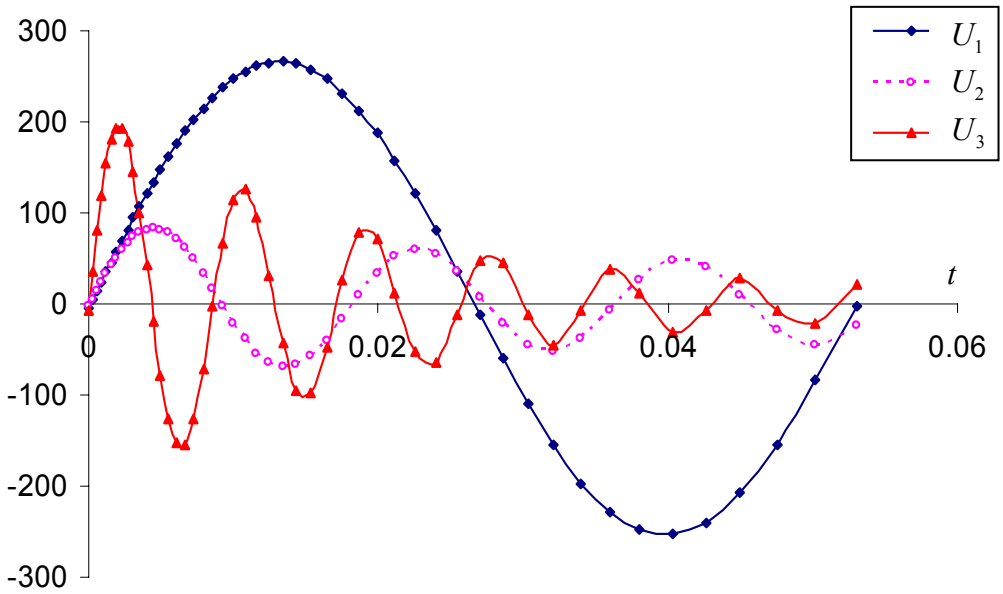

Figure 5.16 Modal Controls

Note that in this trimodal solution the plots for *mode*1 and *mode*2 are identical to the plots in Figure 5.5 and 5.6. Variations of the control forces are shown in Figure 5.17. Comparing with these plots in Figure 5.13 (which were obtained for $t_f = 0.079311$) one

can observe that the forces vary in a somewhat similar manner, however, the maximum values are now higher. Namely the values are $1231N$ for F_3, and $350N$, $392N$ for F_1 and F_2 respectively.

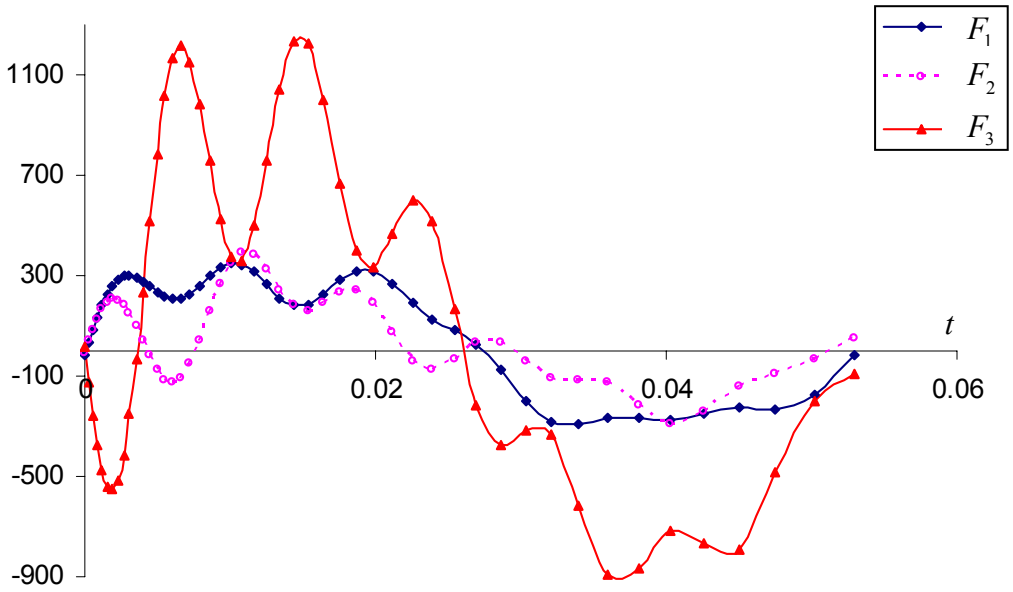

Figure 5.17 Control Forces

The displacements for particular nodes are displayed in Figure 5.18. The plots show a close resemblance to the two actuator case shown in Figure 5.8.

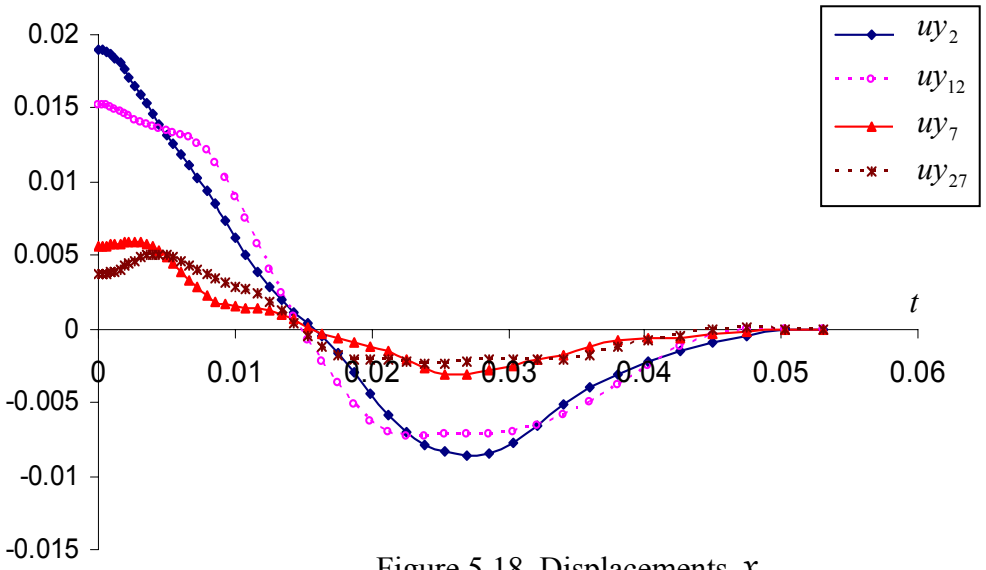

Figure 5.18 Displacements $x_{(3)}$

Again, for verification purposes the control forces from Figure 5.17 (the beam analogy) are applied to the DYNAMIC MODEL to run the transient dynamic analysis of the structure. The structure's response, represented by the displacement patterns of nodes 2, 7, 12 and 27, is shown in Figure 5.19. The residual vibrations for $t > t_f$ are now slightly reduced because of the addition of the third actuator to control the three modes of vibration.

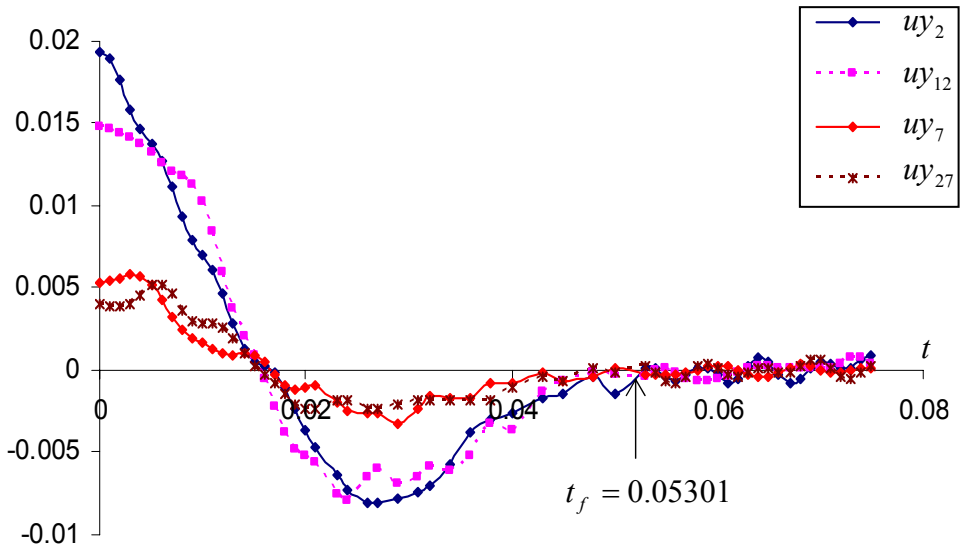

Figure 5.19 Displacements from Transient Dynamic Analysis

5.4.5 Case3: Four Actuators, and t_f given

In order to further reduce the spill over effect, four actuators are placed at nodes 2, 12, 7 and 27 to generate forces F_1, F_2, F_3 and F_4 respectively (Figure 5.20). Once again **Step 1** and **2** of the BAA will be the same as before, except the BEAMS MODEL now consists of four fictitious analogous beams instead of three. The parameters of these beams are calculated from Eq. (4.42-b,c,d).

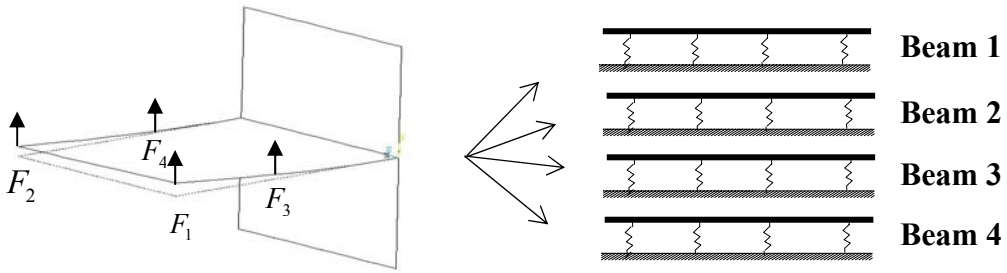

Figure 5.20 Four Actuators

The maneuver time $t_f = 0.05301$ was assumed again to compare it to the previous cases. The control forces are shown in Figure 5.21. The maximum values of these forces are $397N$ and $428N$ for F_1 and F_2 respectively, and $492N$ and $542N$ for F_3 and F_4 respectively. Thus, in comparison to case 3 the values of F_1 and F_2 are slightly increased. Since F_3 and F_4 now play a similar role as F_3 in case 3, their maximum values are now about half of the maximum of F_3 for case 3.

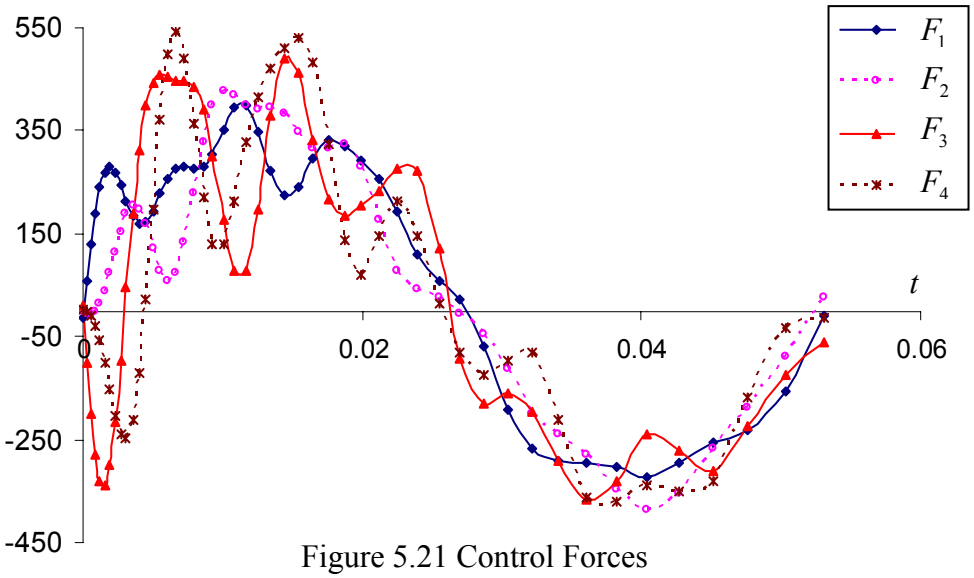

Figure 5.21 Control Forces

The corresponding displacements $x_{(4)} = \Phi_1\eta_1 + \Phi_2\eta_2 + \Phi_3\eta_3 + \Phi_4\eta_4$ are shown in Figure 5.22 and are very similar to the displacements $x_{(3)}$ on Figure 5.18.

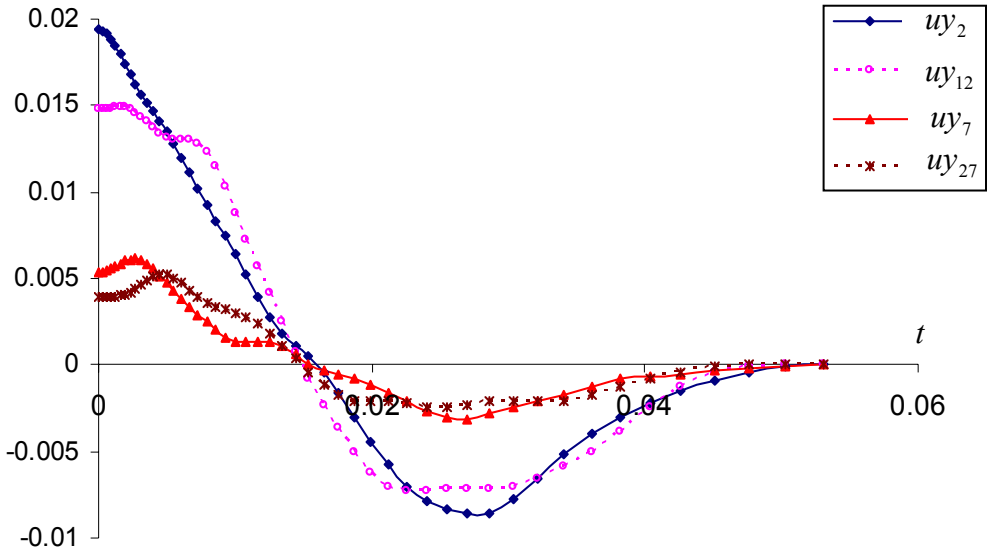

Figure 5.22 Displacements $x_{(4)}$

Once again the forces from Figure 5.21 are used to run the transient dynamics of the DYNAMIC MODEL for verification of the results from the beam analogy. The structure's response, represented by the displacement patterns for nodes 2, 7, 12 and 27, is shown in Figure 5.23. The spillover effect (for $t > t_f$) is further reduced because of the addition of the fourth actuator and control of the four modes of vibrations.

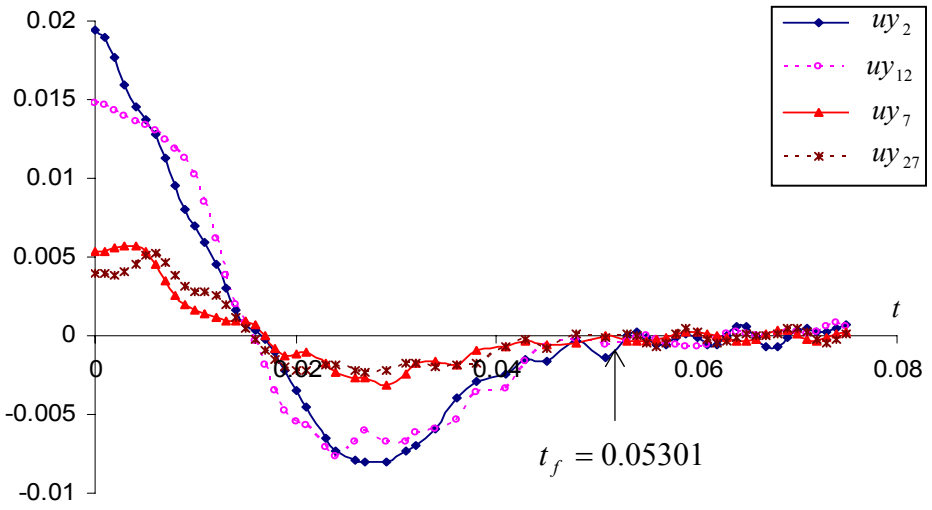

Figure 5.23 Displacements from Transient Dynamic Analysis

5.5 Effect of Placement of Actuators on the Fin Structure

As explained before the beam analogy is a very effective tool in order to determine the magnitudes of the control forces, the control duration etc., as explained in the previous sections by using 2, 3 and 4 actuators on the fin structure.

In a similar manner the efficiency of particular placements of an actuator can be examined. When the actuators' location is changed one has to follow the same algorithm with only the $\widetilde{\Phi}$ matrix modified accordingly (placement matrix B_a in Eq. (4.12) is different). After keeping the same η's and all other parameters as in the case of two actuators, change the position of the actuators from node numbers 2 and 12 to 7 and 27 respectively. The actuator forces are obtained using the following matrix:

$$\begin{bmatrix} F_1^{(7)} \\ F_2^{(27)} \end{bmatrix} = \begin{bmatrix} \Phi_1{}^{(7)} & \Phi_1{}^{(27)} \\ \Phi_2{}^{(7)} & \Phi_2{}^{(27)} \end{bmatrix}^{-1} \begin{bmatrix} U_1 \\ U_2 \end{bmatrix} \tag{5.2}$$

these superscripts are introduced to distinguish them from the forces F_1 and F_2 presented in Case1.

After using Eq. (5.2) the control forces are as shown in Figure 5.24.

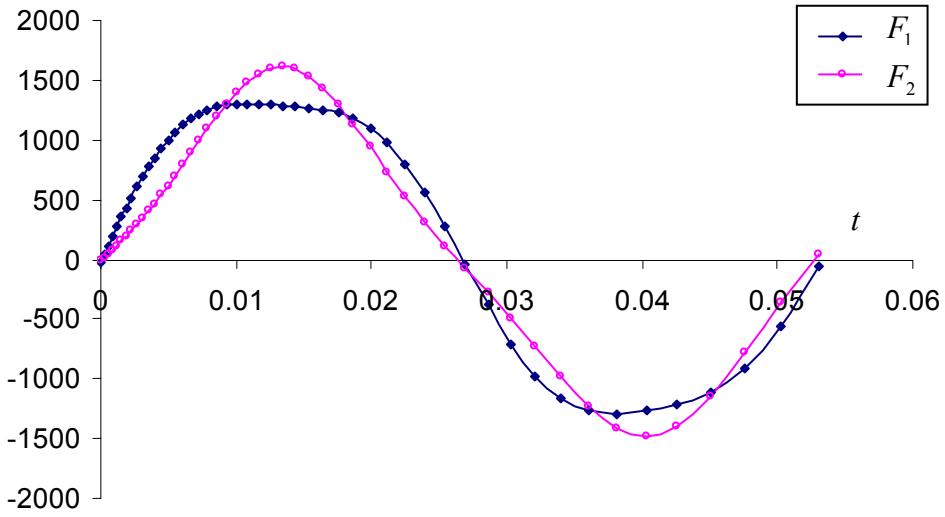

Figure 5.24 Control Forces

By comparing Figure 5.24 with Figure 5.7 one can easily observe that the magnitudes of the control forces are much higher in Figure 5.24. Since the structure's responses under the above sets of forces are similar, this shows that actuator placement has a considerable impact on the magnitude of these forces (smaller actuators may be utilized if they are placed appropriately).

5.6 Impact of Optimization Parameters

In the beam analogy, beam length i.e. maneuver time is obtained by minimizing performance index in a certain form. This form for the performance index includes weighting matrices with the optimization parameters for the energies and the control forces. These optimization parameters can be changed for manipulating the magnitude of the optimal control forces, the maximum deflection, maneuver time, etc.

In general, the weighting matrices Q_d, Q_v and R formulated as linear combinations of M, C, and K (which, by definition, are positive definite for any structure modeled properly by the FEM) have *nine* different optimization parameters. So some

understanding of effects of these parameters is beneficial in solving practical problems. Here the meanings of α_2, β_1 and γ_2 are briefly discussed.

The performance is defined as:

$$J = 1/2 \int_0^{t_f} [\alpha_2 x^T K x + \beta_1 \dot{x}^T M \dot{x} + \gamma_2^{-1} F_c^T K^{-1} F_c + \Gamma] dt \rightarrow \min. \quad (5.3)$$

It can be seen that α_2 weights the strain energy, β_1 weights the kinetic energy, $1/\gamma_2$ weights control force, and Γ weights the time of the optimal maneuver.

The effects of these parameters, for the fin structure (case 1 section 5.4.1) in which the performance index was assumed as given by Eq. (5.3), are presented next. The values used before i.e. $\alpha_2 = \beta_1 = 1$, $\gamma_2^{-1} = 100$ and $\Gamma = 0.5$ are considered nominal.

The control force optimization parameter (γ_2)

The parameter $1/\gamma_2$ is weighting the control force. For the case analyzed $\alpha_2 = 1$, $\beta_1 = 1$, $\Gamma = 0.5$, and $\gamma_2^{-1} = 75, 100, 125, 150$ were assumed. Maximum forces for the two actuators are represented by F_{1Max} and F_{2Max} respectively. The effect of γ_2^{-1} on those forces is shown in Figure 5.25.

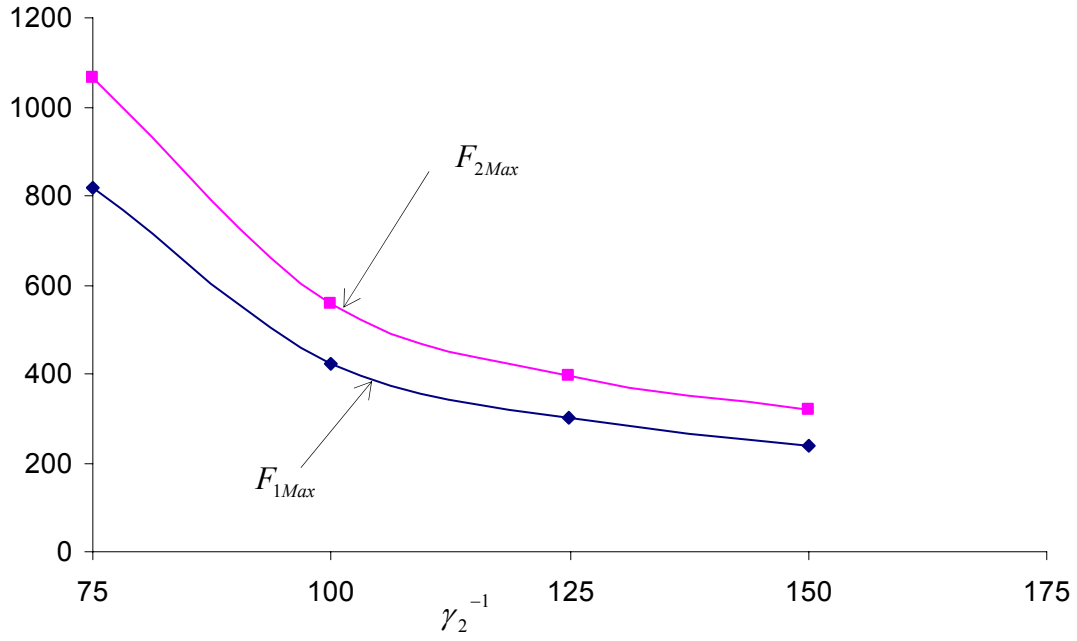

Figure 5.25 Impact of γ_2^{-1} on the Maximum Control Forces for Two Actuators

In general, the increase in the γ_2^{-1} results in the decrease in the resulting force and *vice versa.*

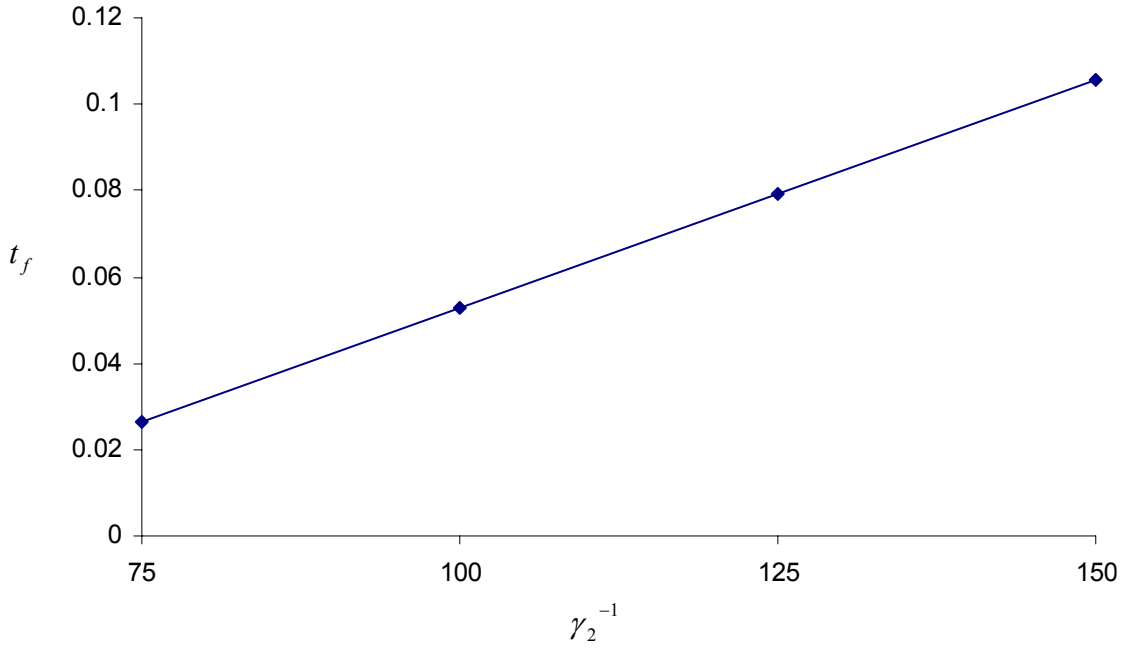

Figure 5.26 Impact of γ_2^{-1} on the Maneuver Time t_f

Since larger values for γ_2^{-1} decrease the maximum forces for both the actuators, this results in an increase in the maneuver time (Figure 5.26).

The strain energy optimization parameter (α_2)

The parameter α_2 is weighting the strain energy. For the case analyzed $\alpha_2 = 1,5,10,15$, $\beta_1 = 1$, $\Gamma = 0.5$ and $\gamma_2^{-1} = 1$ were assumed. The increase in α_2 results in an increase of the maximum forces for both the actuators (Figure 5.27).

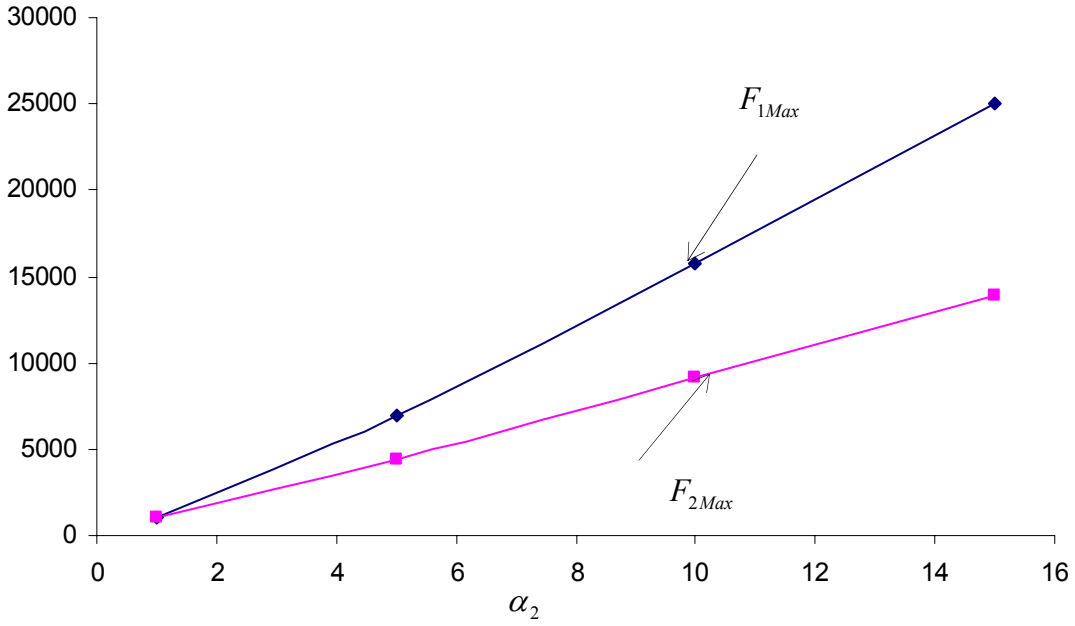

Figure 5.27 Impact of α_2 on the Maximum Control Forces for the Two Actuators

This increase in the forces results in a decrease of the maneuver time (Figure 5.28)

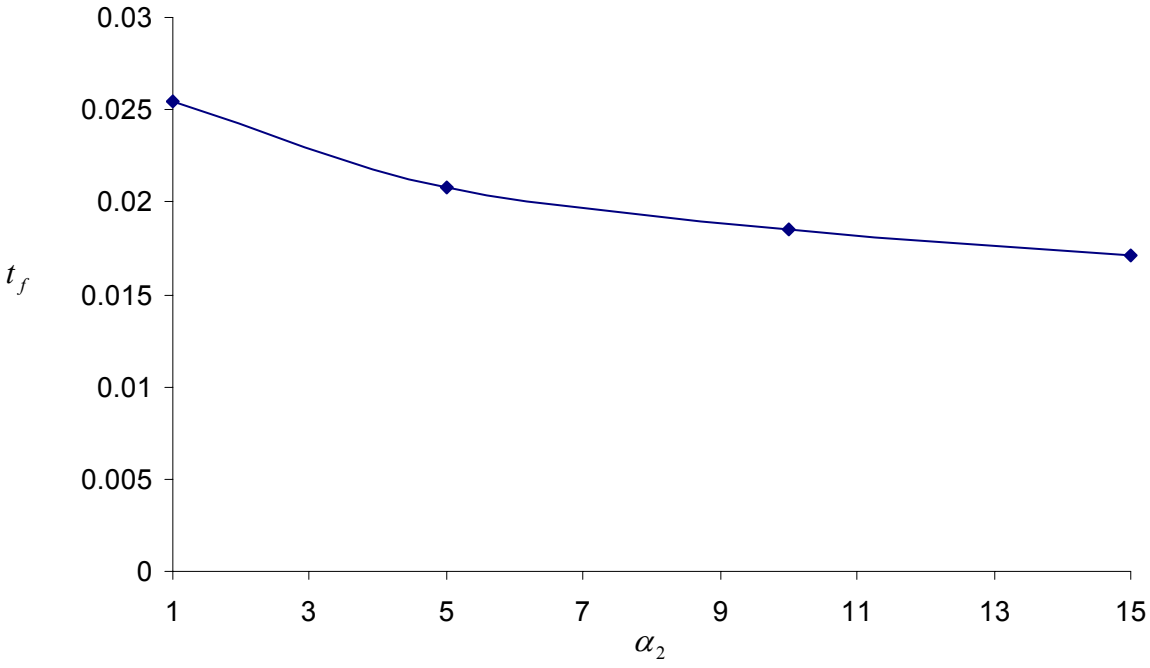

Figure 5.28 Impact of α_2 on the Maneuver Time t_f

Impact of kinetic energy optimization parameter (β_1)

β_1 is the weighting parameter for kinetic energy. For the case analyzed $\alpha_2 = 1$, $\beta_1 = 1, 5, 10, 15$, $\Gamma = 0.5$ and $\gamma_2^{-1} = 1$ were assumed. The increase in β_1 results in an increase in the maximum force for the first actuator but shows decrease in the maximum force for the second actuator (Figure 5.29).

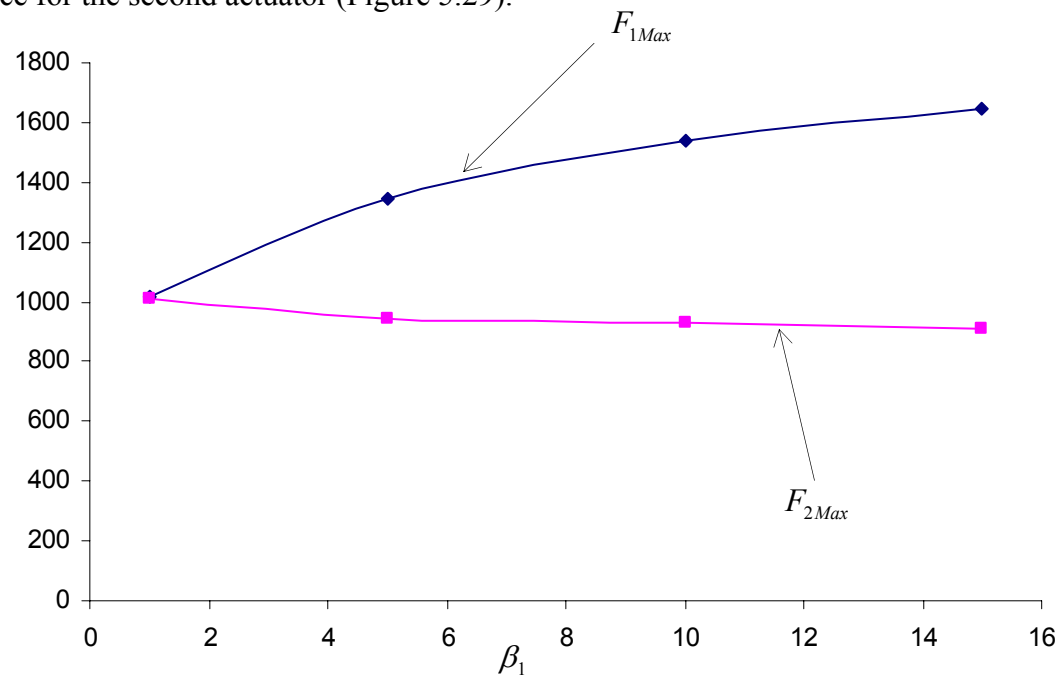

Figure 5.29 Impact of β_1 on the Maximum Control Forces for the Two Actuators

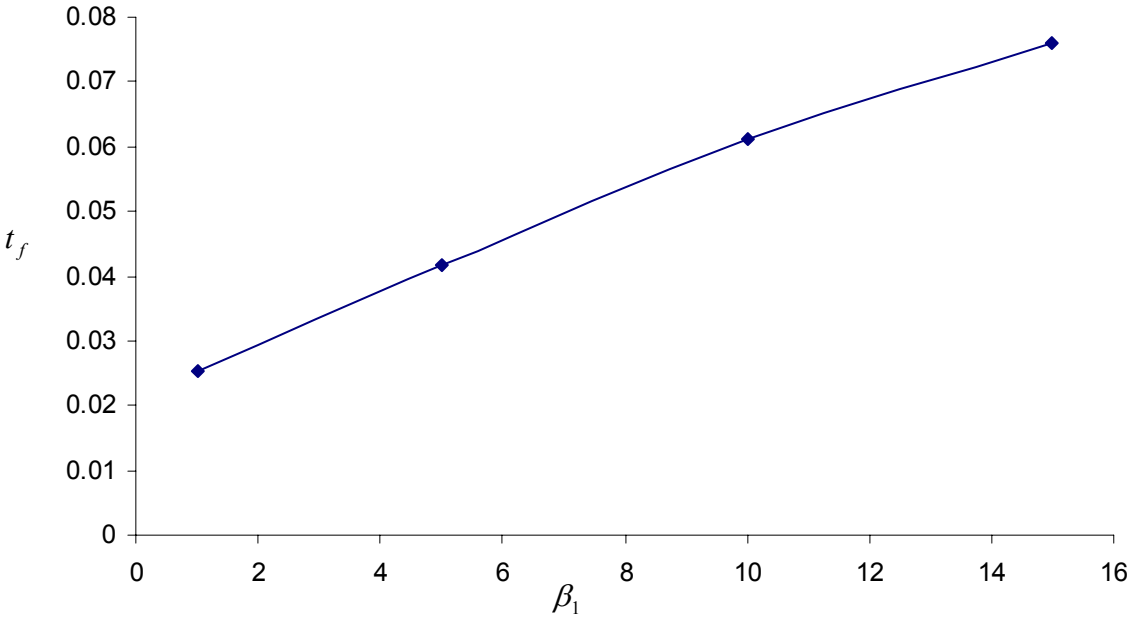

Figure 5.30 Impact of β_1 on the Maneuver time t_f

Increase in β_1 shows an increase of the maneuver time (Figure 5.30).

The maneuver time weighting parameter (Γ)

Γ is the optimization parameter for the maneuver time. For the case analyzed $\alpha_2 = 1$, $\beta_1 = 1$, $\gamma_2^{-1} = 100$ and $\Gamma = 0.001, 0.01, 0.2, 0.5, 2$. The increase in Γ results in a decrease of the maneuver time (Figure 5.32). This causes an increase of the maximum control forces for both the actuators (Figure 5.31). One interesting property to observe here is that $t_f \to \infty$ (Figure 5.32), and $F_i \to$ *to steady state* (Figure 5.31) if $\Gamma \to 0$.

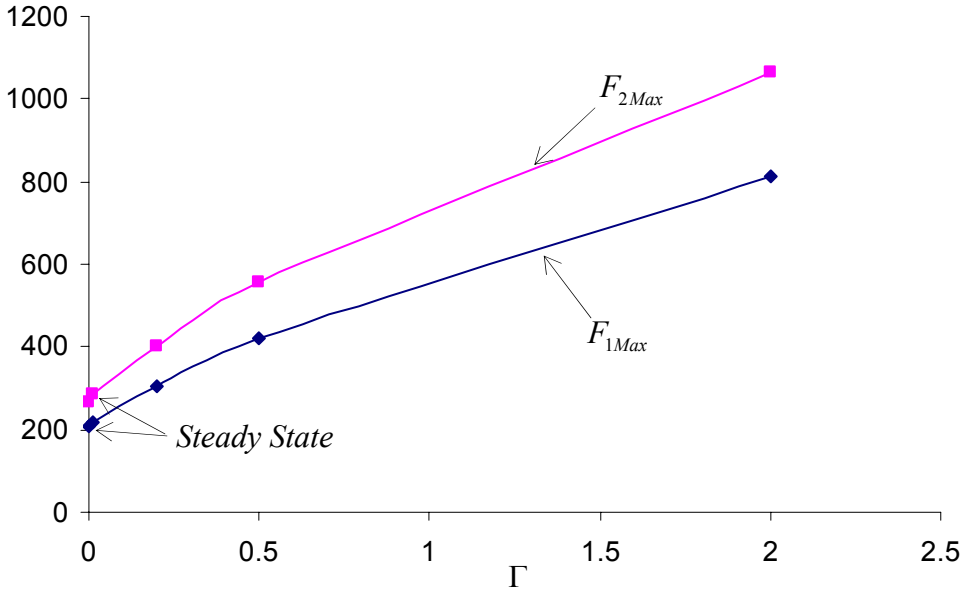

Figure 5.31 Impact of Γ on the Maximum Control Forces for the Two Actuators

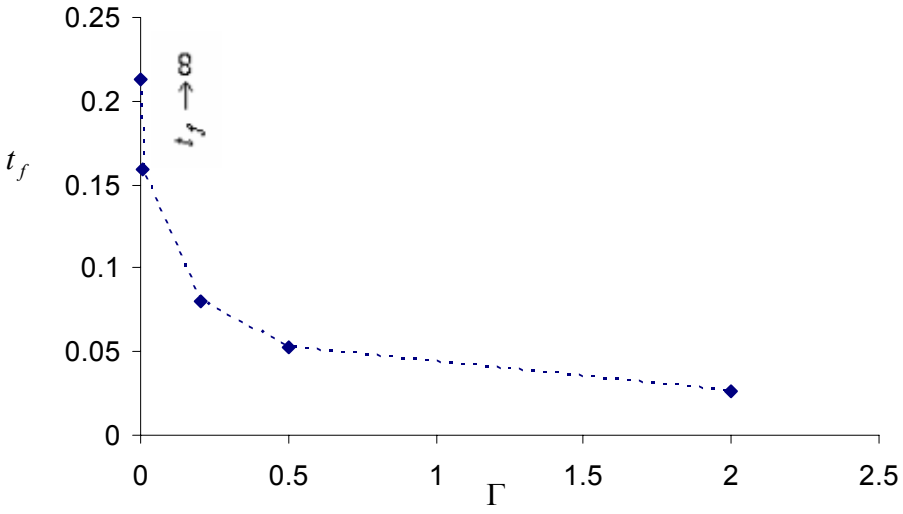

Figure 5.32 Impact of Γ on the Maneuver time t_f

Chapter 6. Closed Loop Control

6.1 Introduction

The beam analogy was successfully implemented in the previous chapter to problems related to open loop control, in which the optimal control forces and the trajectories were obtained as a function of time. Here the beam analogy is used to determine optimal gains for closed loop control of active optimal vibration in continuous structures. An algorithm for a direct calculation of optimal gains for closed loop control of time-invariant problems without using Riccati's equation is discussed in detail. The number and size of beam elements should be properly selected for this application. Also, using a proper spacing ratio and beam length is very important and is discussed in the last part of this chapter.

6.2 Time invariant control and constant gain

If the performance index from Eq. (3.4) is written in the form:

$$J = 1/2\int_0^\infty (z^T Qz + F_c{}^T RF_c)dt \rightarrow \min \tag{6.1}$$

Such a problem is called a time invariant problem. Riccati's equation for the time invariant cases was discussed in chapter 3 in section 3.5.2, where it was indicated that if $t_f \rightarrow \infty$, control forces can be obtained in terms of states i.e. $F_c = -Gz(t),$ and where G is a constant matrix known as the feedback gain matrix. Thus, the forces in this control can be obtained by feeding back output (using some sensors) from the system to the controller (the gain matrix in this case). By doing this the control forces instead of depending on time will depend on the particular state of the system. Moreover, control forces will not depend on the initial disturbance of the system.

The modal controls for time-invariant problems can be written in the form:

$$U_i(t) = -g_{id}\eta_i(t) - g_{iv}\dot{\eta}_i(t) \qquad i=1\ldots s \tag{6.2}$$

where g_{id} and g_{iv} are constants referred to as the modal gains for position and velocity, respectively. The optimal gains are typically obtained by solving the corresponding Riccati equations (in the form of a set of nonlinear algebraic equations as explained in

chapter 3 section 3.5.2). This is difficult to solve due to its nonlinearity. Theoretically $t_f \to \infty$ is needed to obtain optimal gains, but for numerical reasons when using the beam analogy the beams should be of a finite length. Determination of such a finite length is referred to as the effective length and is discussed later. First some compact form of the optimality condition and its characteristics are presented.

6.3 Optimal Vibration Control

As is known from chapter 4 the optimality equation and the corresponding BCs in terms of the modal variables can be written in the form of Eqs. (4.38) and (4.30). For the time-invariant problems it is assumed that the initial BCs in Eq. (4.30) can be arbitrary, and the final BCs are in the form:

$$\eta_i^f = \dot{\eta}_i^f = 0 \quad \text{and} \quad t_f \to \infty \tag{6.3}$$

Eq. (4.38) can be rewritten in a somewhat more compact form as:

$$\dddot{\eta}_i + 2\varsigma_i \lambda_i^2 \ddot{\eta}_i + \lambda_i^4 \eta_i = 0 \tag{6.4}$$

where the following *new optimal control parameters* are introduced:

$$\lambda_i^4 = \omega_i^4 + \hat{R}_{ii}^{-1}\hat{Q}_{iid} = \omega_i^4 + (\gamma_1 + \gamma_2\omega_i^2 + 2\gamma_3\omega_i\xi_i)(\alpha_1 + \alpha_2\omega_i^2 + 2\alpha_3\omega_i\xi_i) \tag{6.5}$$

$$\varsigma_i = [(1-2\xi_i^2)\omega_i^2 - \frac{1}{2}\hat{R}_{ii}^{-1}\hat{Q}_{iiv}]\lambda_i^{-2} \tag{6.6}$$

As can be seen, λ_i and ς_i are dependent on the parameter α, β and γ.

Since $\hat{R}_{ii} > 0$, $\hat{Q}_{iid} \geq 0$, $\hat{Q}_{iiv} \geq 0$ for non-negative α, β and γ, these optimal control parameters satisfy the following: $\lambda_i \geq \omega_i$, and $\varsigma_i \leq 1$.

Again the performance index is assumed as:

$$J = 1/2\int_0^\infty [\alpha_2 x^T K x + \beta_1 \dot{x}^T M \dot{x} + \frac{1}{\gamma_2} F^T K^{-1} F]dt \to \min \tag{6.7}$$

The beam equation and its corresponding BCs for the beam analogy are discussed next.

6.4 The Beam Analogy

As explained in the chapter 4, the governing equation and corresponding BCs for a straight beam of length L loaded axially by force P_i and supported along its entire length by an elastic foundation of the stiffness k_{fi} (Figure1a) is given by Eqs, (4.39) and (4.40). Eq. (4.39) with the BCs (4.40) that define the static problem of the beam is clearly similar to the optimality equation (4.38) with the BCs (4.30). This similarity permits forming an analogy between the beam's deflection $v_i(y)$ (Figure 6.1a) and the modal variable $\eta_i(t)$ (Figure 6.1b) and was discussed in detail in the chapter 4**.**

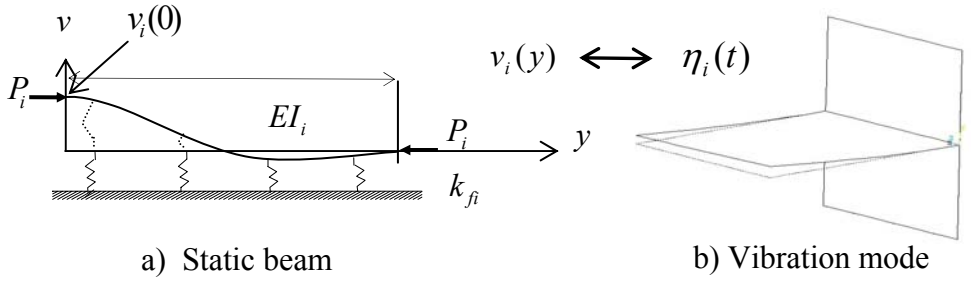

a) Static beam b) Vibration mode

Figure 6.1 The Beam Analogy

Here for the time invariant case the boundary conditions for the beam, equivalent to the conditions (4.30) and (6.3), will be:

$$v_i(0) = \eta_i(0),\ \theta_i(0) = \dot{\eta}_i(0) \text{ and } v_i(L) = \theta_i(L) = 0 \text{ where } L \to \infty \qquad (6.8)$$

The analogy requires building a set of fictitious analogous beams and then solving them by FEM. For numerical reasons these beams should be of finite length (as explained before). However, to obtain constant optimal gains for the time-invariant problems one has to consider infinite time, or the beams of infinite length (i.e.: $L \to \infty$) in the beam analogy. Therefore a practical question arises as to what should be the 'effective time', or the corresponding 'effective finite beam length', in order to obtain results representing the case of theoretically infinite control time. The above question is answered by analyzing the well known behaviour of beams on elastic foundations.

6.5 Determination of Effective Beam's Length

Due to the boundary condition (6.8), the left end of the fictitious analogous beam is always displaced to represent the initial disturbance (4.30). On the other hand the right end must be free of any deflections and rotations to represent conditions (6.3). The beam's deflection should disappear from left to right, which would illustrate the pattern of amplitude's reduction of the corresponding modes of vibration with time.

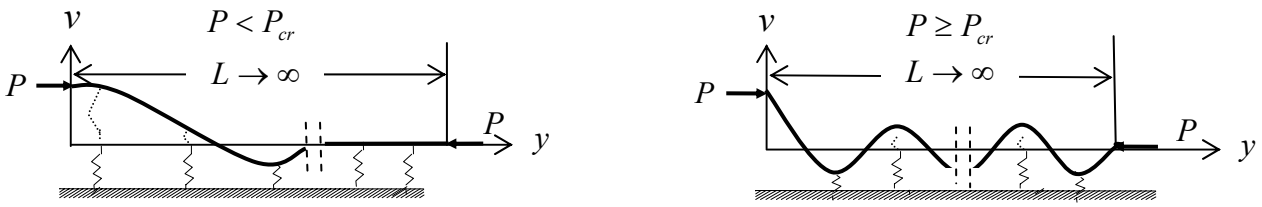

a) Decaying Deflection b) Sustained Deflection

Figure 6.2 Beams on Elastic Foundations

From the studies of elastic beams on elastic foundations [Hetenyi, M., 1971] it is known that the deflections of the beam will be gradually decreasing with the distance from the left end (Figure 6.2a) only if P_i is smaller than the critical compressive force $P_{cr} = 2\sqrt{EIk_f}$, otherwise the beam will be deflected over its entire length, as indicated in Figure 6.2b.

Therefore, the value of P calculated from (4.42-c) and imposed on the fictitious beam will be decisive as to whether the vibrations die out or continue (the subscript *i* is omitted in this part of the chapter for convenience).

Comparing the coefficients in Eqs. (6.4) and (4.39) the following correspondence is obtained:

$$2\varsigma\lambda^2 = \frac{P}{EI} \tag{6.9}$$

$$\lambda^4 = \frac{k_f}{EI} \tag{6.10}$$

Combining (6.9) and (6.10) the following is obtained:

$$\varsigma = \frac{P}{2EI\lambda^2} = \frac{P}{2\sqrt{EIk_f}} = \frac{P}{P_{cr}} \tag{6.11}$$

The requirement $P < P_{cr}$ for the beam deflection to decay to zero, because of the correspondence (4.42-a), translates into $\varsigma < 1$, which is needed for the vibrations to be attenuated. Note that, according to Eq. (6.6), the case $\varsigma = 1$ is possible only if ξ=0 (negligible structural damping) and if $\alpha_i = \beta_i = 0$ is assumed, which results in $\hat{Q}_d = \hat{Q}_v = 0$. Since such a case represents sustained vibrations, the above combination of the optimization constants cannot be used for the time-invariant problems (that is at least one of the matrices *C*, Q_d, or Q_v must be non- zero in order to consider $t_f \to \infty$ in Eq. (3.2)).

The beam's solutions, as presented in [Hetenyi, M., 1971], depend on the two *beam parameters* defined as:

$$\delta = \sqrt{\sqrt{\frac{k_f}{4EI}} + \frac{P}{4EI}} \tag{6.12}$$

$$\tau = \sqrt{\sqrt{\frac{k_f}{4EI}} - \frac{P}{4EI}} \tag{6.13}$$

Using (6.9), (6.10), (6.12), and (6.13) the *beam parameters* can be expressed in terms of the *optimal control parameters* as follows:

$$\delta = \lambda\sqrt{\frac{1+\varsigma}{2}} \tag{6.14}$$

$$\tau = \lambda\sqrt{\frac{1-\varsigma}{2}} \tag{6.15}$$

Since $\varsigma < 1$, the parameter τ is always positive. Its value defines the character of the solution functions. According to [Hetenyi, M., 1971] the beam's deflection for infinite length has the following form (where C_1 and C_2 are integration constants to be calculated from the initial conditions given in terms of the initial disturbance):

Case1: If $1 > \varsigma > -1$ then $0 < \tau < \lambda$ and $v = e^{-\tau\alpha}(C_1 \cos\delta y + C_2 \sin\delta y)$

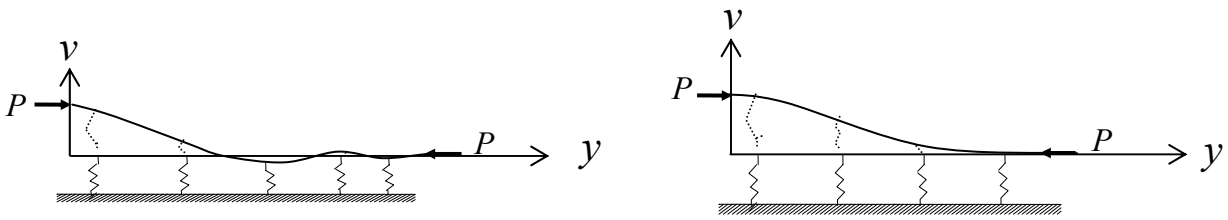

a) Underdamped Case b) Critical Case

Figure 6.3 Deflection Patterns Representing Modes of Vibration

In terms of control, this case represents underdamped vibrations. The amplitudes of the oscillations will decay to zero.

Case 2: If $\varsigma = -1$ then $\tau = \lambda$ and $v = e^{-\tau y}(C_1 + C_2 y)$

This case will represent the critical damping condition with no oscillations.

Case 3: If $\varsigma < -1$ then $\tau > \lambda$ and $v = C_1 e^{-\tau_1 y} + C_2 e^{-\tau_2 y}$, where $\tau_1, \tau_2 = \lambda\sqrt{-\varsigma \pm \sqrt{\varsigma^2 - 1}}$

This case will clearly represent an overdamped case.

Let the effective length L_{eff} be defined as the length of the beam for which the left hand side (LHS) boundary conditions do not affect the right hand side (RHS) boundary conditions, and vice versa. In statics, such beams are referred to as long beams. Since the attenuation of a particular mode is governed by the exponent τL, any initial disturbance will be reduced by 95% when $\tau L \cong 3$. After some numerical experimentation it has been found that for optimal control applications the threshold of negligible vibrations should be reduced to 1%, which corresponds to $\tau L > 4.6$ (it provides sufficient accuracy in calculating gains as explained in the next section). Using (6.15) the effective beam's length or effective control time will be defined by:

$$L_{eff} = t_{eff} \geq \frac{6.505}{\lambda_1\sqrt{1-\varsigma_1}} \tag{6.16}$$

The control parameters λ_1 and ς_1 are used to determine the control time required to suppress all the modes. This is because $\lambda_1\sqrt{1-\varsigma_1} \leq \lambda_2\sqrt{1-\varsigma_2} \leq \lambda_3\sqrt{1-\varsigma_2}.....$, which means that to eliminate vibrations of the first mode the longest period is required.

6.6 Optimal Modal Gains from the Beam Analogy

Once the effective beam length (or the effective time for the control problem) is correctly determined, the beam analogy can be run. It will provide the values of modal displacements $\eta_i(t)$, modal velocity $\dot{\eta}_i(t)$ and modal control $U_i(t)$ for $t = 0, t_1, t_2 \ldots$ corresponding to the sequence of nodal points along the beam. A line representing $U_i(t)$ as a function of $\eta_i(t)$ and $\dot{\eta}_i(t)$ is referred to as the modal trajectory. In the coordinate system η_i, $\dot{\eta}_i$ and U_i such a line will generally have a spiral shape converging to the plot's origin as shown in Figure 6.4a (this figure is plotted using U_1, η_1 and $\dot{\eta}_1$ calculated for the example discussed in section 6.9.1). According to Eq. (6.2) the modal trajectory must be flat and entirely on a certain plane *S*. If such a plane is identified then, the modal gains g_{id} and g_{iv} can directly be related to its slopes or to the angles φ_d and φ_v indicated in Figure 6.4b. Note, however, that from the beam analogy the modal trajectory is obtained only in the parametric form, and the interceptions of the plane *S* with planes U_i, η_i (line *OA*) and $U_i, \dot{\eta}_i$ (line *OB*) are not directly available. Also, if the beam used in the calculations is not sufficiently long, or if some calculation errors are present, then the trajectory will not be flat and no plane can be identified. There are several methods to verify correctness of the analysis, and to calculate slopes of the plane (if the analysis is correct). One method could be to plot the modal trajectory in the coordinates $\overline{\eta}_i$ and $\dot{\overline{\eta}}_i$ rotated in such a way that the plane *S* is seen as a straight line (Figure 6.4c).

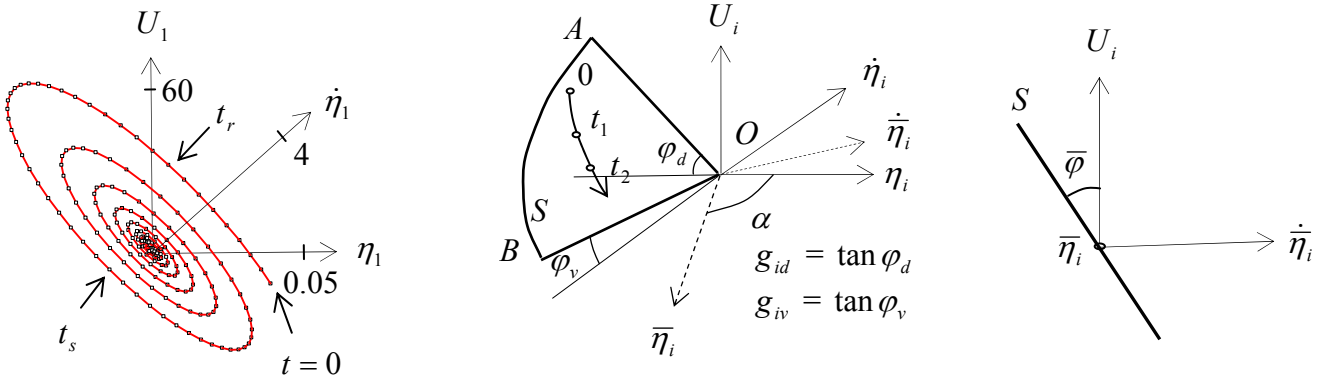

a) Modal Trajectory b) Parameters of Plane *S* c) Flatness Test

Figure 6.4 The Modal Coordinates

If the straight line representation of plane S is obtained (via rotating the coordinate system by an angle α), and if the inclination of this line in the new coordinate system is $\overline{\varphi}$,

than the gains can be calculated from:

$$g_v \tan\alpha - g_d = 0 \tag{6.17}$$

$$g_d \sin\alpha + g_v \cos\alpha = \tan\overline{\varphi} \tag{6.18}$$

The geometrical manipulations indicated in Figure 6.4 can be done automatically using graphical software (such as **ORIGIN 6,** for example).

The gains can also be calculated by simply considering some points along the flat trajectory (say, at t_r and t_s). At these points, for known values of the modal controls and modal variables, the gains can be determined from:

$$U_i(t_r) = -g_{id}\eta_i(t_r) - g_{iv}\dot{\eta}_i(t_r) \tag{6.19}$$

$$U_i(t_s) = -g_{id}\eta_i(t_s) - g_{iv}\dot{\eta}_i(t_s) \tag{6.20}$$

For practical reasons the instances t_r and t_s should be selected such that the corresponding points on the plane S are separated by the sufficient distance and are sufficiently away from the origin. The above methods will be discussed in more detail in section 6.9 where the numerical example is presented.

6.7 Optimal Gain Matrix for the System

According to Eq. (6.2) the vector of modal controls can be written as

$$U = -g \cdot \begin{bmatrix} \eta \\ \dot{\eta} \end{bmatrix} \tag{6.21}$$

where $g = \begin{bmatrix} g_d & g_v \end{bmatrix}$ and g_d and g_v are diagonal matrices of modal gains (with the terms g_{id} and g_{iv} along the diagonals) calculated from the beam analogy as explained in the previous section. Substituting (6.21) into Eq. (4.7), the system's response in the modal space can be determined. The 'effective' damping $\overline{\Delta}_{ii} = \Delta_{ii} + g_{iv}$, and the 'effective' frequency $\overline{\omega}_i^2 = \omega_i^2 + g_{id}$ will characterize this response. As long as $g_{iv} > -\Delta_{ii}$ and

$g_{id} > -\omega_i^2$ the system's vibrations will be continuously decaying. In particular, the attenuation should always result for positive values of the modal gains.

Similarly as in [Meirovitch, L., and Baruh, H., 1982] it was assumed that n_a actuators will control $s = n_a$ lowest vibration modes, with the modes higher than s uncontrolled. Practicality of such an assumption is normally justified by the higher energy needed to excite the higher modes (resulting in small amplitudes of disturbance for higher modes) and by a larger effect from structural damping, always present in physical systems, on the higher modes (consequently, such modes will be damped out naturally). If the number of modes considered, *s*, is equal to the number of actuators, then the vector of modal gains is related to the vector of control forces by the following relation:

$$F_c = \widetilde{\Phi}^{-1} U \tag{6.22}$$

where as already explained, $\widetilde{\Phi} = \Phi^T B_a$, and where B_a is the placement matrix for actuators and it has all *zero* components except where the actuators are positioned.

Similar to the controllability of the structure (in chapter 4 section 4.2) one more property known as observability can be introduced in reference to control of dynamic systems. In the next section observability is explained along with some examples.

6.7.1 Observability

As explained in chapter 2 section 2.3 the system state (in the form of error) is needed so that control forces can be obtained by feeding it to the gain matrix. States can be obtained from the system's output by using some sensors. Like actuators sensors have to be placed at certain specified locations on the system. If the actuators and the sensors are positioned on the structure to be controlled at the same places, then this kind of system is called collocated, and if they are positioned at different places then it is called a non-collocated system.

As explained before controllability measures the particular actuator input configuration‘s ability to control all system states, in a similar way observability measures the particular sensor output configuration's ability to obtain the information needed to estimate all system states.

An important difference can be seen here between classical control and control using the beam analogy, in classical control the matrix A (Eq. (2.2)) is the system's matrix but here it will take the form of a modal displacement matrix Φ because here the modal space is used.

Now assume that there are n_0 sensors (where $2s \le n_0 \le n$) monitoring the system's response (the output) in terms of the DOFs and their derivatives in the following general way:

$$y_i = \sum_{j=1..m} C_d^{ij} x_j + C_v^{ij} \dot{x}_j \qquad i = 1..n_0 \quad \text{or} \quad y = \widetilde{C} \cdot \begin{bmatrix} x \\ \dot{x} \end{bmatrix} \tag{6.23}$$

where $\widetilde{C} = \begin{bmatrix} C_d & C_v \end{bmatrix}$ is a known matrix of dimensions $n_0 \times 2n$.

In the beam analogy not all DOFs of the structure are considered since only a finite number of modes using modal space are controlled. Here also Eq. (6.23) is calculated in the form of modal variables using $x = \Phi\eta$ given by Eq. (6.24)

$$y = \hat{C} \cdot \begin{bmatrix} \eta \\ \dot{\eta} \end{bmatrix} \tag{6.24}$$

where matrix $\hat{C} = \begin{bmatrix} \hat{\Phi} & \breve{\Phi} \end{bmatrix}$ has the dimensions $n_0 \times 2s$

where $\hat{\Phi} = C_d \Phi$ and $\breve{\Phi} = C_v \Phi$

Here one can see that the system's matrix of n DOFs now reduces to the modal displacement matrix of dimension $n_0 \times 2s$.

Inverting Eq. (6.24), the modal variables can be recovered from the measurement vector as:

$$\begin{bmatrix} \eta \\ \dot{\eta} \end{bmatrix} = H \cdot y \tag{6.25}$$

where $H = (\hat{C}^T \hat{C})^{-1} \hat{C}^T$

The system is observable if H can be inverted.

6.7.2 Examples

Some examples to demonstrate the observability of the system are shown by using the fin structure (Figure 5.2) and for controlling *two* or *four* modes with *two* or *four* actuators.

In the example a collocated system is assumed, i.e. the location of sensors are same as that of the actuators. As in chapter 5 in section 5.4.1 actuators are placed at node uy_2 and uy_{12}. Sensors are also placed on the structure in a similar manner at uy_2 and uy_{12}. This way the output vector will be:

$$y_d{}^T = \begin{bmatrix} uy_2 & uy_{12} \end{bmatrix} \tag{6.26}$$

The output vector will have two components, and therefore $n_0 = 2$.

Matrix $\hat{C}$ in Eq (6.24) will have the form:

$\hat{C} = \begin{bmatrix} \bar{\Phi} & 0 \\ 0 & 0 \end{bmatrix}$ where $\bar{\Phi} = C_d \Phi = \begin{bmatrix} .28181 & .40179 \\ .28181 & -.40179 \end{bmatrix}$ as $C_d = \begin{bmatrix} 1 & 0 \\ 0 & 1 \end{bmatrix}$ (because sensors are placed at node 2 and 12 only, the rest of the values will be *zero*). The Φ matrix is the same as it was in chapter 5 section 5.4.1.

Clearly the *C* matrix is singular as its inverse does not exist. This shows that the system is not observable.

To make it observable, assume that the displacement readings are automatically differentiated, to obtain the displacement velocity readings i.e.: $\dot{y}_d{}^T = \begin{bmatrix} u\dot{y}_2 & u\dot{y}_{12} \end{bmatrix}$ and therefore $n_0 = 4$.

In that case

$$\hat{C} = \begin{bmatrix} \bar{\Phi} & 0 \\ 0 & \bar{\Phi} \end{bmatrix} \tag{6.27}$$

and $(\hat{C}^T \hat{C})^{-1} (\hat{C})^T$ exists hence the system is observable.

In the case of four actuators again:

$\hat{C} = \begin{bmatrix} \bar{\Phi} & 0 \\ 0 & \bar{\Phi} \end{bmatrix}$ but here

$\widehat{\Phi} = C_d \Phi$ is 4×4 matrix since the first four modes of the fin structure are controlled and $n_0 = 8$. The Φ matrix is the same as it was in Chapter 5 section 5.4.5 and again $(\hat{C}^T \hat{C})^{-1} (\hat{C})^T$ exists so the system is observable.

to obtain constant gains using (6.21) and (6.22) use:

$$F_c = -\widetilde{\Phi}^{-1} \cdot g \cdot (\hat{C}^T \hat{C})^{-1} \hat{C}^T \cdot y = -G \cdot y \tag{6.28}$$

where the optimal gain matrix for the system, *G* (dimension $n_a \times n_0$) is defined as:

$$G = \Phi^{-1} g (\hat{C}^T \hat{C})^{-1} \hat{C}^T \tag{6.29}$$

in Eq. (6.28) any measurement noise is neglected.

In the next section an algorithm called the Gain Algorithm (GA) is presented to get control forces from the constant feedback gain matrix.

6.8 Gain Algorithm

The Gain Algorithm (GA) to obtain the optimal gains from the beam analogy contains seven steps shown in Figure 6.5. Some more important details involving the particular steps will be explained on the examples that follow. This algorithm is a modification of the BAA already presented in Figure 5.1, chapter 5. Note that no iterations are required. Also note that the matrix of modal gains can be calculated for the structure independently of the locations of actuators and sensors, and that the initial disturbances for simulating the structure's response can arbitrarily be assumed.

START

↓

Step1 Generate a **DYNAMIC MODEL** of the structure
Run modal analysis to obtain Ω and Φ

↓

Set optimization parameters α_i, β_i, *and* γ_i

Step2 Determine the parameters of the analogous **BEAMS**
Calculate length of the analogous beam's L_{eff} from Eq. (6.16)

↓

Step3 Generate static **BEAMS MODEL** to solve Optimality Equation
Determine v, θ, M_b, and T

↓

Step4 Transfer the **BEAMS MODEL** results back to the modal solutions
Calculate control forces $F_c(t)$, and response $y(t)$

↓

Plot the modal trajectory for the first mode using $\eta_1(t)$, $\dot{\eta}_1(t)$ and $U_1(t)$

Step5 Rotate coordinate system to verify whether the trajectory is plane
Calculate g_{1d} and g_{1v}, and repeat the calculations for the remaining modes to obtain g_{id} and g_{iv}

↓

Step6 Calculate G from Eq. (6.29)

↓

Step7 Verify the *G*'s values by substituting the results from **Step 4** for selected time instances into in the relation $F_c(t) = -G \cdot y(t)$

Figure 6.5 Flowchart of the GA

6.9 Numerical Example

Again consider the same fin structure (Figure 5.2) with all the values exactly the same as before (see chapter 5 section 5.4), the only difference is that it was previously controlled by the open loop control method and this time a feedback gain matrix is obtained for the closed loop control system. Step 1 and 2 are exactly the same as before the only difference is in the calculation of the effective length.

As discussed in section 6.5 an infinite process ($t_f \to \infty$) for time invariant control problems can be modelled in the beam analogy method by finite beams of the sufficient length L_{eff}. For the problem considered this length is $L_{eff} = 0.549m,$ as determined from Eq. (6.16). This completes **Step2** of the GA.

6.9.1 Optimal Gains for Two Actuators

The use of the GA will first be demonstrated on the case of two actuators placed at nodes 2 and 12 generating two forces F_1 and F_2 (Figure 6.6). Only the two lowest modes of the fin vibrations will be controlled. Also, for simplicity of presentation assume that the two sensors will monitor the vertical displacements at nodes 2 and 12 (collocated control). Two static analogous beams are needed to analyze the problem. The parameters of these beams, as calculated from Eq. (4.42-b,c,d), are shown in Figure 6.6. Both beams are 0.549 *m* long.

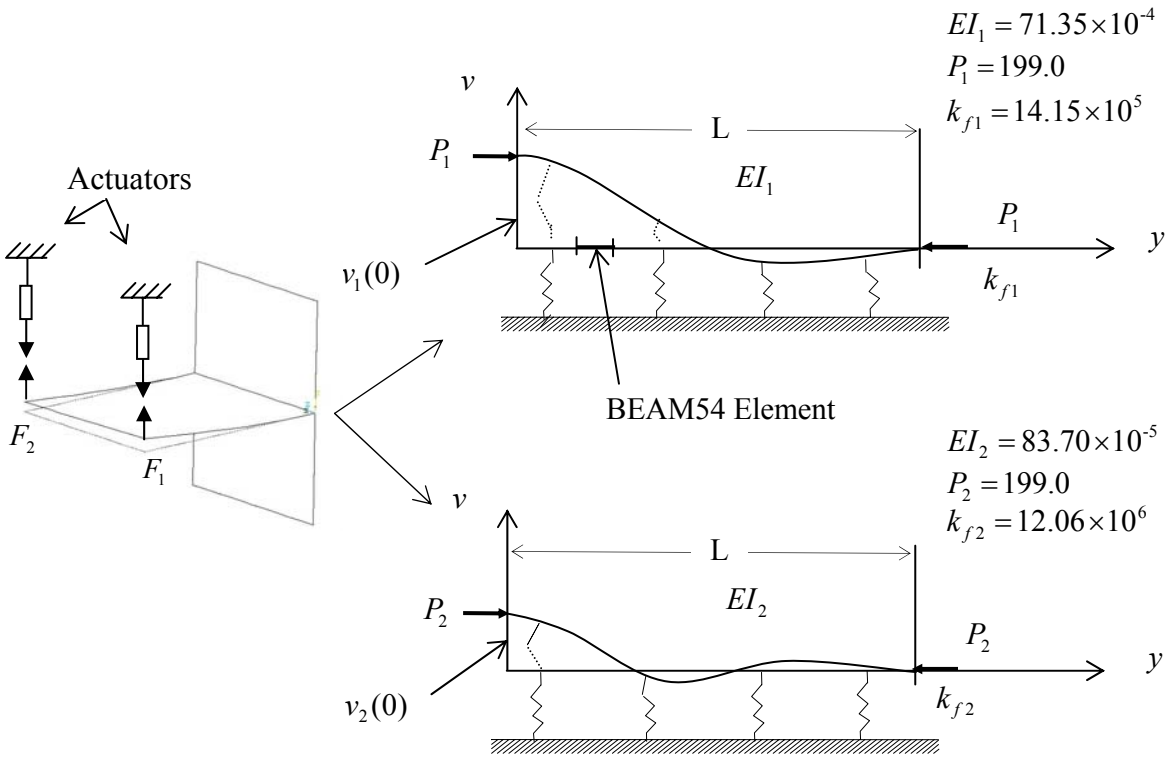

Figure 6.6 Analogous Beams for 2 Actuators

The analogous beams are meshed with BEAM54 elements (200 elements for each beam). The deflections and rotations at the left end of the beams are the same as the initial values of the modal variables i.e.: $v_1(0) = 0.05819,\ \theta_1(0) = 0,\ v_2(0) = 0.004670$ and $\theta_2(0) = 0$. The beams are then solved by ANSYS to obtain the static deflections, rotations and bending moments in terms of the coordinate *y*. This completes **Step 3** of the algorithm.

Now the results obtained from the fictitious static BEAMS MODEL can be converted into the optimal time variation of modal variables and controls (**step 4**). The modal variables and modal velocities of the structure are numerically identical to the displacements and slopes of analogous beams (see Eq. (4.44)) and are shown in Figure 6.7 and 6.8. The abscissa represents the time variable (in seconds).

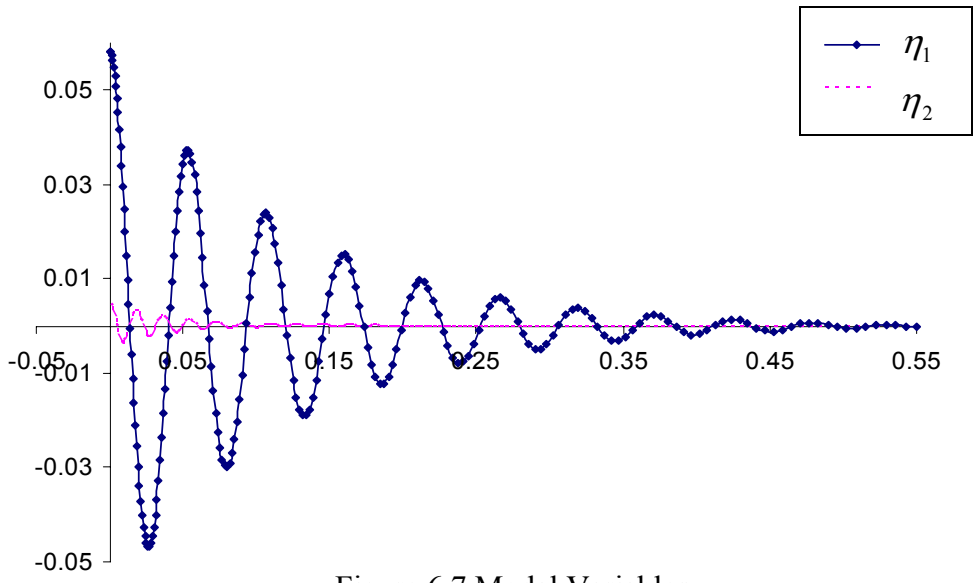

Figure 6.7 Modal Variables

Comparison for Modal Variables

Here the modal variables obtained in Figure 5.5 (chapter 5 section 5.4.1 finite time, i.e. $t_f = 0.05301$ case) and what was obtained in Figure 6.7 are compared. In the finite time case in Figure 5.5, the variable η_1 attained *zero* value in less then a cycle and η_2 attained *zero* after *two* complete cycles. In figure 6.7 one can easily see that η_1 completed almost *eleven* cycles before attaining a *zero* value and η_2 was almost zero after *six* cycles.

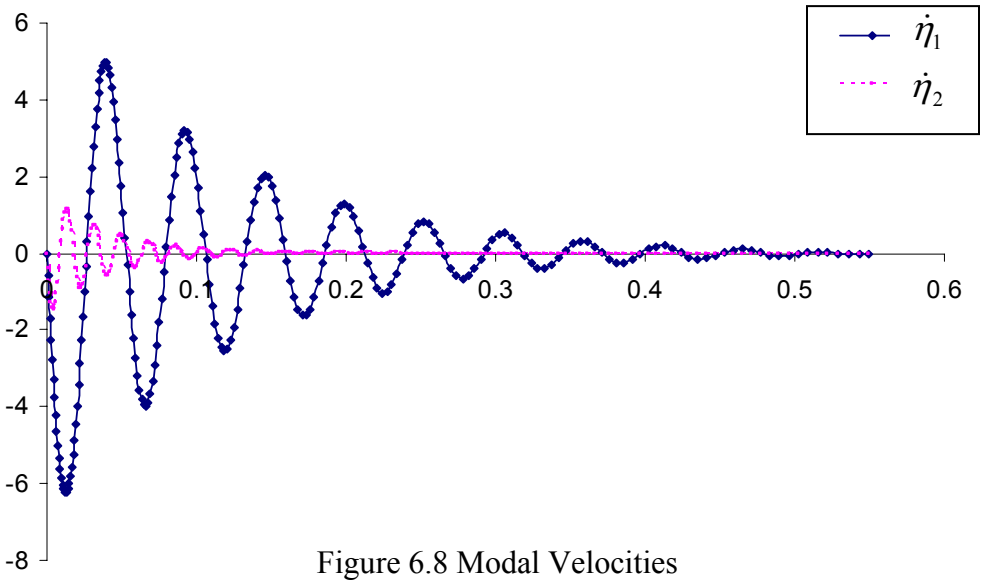

Figure 6.8 Modal Velocities

The modal controls are obtained from Eq. (4.45), and are plotted in Figure 6.9.

Note that since the initial disturbance is only slightly asymmetric the modal variable and control for the 2nd mode are small in comparison with the corresponding values for the 1st mode.

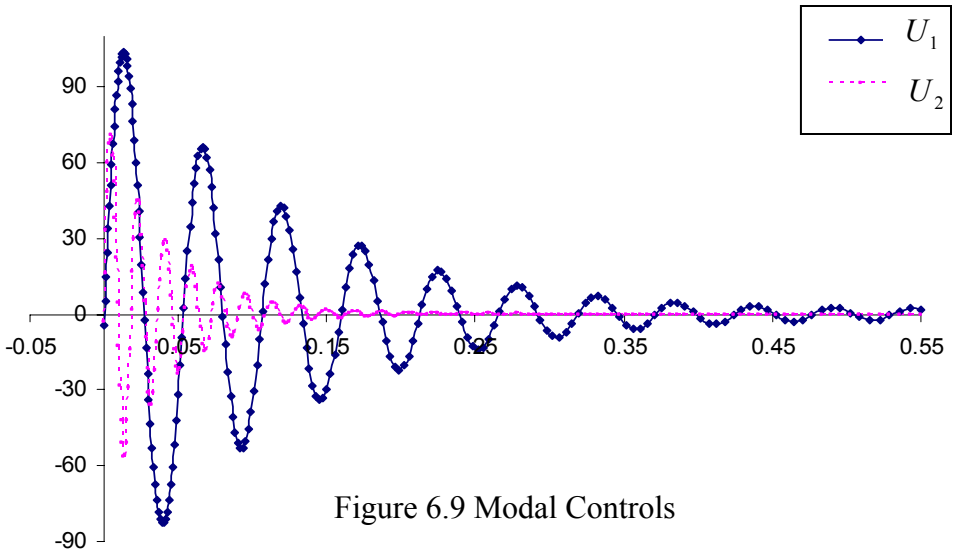

Figure 6.9 Modal Controls

Comparison for Modal Controls

Here Figure 6.9 is compared with Figure 5.6 (chapter 5 section 5.4.1 with finite time case). In Figure 5.6, U_1 had a maximum value of around 280 and was almost *zero* in one cycle, and U_2 with a maximum value of 85 was not completely *zero* even after *three* complete cycles.

On the other hand in the infinite time period case (Figure 6.9), U_1 had a maximum value of 110 (this is less compared to the finite time case) and was at almost zero in *eleven* cycles. While U_2 with a maximum value of 70 was zero after *eleven* cycles (with much smaller time periods).

The magnitudes of the control forces can be obtained from Eq. (4.46), which for the two modes considered takes the form: $\begin{bmatrix} F_1 \\ F_2 \end{bmatrix} = \widetilde{\Phi}^{-1} U = \begin{bmatrix} .28181 & .28181 \\ .40179 & -.40179 \end{bmatrix}^{-1} \begin{bmatrix} U_1 \\ U_2 \end{bmatrix}$ (6.30)

Such a form is the result of matrix B_a containing unit value entries corresponding to the uy_2 and uy_{12} positions and zeros everywhere else. Substituting *U's* from Figure 6.9 one obtains the control forces as shown in Figure 6.10.

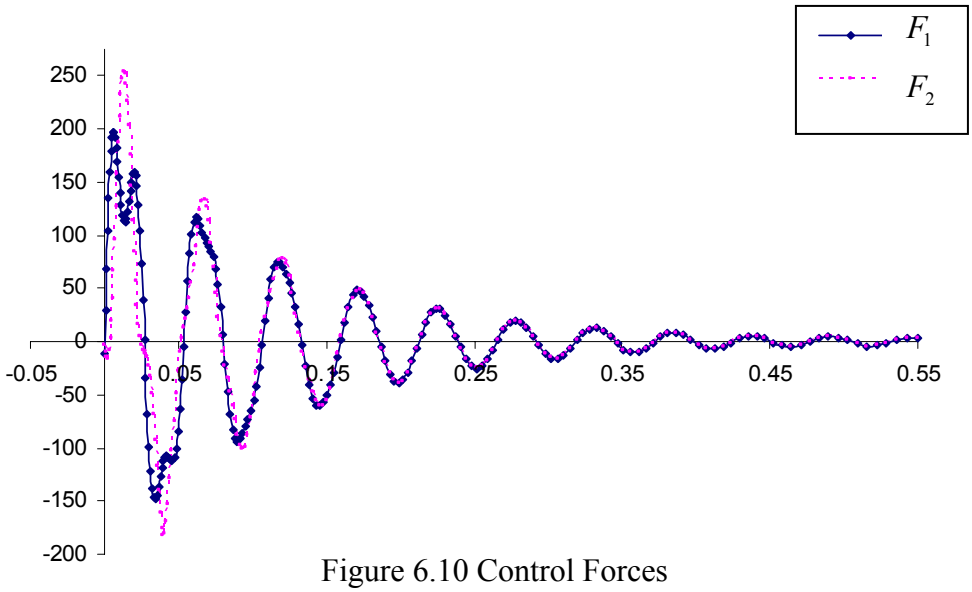

Figure 6.10 Control Forces

Note that forces F_1 and F_2 are visibly different only at the beginning of the process. After the effects associated with the 2nd mode are eliminited (for $t \geq 0.1s$) the actuators act almost identically. Also note that these forces will not excite higher modes (no spillover effect) by virtue of Eq. (6.21) all $U_i = 0$ if $i > s$ ($s = 2$ for this case).

If control forces in Figure 5.7 are compared (see finite time period Chapter 5 Section 5.4.1), the forces are of higher magnitudes (the maximums for F_1 and F_2 are $423N$ and $557N$ respectively) for both the actuators.

The histograms for any DOFs over the entire process can be obtained from Eq. (4.43) in the form $x^{(2)} = \Phi_1\eta_1 + \Phi_2\eta_2$. The symbol $x^{(j)}$ denotes the values calculated using $j = 2$ modes only. For example the vertical displacements at the nodes 2 and 12 are as shown in Figure 6.11.

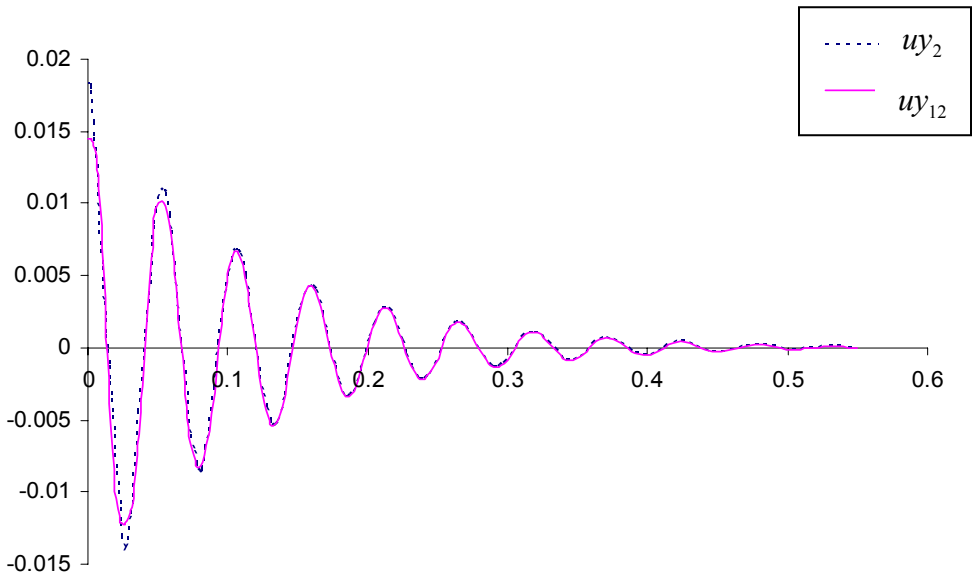

Figure 6.11 The vertical displacements at nodes 2 and 12

The nodal velocities can be calculated from $\dot{x}^{(2)} = \Phi_1\dot{\eta}_1 + \Phi_2\dot{\eta}_2$ where the modal velocities are shown in Figure 6.8.

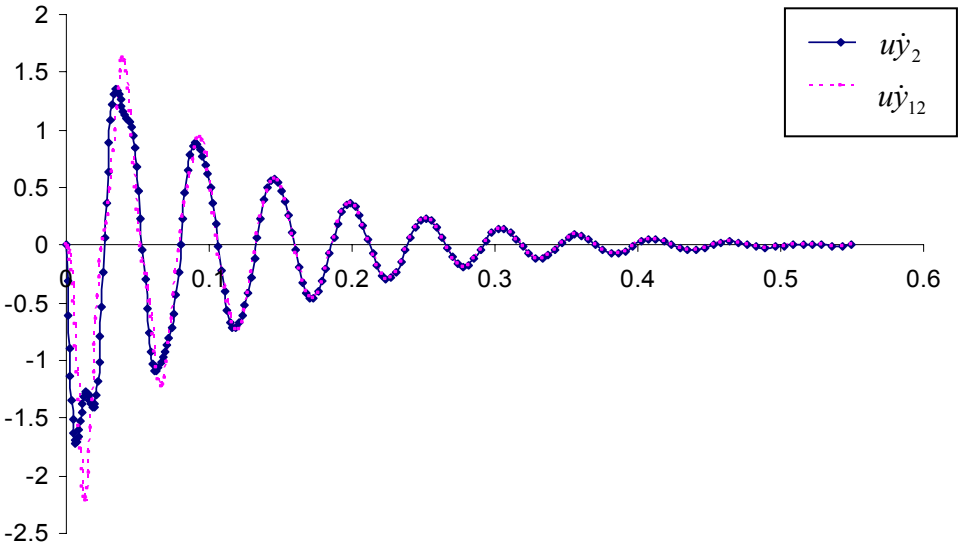

Figure 6.12 The Vertical Velocities of Nodes 2 and 12

The vertical velocities of nodes 2 and 12 are plotted in Figure 6.12. This completes **Step 4**. The plots in Figures 6.10, 6.11 and 6.12 will be used later to verify the gains for the system (see **Step 7**).

The phase diagrams (i.e. : $U_i(t)$ vs. $\eta_i(t), \dot{\eta}_i(t)$) are obtained in **Step 5**. The modal trajectory plot for the first mode, using the results presented in Figures 6.7, 6.8 and 6.9, was shown in Figure 6.4a. The plot was generated with the help of the software **ORIGIN 6** and can be rotated to obtain the image shown in Figure 6.4c. However, due to the large difference in the numerical scales of $\eta_i(t), \dot{\eta}_i(t)$ and $U_i(t)$ axes (see Figure 6.4a), reading the angles φ_d and φ_v from the plot is somewhat difficult, therefore **ORIGIN 6** was only used to confirm the trajectory's flatness. For the values of the modal gains the method of two time instances, Eq. (6.19) and (6.20), was found to be more convenient to use and reasonably accurate.

For example, if several t_r and t_s are somewhat randomly chosen the numerical values of these modal gains for the first mode are calculated from Eq. (6.19) and (6.20) and listed in Table 6.1.

t_r	t_s	g_{1d}	g_{1v}
7.01E-04	1.41E-03	69.96	16.73
2.85E-03	3.59E-03	69.97	16.73
6.61E-03	7.39E-03	70.01	16.73
1.48E-02	1.57E-02	70.06	16.73
2.60E-02	2.70E-02	69.99	16.74

Table 6.1 Modal Gains for First Mode

As can be seen from Table 6.1, scatter of the results is relatively small. This proves that the L_{eff} used in the beam analogy is long enough, and the resulting modal trajectory is sufficiently flat. Averaging these values $g_d = 70.00$ and $g_v = 16.73$, one can then calculate $\varphi_d = 89.18^0$ and $\varphi_v = 86.57^0$ (see Figure 6.4b). On the plot in Figure 6.4a

generated by **ORIGIN 6,** these angles are actually 3.20^0 and 45.20^0 respectively, due to the distortion caused by the different coordinate scales.

Using a similar procedure g_d and g_v can be calculated for the second mode (see Table 6.2):

t_r	t_s	g_{2d}	g_{2v}
7.01E-04	1.41E-03	596.63	48.87
3.59E-03	4.33E-03	597.90	48.87
6.61E-03	7.39E-03	597.96	48.87
6.61E-03	7.39E-03	597.43	48.87
8.97E-03	9.78E-03	596.88	48.88

Table 6.2 Modal Gains for Second Mode

Both the modal gains are positive for both the modes, which means the conditions mentioned in Section 6.7 ($g_{iv} > -\Delta_{ii}$ and $g_{id} > -\omega_i^2$) are satisfied. As in the case presented structural damping is vanishing, i.e.: $\Delta_{ii} = 0$.

6.9.2 Physical Gain Matrix for First Two Modes

With two sensors reading the vertical displacement of the nodes where the actuators are attached, the displacement readings vector is defined as $y_d{}^T = [uy_2 \quad uy_{12}]$. Also, assume that the displacement readings are automatically differentiated to obtain the displacement velocity readings i.e.: $\dot{y}_d{}^T = [u\dot{y}_2 \quad u\dot{y}_{12}]$ (as explained in section 6.7.2). This way the output vector $y^T = [y_d^T \quad \dot{y}_d^T]$ will then have four components, and therefore $n_0 = 4$. Matrix $\hat{C}$ will have the form given by Eq. (6.27).

Note that a control system with any other set of sensors for which the matrix $\hat{C}^T\hat{C}$ is not singular will be treated identically.

The system's gains *G* can now be calculated from Eq. (6.29) by directly substituting matrices $\widetilde{\Phi}^{-1}$ and $\hat{C}$ from (6.30) and (6.27) respectively, and the modal gains, *g*, from Tables 6.1 and 6.2.

However, for problems with actuators and sensors at the same locations one has $C_d = B^T$ and $(\hat{C}^T\hat{C})^{-1}(\hat{C})^T = \widetilde{\Phi}^{-1}$. Therefore, for collocational systems Eq. (6.28) can be simplified to the form:

$$F_c = -\widetilde{\Phi}^{-1} \cdot g \cdot \begin{bmatrix} \widetilde{\Phi}^{-T} & 0 \\ 0 & \widetilde{\Phi}^{-T} \end{bmatrix} \cdot y = -G_d y_d - G_v \dot{y}_d \tag{6.31}$$

where

$$G_d = \widetilde{\Phi}^{-1} g_d \widetilde{\Phi}^{-T} \text{ and } G_v = \widetilde{\Phi}^{-1} g_v \widetilde{\Phi}^{-T} \tag{6.32}$$

For the case of two actuators:

$g_d = \begin{bmatrix} 70.00 & 0 \\ 0 & 597.36 \end{bmatrix}$ and $g_v = \begin{bmatrix} 16.73 & 0 \\ 0 & 48.87 \end{bmatrix}$ (see Table 6.1 and 6.2 in section 6.9.1).

Substituting into (6.32) one obtains:

$$G_d = \begin{bmatrix} 1145.43 & -704.72 \\ -704.72 & 1145.43 \end{bmatrix} \text{ and } G_v = \begin{bmatrix} 128.34 & -23.01 \\ -23.01 & 128.34 \end{bmatrix} \tag{6.33}$$

For verification purposes, the control forces at a particular instant in time can be obtained from Eq. (6.31) by using the gains (6.33) and the values of $y_d(t)$ and $\dot{y}_d(t)$. For example at $t_1 = 0.0676$, the plots in Figure 6.11 and 6.12 give :

$y_d^T(t_1) = \begin{bmatrix} -0.000866 & -0.000681 \end{bmatrix}$ and $\dot{y}_d^T(t_1) = \begin{bmatrix} -0.973 & -1.22 \end{bmatrix}$ respectively.

Substituting into (6.31) one obtains:

$$\begin{bmatrix} F_1(t_1) \\ F_2(t_1) \end{bmatrix} = -G_d \cdot y_d(t_1) - G_v \cdot \dot{y}_d(t_1) = \begin{bmatrix} 97.40 \\ 134.40 \end{bmatrix} \tag{6.34}$$

which is the same as the result obtained from the beam analogy (see plot in Figure 6.10). This confirms that the gains were calculated correctly.

6.9.3 Consequences of Insufficient Beam Length

In the previous section the modal gains g_d and g_v were determined after calculating the effective length using Eq. (6.16). To explain the consequences of using beams that are too short, consider the beam length of $L = 0.05301$ (finite beam length from the case 1 section 5.4.1).

The GA was followed step by step and the trajectory was plotted (Figure 6.13) using **ORIGIN 6** in **Step5**, i.e. checking the flatness of the trajectory. For this case efforts have been made to manipulate (in **ORIGIN 6**) the trajectory to get it into a single plane. Figure 6.13 is the best manipulation that was obtained, clearly the trajectory is not flat.

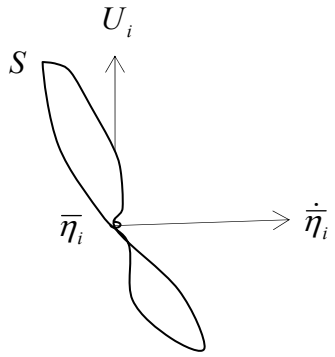

Figure 6.13 Trajectory from Insufficient Beam Length

6.9.4 Optimal Gains for Four Actuators

Consider four actuators attached vertically at nodes 2, 12, 7 and 27 (see Figure 5.2 for the nodes location) to control four vibration modes. The set of four analogous beams (Figure 6.14) has to be considered.

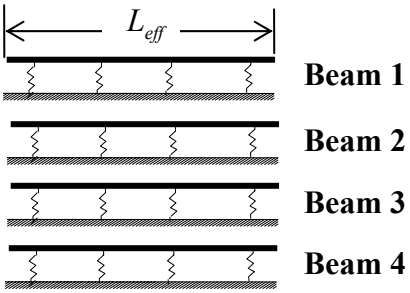

Figure 6.14 Four Analogous Beams

The modal gains for four modes are obtained using a procedure that is identical to the one used for two modes discussed earlier.

These results are listed in Table 6.3. The pairs of t_r and t_s were the same as shown in Table 6.1.

i	g_{id}	g_{iv}
1	70.00	16.73
2	597.36	48.87
3	2774.16	104.70
4	8011.66	175.48

Table 6.3 Modal Gains for Four Modes

One can observe that for the first two modes the modal gains are the same as determined in section 6.9.2 (see Tables 6.1 and 6.2).

Now matrix $\widetilde{\Phi}$ is obtained as:

$$\widetilde{\Phi} = \begin{bmatrix} .28181 & .28181, & .091711 & .091711 \\ .40179 & -.40179 & 21356, & -.21356 \\ .24162 & .24162 & -.24127 & -.24127 \\ .44086 & -.44086 & -.31912 & .31912 \end{bmatrix} \tag{6.35}$$

Assuming as before the collocated sensors $y_d{}^T = [uy_2 \quad uy_{12} \quad uy_7 \quad uy_{27}]$ and $\dot{y}_d{}^T = [u\dot{y}_2 \quad u\dot{y}_{12} \quad u\dot{y}_7 \quad u\dot{y}_{27}]$ meaning that the output y has now $n_0 = 8$ components. The system's gain matrix can again be determined from Eq. (6.32). Following the procedure discussed in section 6.9.2:

$$G_d = \begin{bmatrix} 2998.01 & -1311.84 & -5130.67 & 970.76 \\ -1311.84 & 2998.01 & 970.76 & -5130.67 \\ -5130.67 & 970.76 & 14028.70 & -223.26 \\ 970.76 & -5130.67 & -223.26 & 14028.70 \end{bmatrix}$$

$$G_v = \begin{bmatrix} 122.67 & -8.57 & -94.60 & -11.87 \\ -8.57 & 122.67 & -11.87 & -94.60 \\ -94.60 & -11.87 & 477.06 & 94.57 \\ -11.87 & -94.60 & 94.57 & 477.06 \end{bmatrix}$$

This calculation would be similar if the number and location of sensors or actuators were altered. If the sensors and actuators are not collocated, then one has to use Eq. (6.29), instead of Eq. (6.32), to determine the system's optimal gains.

6.10 Comment on the Meshing of Analogous Beams

As discussed previously the static analogous beams are modelled in the spatial domain and modal results are calculated after applying the boundary conditions to the beams. Now the question arises as to how many beam elements and of what size are needed for sufficient accuracy? The answer to this question depends on the periods of the vibrations of the modes to be controlled.

Remember that each element represents the time step Δt. The highest mode is attenuated first, and if the period of vibration of the highest mode control is T_s, then for an accurate integration the elements length at the beginning should be about $\frac{T_s}{10}$.

The first mode is attenuated last, so the elements on the RHS of the beam should have the length of about $\frac{T_1}{10}$. For minimum computational effort the element length should vary from $\frac{T_s}{10}$ to $\frac{T_1}{10}$.

To develop the distribution of elements over the entire beam, a method called the spacing ratio is used. This is defined as the ratio of last division size to the first division size. In ANSYS, if the spacing ratio > 1.0, divisions increase, if < 1.0, divisions decrease. The ratio defaults to 1.0 (uniform spacing).

The spacing ratio can be defined mathematically as:

$$sp = \frac{a_0}{a_0 q^{n-1}} = q^{n-1} \tag{6.36}$$

where a_0 is the size of first element, $a_0 q^{n-1}$ is the size of the last element, q is the ratio between two consecutive elements and n is the total number of elements.

As mentioned before the spacing ratio can be assumed as:

$$sp = \frac{\mathrm{T_1}}{\mathrm{T_s}} \tag{6.37}$$

For the fin structure (the same as used in section 6.9) to control the first two modes, $T_1 = .0530$ and $T_s = 0.0181$. So here the *sp* needed is nearly equal to 3. Now the number and the size of each element over the total length L must be found, which would give approximately this spacing ratio. The whole beam (length *L*) is divided into two sections of lengths L_{11} and L_{22} (Figure 6.15).

Where L_{11} can be obtained from:

$$L_{11} = \frac{L}{mm}$$

where mm is a parameter. In the present case $mm = 2.5$ is assumed.

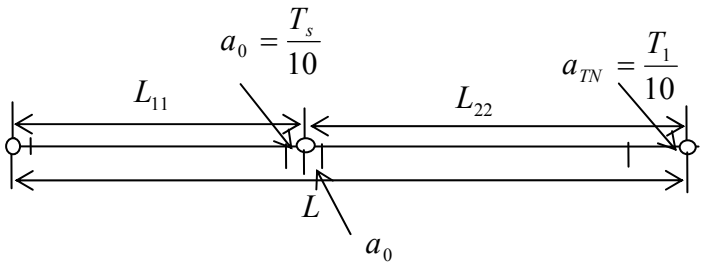

Figure 6.15 Two Divisions of Beam Model

The section L_{11} is divided into el_{11} elements of size a_0 for better accuracy of the control forces at the beginning. If el_{TN} is the total number of elements over the length L then

$$el_{11} = \frac{el_{TN}}{nn}$$

where nn is a parameter (in the case presented $nn = 1.667$ is assumed).

In the second section (length L_{22}) the elements with varying size (increasing) are used.

The number of elements over the length L_{22} is el_{22} where:

$L = L_{11} + L_{22}$ and $el_{TN} = el_{11} + el_{22}$

Because, over the length L_{22} the elements obey the geometrical series rule, one can write:

$$L_{22} = a_0 + a_0 q + ... + a_0 q^{el_{22}-1} \tag{6.38}$$

From which:

$$a_0 = \frac{L_{22}(q-1)}{q^{el_{22}}-1} = \frac{L_{22}}{\frac{q^{el_{22}}-1}{q-1}} \tag{6.39}$$

or using the sp parameter:

$$a_0 = \frac{L_{22}}{\frac{sp^{\frac{el_{22}}{el_{22}-1}}-1}{sp^{\frac{1}{el_{22}-1}}-1}} \tag{6.40}$$

It is desirable for the size of the first element in the length L_{22} of the beam to be equal to the size of last element in the length L_{11} (to avoid a large difference in the size of elements due to the change of section (i.e. from L_{11} to L_{22})), therefore:

$$a_0 = \frac{L}{mm.el_{11}} = \frac{L\left[1-\frac{1}{mm}\right]}{\frac{x^{el_{22}}-1}{x-1}} \quad \text{where } x = sp^{\frac{1}{el_{22}-1}} \tag{6.41}$$

or

$$(x-1)\cdot el_{11}(mm-1) = x^{el_{22}} - 1 \tag{6.42}$$

For the assumed *mm* and *nn* the value of sp can be obtained from Eq. (6.42).

For the calculation of spacing ratio to control the first two modes of the fin structure, the total length is $L = 0.549$ (Chapter 6 Eq. (6.16)), and $el_{TN} = 60$ for $mm = 2.5$ and $nn = 1.667$. The following can therefore be calculated:

$L_{11} = 0.2196,\ L_{22} = 0.3294$, $el_{11} = 36$ and $el_{22} = 24$

Finally from Eq. (6.42) the spacing ratio $sp = 4.21$ is obtained; the value of $sp = 5$ was used for convenience.

To see the difference, the modal controls and the control forces for $sp = 1$ (60 elements) and $sp = 5$ (60 elements) respectively, Figures 6.16, 6.17, 6.18, and 6.19 are plotted below.

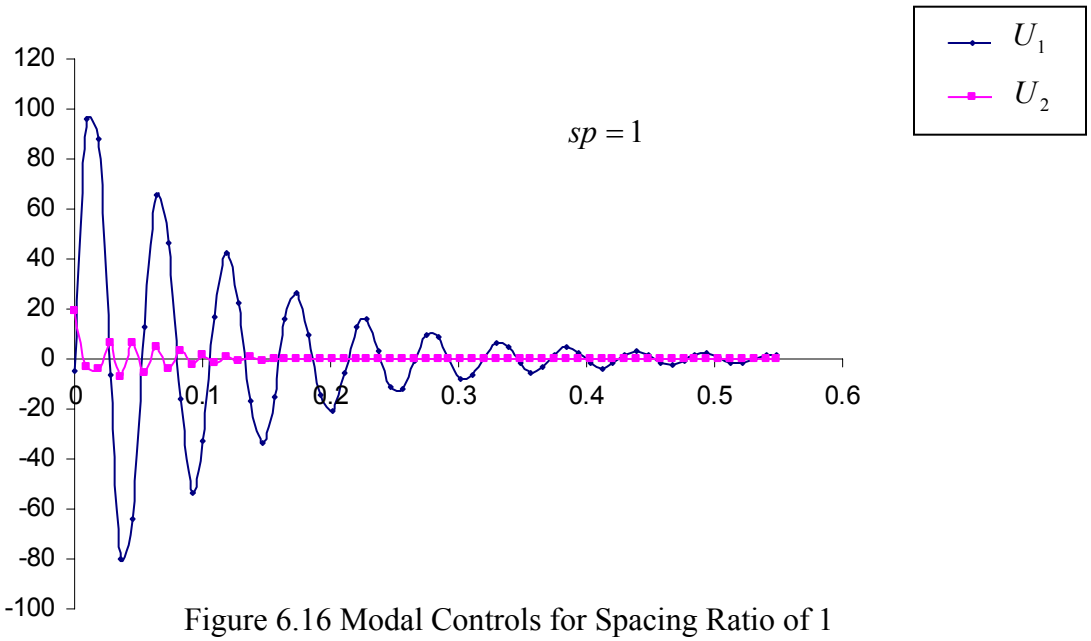

Figure 6.16 Modal Controls for Spacing Ratio of 1

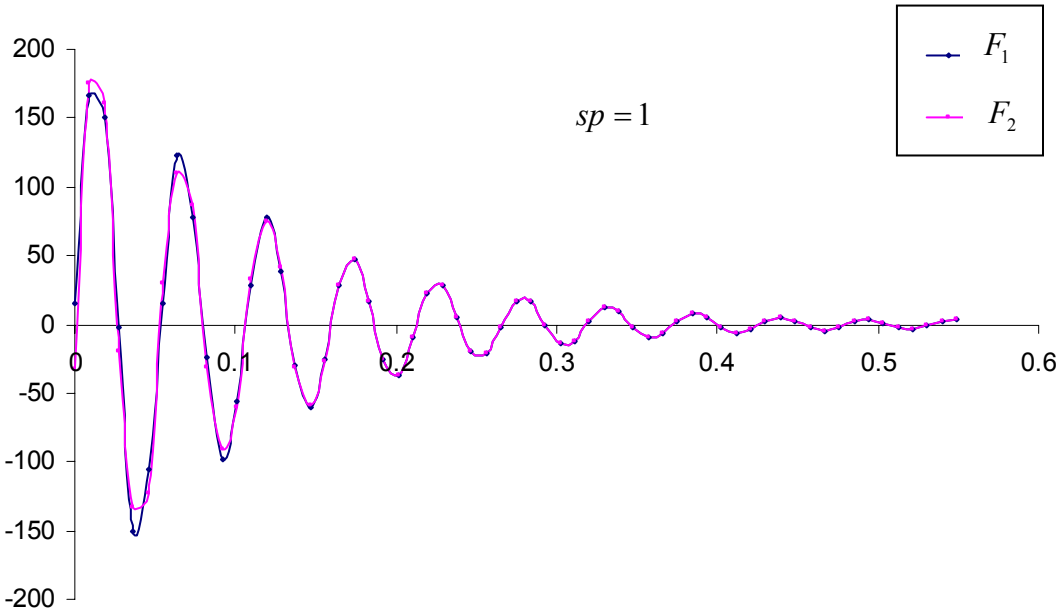

Figure 6.17 Control Forces for Spacing Ratio of 1

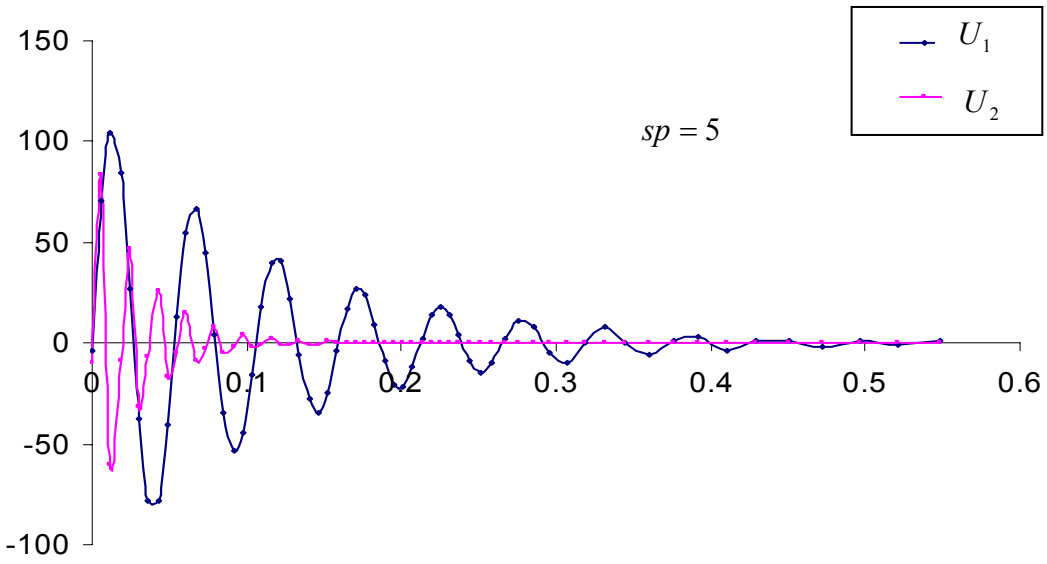

Figure 6.18 Modal Controls for Spacing Ratio of 5

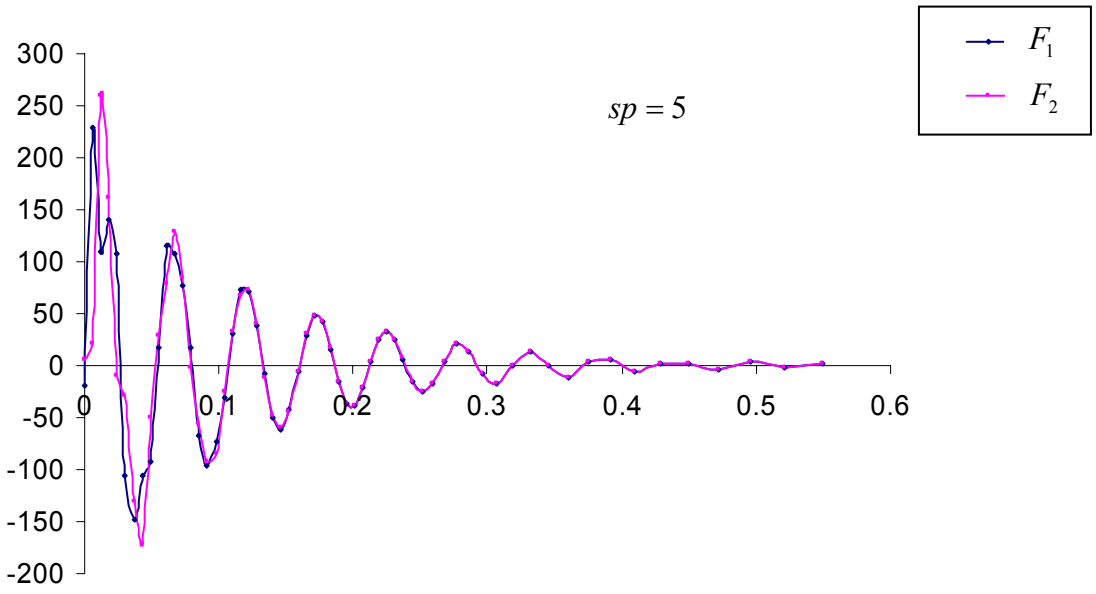

Figure 6.19 Control Forces for Spacing Ratio of 5

Clearly, the modal controls and control forces obtained by assuming 60 elements and $sp = 5$ (Figure 6.18 and 6.19) are very similar with what was obtained using 200 elements in chapter 6 Figure 6.9 and 6.10 on the other hand the equal division ($sp = 1$) is not capable of recreating the fast oscillations at the beginning of the control process (for $t \le 0.1$).

6.11 Comment on Solving the Target Condition ($H(t_f) = 0$)

In step 3 of the BAA (chapter 5 Figure 5.1) the value of the optimum L must be found by satisfying the target condition, i.e. $H(t_f) = 0$. For this purpose ANSYS design optimization module was used. If the behaviour of the L *v*s. $\hat{H}(t_f)$ is plotted, where $\hat{H}(t_f) = \ddot{\eta}_i^T \hat{R}_{ii} \ddot{\eta}_i$, it will be varying as in Figure 6.20.

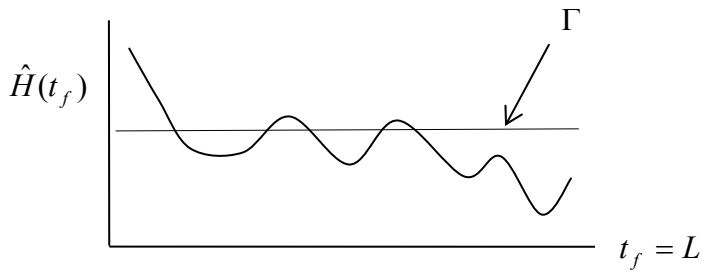

Figure 6.20 Target Condition Behaviour

Since $\hat{H}(t_f)$ must be equal to Γ to meet the target condition (as $H(t_f) = \hat{H}(t_f) - \Gamma = 0$), This means that there may be several local solutions, and the first solution that represents the optimum may be accidentally skipped.

To get an idea about this numerical difficulty, the actual values of $\hat{H}(t_f) = \hat{H}(L)$ are plotted in Figure 6.21.

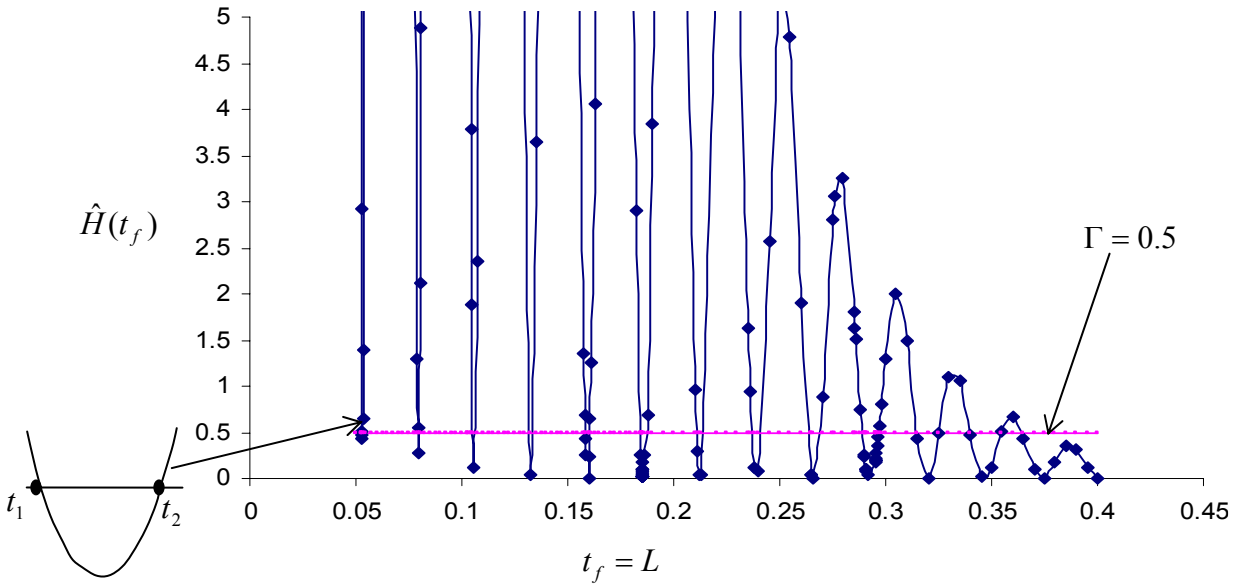

Figure 6.21 Behaviour of $\hat{H}(t_f)$ to Control First Two Modes of Fin structure

For example if $\Gamma = 0.5$, *twenty-five* values of t_f^k can be obtained, which satisfy the target condition (Figure 6.21). It can be demonstrated that each t_f^k results in an extremal value of the objective; i.e. $\delta J(t_f^k) = 0,$ with $\delta J(t_f^k) \to \min$ if the slope of $\hat{H}(t_f)$ is negative, and $\delta J(t_f^k) \to \max$ if the slope is positive (see Figure 6.22). Also, the global minimum is at $t_f^1,$ the smallest root of the target condition.

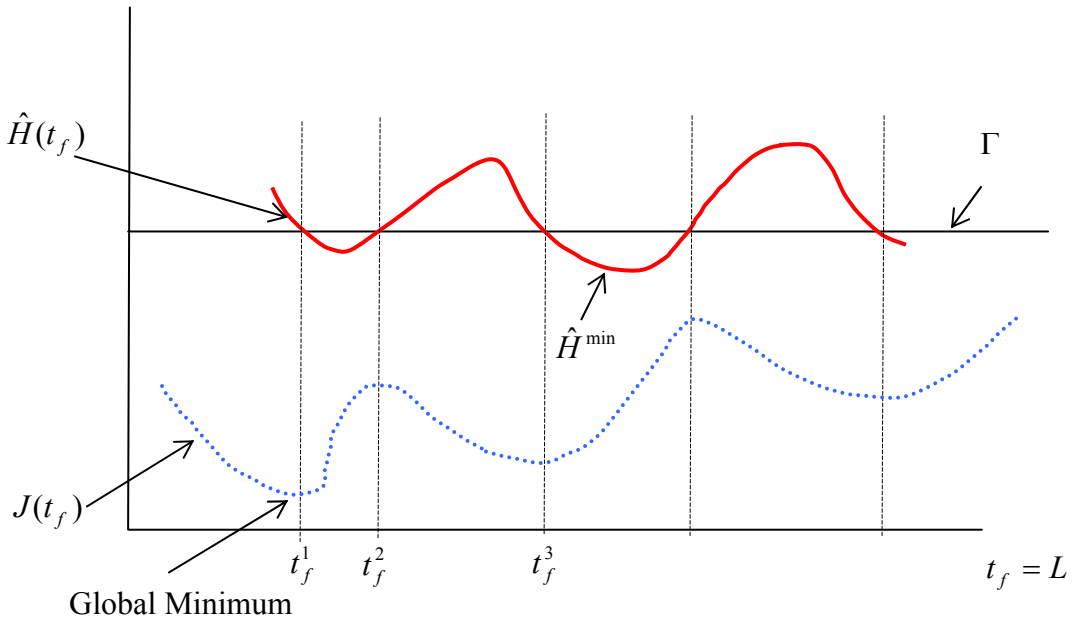

Figure 6.22 Global Optimum Point

The plots in Figure 6.21 and Figure 6.22 have several minima with the values of $\hat{H}^{\min}$ decreasing as t_f increases. It should be noted that $\hat{H}^{\min}$ are always positive and drop to *zero* only if $t_f \to \infty$ as shown in Figure 6.23.

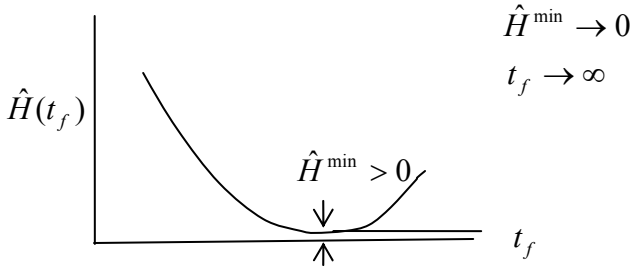

Figure 6.23 Behaviour of $\hat{H}(t_f)$ for Longer Times

Chapter 7 Conclusion and Future Work

7. 1 Conclusions

The control forces and the optimal trajectories for the active vibrations attenuation of structures are determined by the FEM that solves the corresponding TPBV optimal control problem. Since the optimality condition for the control problem is found to be similar to the problem of static bending of beams, an analogy (referred to as the beam analogy) between these two problems is used. The time domain (of control problems) can be discretized with the help of the 'static' Hermitian beam elements. The analogy is numerically convenient because the elements can be assembled and the solutions obtained by applying the standard FEM software used in structural analysis.

To control higher number of modes effectively and easily for the open loop control systems, generalization of the beam analogy procedure is done using the Beam Analogy Algorithm (BAA) and is based completely on the FEM technique. The BAA combines the FEM model of the analogous beams with a standard FEM model of the structure's dynamics to determine the optimal control forces and to simulate the system's response for the modes considered. The results of the BAA can be independently verified by running the transient dynamic analysis of the FEM structure's dynamic model. As illustrated by the examples, the optimization parameters and the set up of the control problem can be easily changed or modified. It allows for quick assessment of the magnitude of control forces, effectiveness of a particular placement of the actuators, duration of the processes, dynamic response of any part of the structure, etc.

A modified form of the BAA referred to as the Gain Algorithm (GA) was developed for vibration attenuations of the elastic structures for the closed loop control cases. GA uses a fictitious spatial domain and the FEM technique to determine the optimal gains for time-invariant vibration control problem. No iterations are required and Riccati's equation is not used. The method can be used with complex structures modelled using a large number of DOFs (it will affect only the FEM modal analysis required in Step1 of the GA Chapter 6). Also, the numerical effort required for obtaining optimal gains will be minimally changed if more actuators are used to control higher modes, if needed. Comment on the meshing of the analogous beam is presented. It will help in determining

the optimum number of the beam elements to get sufficient accuracy, which in turn will save computation time. Finally, comments to understand the behaviour of the target condition over the maneuver time t_f and to obtain the first optimal point are presented.

7.2 Future Work

In this thesis the total number of modes controlled were assumed equal to the number of actuators placed on the structure. In future work cases in which the number of modes controlled will be more then the number of actuators placed on the structure can be done.

Linear vibration problems were handled in this thesis. Work can be done in the field of nonlinear vibration attenuations problems.

It is also hope that the research presented in this thesis shall be included in future commercial finite element software packages to automatically handle optimal control problems.

REFERENCES

Abdullah, M.M., 1998, "*Optimal Location and Gains of Feedback Controllers at Discrete Locations*," AIAA Journal, 36(11):2109-2116

Athans, M. and Falb, P.L., 1966, "*Optimal Control,"* McGraw-Hill Book Company, New York.

Bathe, K. J., 1996, "*Finite Element Procedures,"* Prentice Hall, Englewood Cliffs, New Jersey

Choi, S. S., Sirisena, H. R., 1977, *"Computation of Optimal Output Feedback Controls for Unstable Linear Multivariable Systems,"* IEEE Transactions on Automatic Control, AC-22 :134-136

Fonseca, I. and Bainum, P., 1995, "*Simultaneous structural and control optimization of large space structures*," Appl. Mech. Rev. 48(11):S175-S179

Fonseca, Ijar M., Bainum, Peter, M. and Paulo Lourenção, T. M., 2002. "*Structural and Control Optimization of a Space Structure Subjected to the Gravity-Gradient Torque*," Acta Astronautica, vol. 51(10):673-681

He, Y. P., McPhee, J., 2002, "*An integrated Approach Using Genetic Algorithm, Multi body Dynamics, and LQG Control Strategy for Design Optimization of Ground Vehicles with Active Suspensions*," Proc. CSME Forum, Queen's University, Kingston, Canada, CD format

Hetenyi, M., 1971, "*Beams on Elastic Foundations,"* 9th edn. The University of Michigan Press, Ann Arbor

Hodges, D. H. and Bless, R. R., 1991, "*Weak Hamiltonian Finite Element Method for Optimal Control Problems*," Journal of Guidance, Control, and Dynamics, 14(1):148-156

Junkins, J.L. and Kim, Y., 1993, *"Introduction to Dynamics and Control of Flexible Structures,"* AIAA Education Series: Washington DC

Kelkar, A. G., Mao Y. and Joshi, S. M., 2001, "*Synthesis of LQ-Optimal Constant–Gain Positive-Real Controllers*," Control and Intelligent Systems, 29 (3): 65-73

Kim, S.J., Hwang, J.S., and Mok, J., 2000, "*Sensor/Actuator Optimal Design for Active Vibration Control of Shell Structure*,*"* Journal of Intelligent Material Systems and Structures, 11(11):848-856

Kim, J., Hwang J.S. and Kim, S.J., 2001, "*Design of Modal Transducers by Optimizing Spatial Distribution of Discrete Gain Weights*," AIAA Journal, 39 (10):1969-1976

Levine, W. S. and Athans M., 1970, "*On the Determination of the Optimal Constant Output Feedback Gains for Linear Variable Systems*," IEEE Transactions on Automatic Control, AC-15:44-48

Lin, Y.H., 1989, "*Optimal vibration suppression in modal space for flexible beams subjected to moving loads*," Journal of Shock and Vibration, 4(1):39-50

Meirovitch, L. and Baruh, H., 1982, *"Control of self-Adjoint Distributed –Parameter System,"* Journal of Guidance, *5* (1):60-66

Mendel, J. M., 1974, "*A Concise Derivation of Optimal Constant Limited State Feedback Gains*,*"* IEEE Transactions on Automatic Control, AC-19 : 447-448

Moerder, D. D. and Calise, A. J., 1985, "*Convergence of a Numerical Algorithm for Calculating Optimal Output Feedback Gains*," IEEE Transactions on Automatic Control AC-30(9):900-903

Pinch, E.R., 1993, "*Optimal Control and Calculus of Variations,"* Oxford University Press, Oxford

Preumont, A., 2002, *"Vibration control of active structures,"* 2nd edn. Kluwer Academic Publishers, Dordrecht, Boston

Saleh, A. and Adeli, H., 1994, "*Parallel algorithms for integrated structural /control optimization,* Journal of Aerospace Engineering," AIAA Journal, 7(3):297-314

Saleh, A. and Adeli, H., 1999, *"Control, optimization, and smart structures*," J. Wiley&Sons, Inc, New York

Szyszkowski, W. and Hoetzel*,* M., 1999, "*Optimal Linear Regulator Problems Solved by The Finite Element Method*," Computers and Structures*,* 70:141-148 .

Szyszkowski, W. and Grewal, I. S., 2000, "*Beam Analogy for Optimal Control of Linear Dynamic Systems*," Computational Mechanics, 25(5): 489-501

Szyszkowski, W. and Grewal, I. S., 2002, "*Optimal vibrations control problems by the finite element method,"* Part *I* and *II*, Communications in Numerical Methods in Engineering, 18(12):861-876

Takahashi, Y. and Robins, M. J., and Auslander, D.M., 1972, "*Control and Dynamic Systems*" Addison Wesley Publishing Company, Reading, Massachusetts

Tzou, H.S. and Anderson, G.L., 1992, "*Intelligent Structural Systems*," Kluwer Academic Publishers, Dordrecht, The Netherlands.

Wang, S. Y., Quek, S. T. and Ang, K. K., 2001 "*LQR Vibration Control of Piezoelectric Composite Plates*," Smart Structure and Devices, Proc. SPIE, 4235:375-386

Warner, M. S. and Hodges D. H., 2000, "*Solving Optimal Control Problems Using hp-Version Finite Elements in Time*," Journal of Guidance, Control, and Dynamics, 14(23): 89-94.

Zhong, W., Lin, J. and Qiu, C., 1992, "*Computational Structural Mechanics and Optimal Control-The simulation of Substructural Chain Theory to Linear Quadratic Optimal Control Problems*," *Int*. Journal for Numerical Methods in Engineering, 33: 197-211.

A. Appendix A

A.1 Example FEM ANSYS Program

The following is an example of ANSYS program to solve the problem of static beams using beam analogy.

```
l1 = 0.53010E-01

/title, 2DOF


                !constants...
alpha1=0        !alphas for Qd
alpha2=1
alpha3=0

b1=1            !betas for Qv
b2=0
b3=0

c1=0            ! gammas for R
c2=1/100
c3=0


/prep7
w1=(14017.15362)**.5 !frequencies 14017.153619
w2=(119435.2415)**.5
damp1=0! damping zeeta
damp2=0


r1=1/(c1+c2*w1**2+c3*2*w1*damp1)        !force wt. parameters
r2=1/(c1+c2*w2**2+c3*2*w2*damp2)
q11=alpha1+alpha2*w1**2+alpha3*2*w1*damp1               !disp. wt. parameters
q12=alpha1+alpha2*w2**2+alpha3*2*w2*damp2
q21=b1+b2*w1**2+b3*2*w1*damp1           !velocit. wt. parameters
q22=b1+b2*w2**2+b3*2*w2*damp2

EI1=r1          !stiffness
EI2=r2
P1=(2*w1**2*r1)-q21+(2*w1*damp1*r1*2*w1*damp1)
P2=(2*w2**2*r2)-q22+(2*w2*damp2*r2*2*w2*damp2)
```

```
kf1=w1**4*r1+q11       !EFS
kf2=w2**4*r2+q12
el1=48              !no. of elements
el2=48
v1=.5819928066e-1!etas
v2=.4670227075e-2
T=0.5    !gamma for time

E=70e9

I1=EI1/E
I2=EI2/E
A1=(12*I1)**.5
A2=(12*I2)**.5

ANTYPE,0
!PSTRES,ON
SSTIF,ON
ET,1,BEAM54
!A1=1
R,1,A1,I1,1,1,,
RMORE,,,,,,,
RMORE,,,,kf1

MP,EX,1,E          !Young's Modulus for steel.
N,1,0.0,0.0
N,(1+el1),l1,0.0
FILL,,,,,,,,10


E,1,2
EGEN,el1,1,1


D,1,ux,0
D,1,uy,v1
D,1,rotz,0
D,1+el1,uy,0
F,(1+el1),fx,(-P1)
D,(1+el1),rotz,0


ET,2,BEAM54
!A2=1
R,2,A2,I2,1,1,,
RMORE,,,,,,,
RMORE,,,,kf2

MP,EX,2,E       !Young's Modulus for steel.
TYPE,2,2
REAL,2
```

```
MAT,2
N,2+el1,0.0,-0.3
N,(2+el1+el2),l1,-0.3
FILL,,,,,,,,10
E,2+el1,2+el1+1
EGEN,el2,1,1+el1


D,2+el1,ux,0
D,2+el1,uy,v2
D,2+el1,rotz,0
D,2+el1+el2,uy,0
F,(2+el1+el2),fx,(-P2)
D,(2+el1+el2),rotz,0
nplot

fini


/solu
solve
fini


/post1
set


esel,s,ELEM,,el1,el1.
*get,A,ELEM,el1,smisc,12
esel,s,ELEM,,(el1+el2),el1+el2.
*get,B,ELEM,(el1+el2),smisc,12.
H=T-(r1*A**2/EI1**2+r2*B**2/EI2**2)
H1=1+abs(H)
esel,all
etable,acceller,smisc,12
etable,velocit,rot,z
etable,disp,u,y
pretab
/format,,,20,20
etable,y,rot,z
etable,ation,smisc,12
plls,acceller,ation
plls,velocit,y
pldispl,1
plls,acceller,ation
plls,velocity,y
H=T-(r1*A**2/EI1**2+r2*B**2/EI2**2)
H1=1+abs(H)
finish
```

A.2 Example ANSYS Program for Transient Dynamic Analysis

The following is an example of ANSYS program to perform transient dynamic analysis of the elastic beam (Mode Superposition).

```
/PREP7
ET,1,SHELL63
R,1,0.02232, , , , , ,     ! Thickness of  Fin Structure
MPTEMP,1,0
MPDATA,EX,1,,7.17e10
MPDATA,PRXY,1,,0.3
MPDATA,dens,1,,2800
K,1,0,0,0,
K,2,1,0,0,
K,3,0,0,0.8,
K,4,1,0,0.8,

/ANG, 1 ,-30.000000,ZS,1
/REP,FAST
/ANG, 1 ,-30.000000,XS,1
/REP,FAST
/ANG, 1 ,30.000000,ZS,1
/REP,FAST


LSTR,      1,      2
LSTR,      2,      4
LSTR,      4,      3
LSTR,      1,      3

FLST,2,4,4
FITEM,2,1
FITEM,2,2
FITEM,2,3
FITEM,2,4
AL,P51X
esize,,10
amesh,1

ET,2,SHELL63!Rigid Plate
R,2,2.11, , , , , ,
K,5,0,0.5,0,
K,6,,0.5,0.8,
K,7,,-0.5,0.8,
K,8,0,-0.5,,
TYPE,   2
MAT,      1
REAL,      2
```

```
l,1,5
l,1,8
l,5,6
l,3,6
l,3,7
l,7,8
al,5,7,8,4
al,4,6,10,9
esize,,10
amesh,2
amesh,3
FLST,2,60,1,ORDE,6
FITEM,2,1
FITEM,2,22
FITEM,2,122
FITEM,2,-150
FITEM,2,232
FITEM,2,-260
!*
/GO
D,P51X, ,0, , , ,ALL, , , , ,
/solu
antype,modal
modopt,subsp,10
!outpr,all,all
solve
save
finish

/solu
antype,trans  !Analysis type (trans=transient dynamic)
trnopt,msup,10   !Solution method (full,reduc,modal,msup)
!nlgeom,off     !Large deformation effects (on,off)
!sstif,on     !Stress stiffening effects (off,on)
!nropt,auto    !Newton-Raphson option (auto,full,modi,init)
        !initial forces imposing initial condtions

f,79,fy,-5047.2
f,113,fy,4127.5
f,120,fy,1129.8
!d,7,ux,0.016
!d,13,ux,0.013
kbc,1
!time,11
deltim,0.001!0.011256806
!autots,on
!outres,,1
!outpr,all
lswrite
timint,on
fdele,79,fy
```

```
fdele,113,fy
fdele,120,fy

!!!!!!!!!!!!!!!!!!!!!!!!!!!!!!!!!!!!!!!!!!!!!!!!!!!!!!!!!!!!!!!!!!!!!!!

!COPY THE FILE FORCE.OUT HERE TILL SPECIFIED BELOW

!!!!!!!!!!!!!!!!!!!!!!!!!!!!!!!!!!!!!!!!!!!!!!!!!!!!!!!!!!!!!!!!!!!!!!!
fdele,2,fy
fdele,12,fy
F,2,fy, -11.322104
F,12,fy, -3.107023
kbc,0
time,.0007+ 0.000000
outres,nsol,10
outpr,nsol,10
lswrite
!!!!!!!!!!!!!!!!!!!!!!!!!!!!!!!!!!!!
fdele,2,fy
fdele,12,fy
F,2,fy, 15.900000
F,12,fy, 2.270000
kbc,0
time,.0007+ 0.000280
outres,nsol,10
outpr,nsol,10
lswrite
!!!!!!!!!!!!!!!!!!!!!!!!!!!!!!!!!!!!
fdele,2,fy
fdele,12,fy
F,2,fy, 44.299999
F,12,fy, 8.080000
kbc,0
time,.0007+ 0.000574
outres,nsol,10
outpr,nsol,10
lswrite
!!!!!!!!!!!!!!!!!!!!!!!!!!!!!!!!!!!!
fdele,2,fy
fdele,12,fy
F,2,fy, 73.699997
F,12,fy, 14.500000
kbc,0
time,.0007+ 0.000883
outres,nsol,10
outpr,nsol,10
lswrite
!!!!!!!!!!!!!!!!!!!!!!!!!!!!!!!!!!!!
fdele,2,fy
fdele,12,fy
F,2,fy, 104.000000
```

F,12,fy, 21.600000
kbc,0
time,.0007+ 0.001210
outres,nsol,10
outpr,nsol,10
lswrite
!!!!!!!!!!!!!!!!!!!!!!!!!!!!!!!!
fdele,2,fy
fdele,12,fy
F,2,fy, 135.000000
F,12,fy, 29.600000
kbc,0
time,.0007+ 0.001550
outres,nsol,10
outpr,nsol,10
lswrite
!!!!!!!!!!!!!!!!!!!!!!!!!!!!!!!!
fdele,2,fy
fdele,12,fy
F,2,fy, 166.000000
F,12,fy, 38.900002
kbc,0
time,.0007+ 0.001910
outres,nsol,10
outpr,nsol,10
lswrite
!!!!!!!!!!!!!!!!!!!!!!!!!!!!!!!!
fdele,2,fy
fdele,12,fy
F,2,fy, 197.000000
F,12,fy, 49.500000
kbc,0
time,.0007+ 0.002280
outres,nsol,10
outpr,nsol,10
lswrite
!!!!!!!!!!!!!!!!!!!!!!!!!!!!!!!!
fdele,2,fy
fdele,12,fy
F,2,fy, 228.000000
F,12,fy, 61.900002
kbc,0
time,.0007+ 0.002680
outres,nsol,10
outpr,nsol,10
lswrite
!!!!!!!!!!!!!!!!!!!!!!!!!!!!!!!!
fdele,2,fy
fdele,12,fy
F,2,fy, 259.000000
F,12,fy, 76.300003

kbc,0
time,.0007+ 0.003090
outres,nsol,10
outpr,nsol,10
lswrite
!!!!!!!!!!!!!!!!!!!!!!!!!!!!!!!!
fdele,2,fy
fdele,12,fy
F,2,fy, 288.000000
F,12,fy, 93.099998
kbc,0
time,.0007+ 0.003530
outres,nsol,10
outpr,nsol,10
lswrite
!!!!!!!!!!!!!!!!!!!!!!!!!!!!!!!!
fdele,2,fy
fdele,12,fy
F,2,fy, 316.000000
F,12,fy, 113.000000
kbc,0
time,.0007+ 0.003980
outres,nsol,10
outpr,nsol,10
lswrite
!!!!!!!!!!!!!!!!!!!!!!!!!!!!!!!!
fdele,2,fy
fdele,12,fy
F,2,fy, 341.000000
F,12,fy, 135.000000
kbc,0
time,.0007+ 0.004460
outres,nsol,10
outpr,nsol,10
lswrite
!!!!!!!!!!!!!!!!!!!!!!!!!!!!!!!!
fdele,2,fy
fdele,12,fy
F,2,fy, 364.000000
F,12,fy, 161.000000
kbc,0
time,.0007+ 0.004970
outres,nsol,10
outpr,nsol,10
lswrite
!!!!!!!!!!!!!!!!!!!!!!!!!!!!!!!!
fdele,2,fy
fdele,12,fy
F,2,fy, 384.000000
F,12,fy, 190.000000
kbc,0

time,.0007+ 0.005500
outres,nsol,10
outpr,nsol,10
lswrite
!!!!!!!!!!!!!!!!!!!!!!!!!!!!!!!!
fdele,2,fy
fdele,12,fy
F,2,fy, 400.000000
F,12,fy, 223.000000
kbc,0
time,.0007+ 0.006050
outres,nsol,10
outpr,nsol,10
lswrite
!!!!!!!!!!!!!!!!!!!!!!!!!!!!!!!!
fdele,2,fy
fdele,12,fy
F,2,fy, 412.000000
F,12,fy, 259.000000
kbc,0
time,.0007+ 0.006640
outres,nsol,10
outpr,nsol,10
lswrite
!!!!!!!!!!!!!!!!!!!!!!!!!!!!!!!!
fdele,2,fy
fdele,12,fy
F,2,fy, 420.000000
F,12,fy, 298.000000
kbc,0
time,.0007+ 0.007250
outres,nsol,10
outpr,nsol,10
lswrite
!!!!!!!!!!!!!!!!!!!!!!!!!!!!!!!!
fdele,2,fy
fdele,12,fy
F,2,fy, 423.000000
F,12,fy, 340.000000
kbc,0
time,.0007+ 0.007900
outres,nsol,10
outpr,nsol,10
lswrite
!!!!!!!!!!!!!!!!!!!!!!!!!!!!!!!!
fdele,2,fy
fdele,12,fy
F,2,fy, 423.000000
F,12,fy, 382.000000
kbc,0
time,.0007+ 0.008570

outres,nsol,10
outpr,nsol,10
lswrite
!!!!!!!!!!!!!!!!!!!!!!!!!!!!!!!!
fdele,2,fy
fdele,12,fy
F,2,fy, 419.000000
F,12,fy, 425.000000
kbc,0
time,.0007+ 0.009280
outres,nsol,10
outpr,nsol,10
lswrite
!!!!!!!!!!!!!!!!!!!!!!!!!!!!!!!!
fdele,2,fy
fdele,12,fy
F,2,fy, 413.000000
F,12,fy, 465.000000
kbc,0
time,.0007+ 0.010000
outres,nsol,10
outpr,nsol,10
lswrite
!!!!!!!!!!!!!!!!!!!!!!!!!!!!!!!!
fdele,2,fy
fdele,12,fy
F,2,fy, 405.000000
F,12,fy, 502.000000
kbc,0
time,.0007+ 0.010800
outres,nsol,10
outpr,nsol,10
lswrite
!!!!!!!!!!!!!!!!!!!!!!!!!!!!!!!!
fdele,2,fy
fdele,12,fy
F,2,fy, 397.000000
F,12,fy, 531.000000
kbc,0
time,.0007+ 0.011600
outres,nsol,10
outpr,nsol,10
lswrite
!!!!!!!!!!!!!!!!!!!!!!!!!!!!!!!!
fdele,2,fy
fdele,12,fy
F,2,fy, 390.000000
F,12,fy, 550.000000
kbc,0
time,.0007+ 0.012500
outres,nsol,10

outpr,nsol,10
lswrite
!!!!!!!!!!!!!!!!!!!!!!!!!!!!!!!!
fdele,2,fy
fdele,12,fy
F,2,fy, 385.000000
F,12,fy, 557.000000
kbc,0
time,.0007+ 0.013400
outres,nsol,10
outpr,nsol,10
lswrite
!!!!!!!!!!!!!!!!!!!!!!!!!!!!!!!!
fdele,2,fy
fdele,12,fy
F,2,fy, 384.000000
F,12,fy, 550.000000
kbc,0
time,.0007+ 0.014400
outres,nsol,10
outpr,nsol,10
lswrite
!!!!!!!!!!!!!!!!!!!!!!!!!!!!!!!!
fdele,2,fy
fdele,12,fy
F,2,fy, 385.000000
F,12,fy, 527.000000
kbc,0
time,.0007+ 0.015400
outres,nsol,10
outpr,nsol,10
lswrite
!!!!!!!!!!!!!!!!!!!!!!!!!!!!!!!!
fdele,2,fy
fdele,12,fy
F,2,fy, 388.000000
F,12,fy, 487.000000
kbc,0
time,.0007+ 0.016400
outres,nsol,10
outpr,nsol,10
lswrite
!!!!!!!!!!!!!!!!!!!!!!!!!!!!!!!!
fdele,2,fy
fdele,12,fy
F,2,fy, 390.000000
F,12,fy, 432.000000
kbc,0
time,.0007+ 0.017500
outres,nsol,10
outpr,nsol,10

lswrite
!!!!!!!!!!!!!!!!!!!!!!!!!!!!!!!!
fdele,2,fy
fdele,12,fy
F,2,fy, 386.000000
F,12,fy, 365.000000
kbc,0
time,.0007+ 0.018700
outres,nsol,10
outpr,nsol,10
lswrite
!!!!!!!!!!!!!!!!!!!!!!!!!!!!!!!!
fdele,2,fy
fdele,12,fy
F,2,fy, 372.000000
F,12,fy, 290.000000
kbc,0
time,.0007+ 0.019900
outres,nsol,10
outpr,nsol,10
lswrite
!!!!!!!!!!!!!!!!!!!!!!!!!!!!!!!!
fdele,2,fy
fdele,12,fy
F,2,fy, 341.000000
F,12,fy, 214.000000
kbc,0
time,.0007+ 0.021200
outres,nsol,10
outpr,nsol,10
lswrite
!!!!!!!!!!!!!!!!!!!!!!!!!!!!!!!!
fdele,2,fy
fdele,12,fy
F,2,fy, 288.000000
F,12,fy, 141.000000
kbc,0
time,.0007+ 0.022500
outres,nsol,10
outpr,nsol,10
lswrite
!!!!!!!!!!!!!!!!!!!!!!!!!!!!!!!!
fdele,2,fy
fdele,12,fy
F,2,fy, 211.000000
F,12,fy, 76.000000
kbc,0
time,.0007+ 0.023900
outres,nsol,10
outpr,nsol,10
lswrite

```
!!!!!!!!!!!!!!!!!!!!!!!!!!!!!!!!
fdele,2,fy
fdele,12,fy
F,2,fy, 109.000000
F,12,fy, 20.100000
kbc,0
time,.0007+ 0.025400
outres,nsol,10
outpr,nsol,10
lswrite
!!!!!!!!!!!!!!!!!!!!!!!!!!!!!!!!
fdele,2,fy
fdele,12,fy
F,2,fy, -10.400000
F,12,fy, -29.400000
kbc,0
time,.0007+ 0.027000
outres,nsol,10
outpr,nsol,10
lswrite
!!!!!!!!!!!!!!!!!!!!!!!!!!!!!!!!
fdele,2,fy
fdele,12,fy
F,2,fy, -135.000000
F,12,fy, -79.099998
kbc,0
time,.0007+ 0.028600
outres,nsol,10
outpr,nsol,10
lswrite
!!!!!!!!!!!!!!!!!!!!!!!!!!!!!!!!
fdele,2,fy
fdele,12,fy
F,2,fy, -251.000000
F,12,fy, -138.000000
kbc,0
time,.0007+ 0.030300
outres,nsol,10
outpr,nsol,10
lswrite
!!!!!!!!!!!!!!!!!!!!!!!!!!!!!!!!
fdele,2,fy
fdele,12,fy
F,2,fy, -341.000000
F,12,fy, -212.000000
kbc,0
time,.0007+ 0.032100
outres,nsol,10
outpr,nsol,10
lswrite
!!!!!!!!!!!!!!!!!!!!!!!!!!!!!!!!
```

```
fdele,2,fy
fdele,12,fy
F,2,fy, -396.000000
F,12,fy, -301.000000
kbc,0
time,.0007+ 0.034000
outres,nsol,10
outpr,nsol,10
lswrite
!!!!!!!!!!!!!!!!!!!!!!!!!!!!!!!!
fdele,2,fy
fdele,12,fy
F,2,fy, -415.000000
F,12,fy, -396.000000
kbc,0
time,.0007+ 0.036000
outres,nsol,10
outpr,nsol,10
lswrite
!!!!!!!!!!!!!!!!!!!!!!!!!!!!!!!!
fdele,2,fy
fdele,12,fy
F,2,fy, -408.000000
F,12,fy, -473.000000
kbc,0
time,.0007+ 0.038100
outres,nsol,10
outpr,nsol,10
lswrite
!!!!!!!!!!!!!!!!!!!!!!!!!!!!!!!!
fdele,2,fy
fdele,12,fy
F,2,fy, -391.000000
F,12,fy, -506.000000
kbc,0
time,.0007+ 0.040300
outres,nsol,10
outpr,nsol,10
lswrite
!!!!!!!!!!!!!!!!!!!!!!!!!!!!!!!!
fdele,2,fy
fdele,12,fy
F,2,fy, -375.000000
F,12,fy, -474.000000
kbc,0
time,.0007+ 0.042600
outres,nsol,10
outpr,nsol,10
lswrite
!!!!!!!!!!!!!!!!!!!!!!!!!!!!!!!!
fdele,2,fy
```

```
fdele,12,fy
F,2,fy, -355.000000
F,12,fy, -376.000000
kbc,0
time,.0007+ 0.045000
outres,nsol,10
outpr,nsol,10
lswrite
!!!!!!!!!!!!!!!!!!!!!!!!!!!!!!!!
fdele,2,fy
fdele,12,fy
F,2,fy, -309.000000
F,12,fy, -236.000000
kbc,0
time,.0007+ 0.047500
outres,nsol,10
outpr,nsol,10
lswrite
!!!!!!!!!!!!!!!!!!!!!!!!!!!!!!!!
fdele,2,fy
fdele,12,fy
F,2,fy, -205.000000
F,12,fy, -92.400002
kbc,0
time,.0007+ 0.050200
outres,nsol,10
outpr,nsol,10
lswrite
!!!!!!!!!!!!!!!!!!!!!!!!!!!!!!!!
fdele,2,fy
fdele,12,fy
F,2,fy, -32.900002
F,12,fy, 26.500000
kbc,0
time,.0007+ 0.05301
outres,nsol,10
outpr,nsol,10
lswrite
!!!!!!!!!!!!!!!!!!!!!!!!!!!!!!!!



!!!!!!!!!!!!!!!!!!!!!!!!!!!!!!!!!!!!!!!!!!!!!!!!!!!!!!!!!!!!!!!!!!!!!!!

!COPY THE FILE FORCE.OUT TILL THIS POINT

!!!!!!!!!!!!!!!!!!!!!!!!!!!!!!!!!!!!!!!!!!!!!!!!!!!!!!!!!!!!!!!!!!!!!!!



fdele,2,fy
```

```
fdele,12,fy
kbc,1
time,.0007+0.053010 +.0007
outres,all,all
outpr,all,all
lswrite


kbc,0
time,0.075
outres,all,all
outpr,all,all
lswrite
save
lssolve,1,52
save
finish



/post26
file,,rdsp
numvar,10
!file,file,rdsp
nsol,2,2,u,y,uy2
nsol,3,12,u,y,uy12
!nsol,3,3,u,y,uy3
nsol,4,7,u,y,uy7
nsol,5,27,u,y,uy27
plvar,2!,3
plvar,2,3,4,5
prvar,2
save
!finish
```